TÉCNICO LISBOA

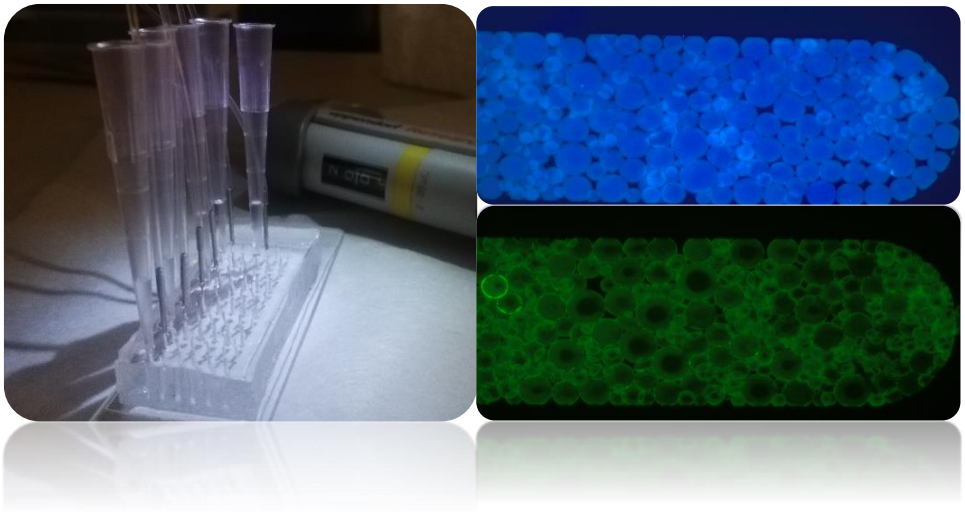

Direct bacterial cell detection in a microfluidic chip

Inês Pereira Domingos

Thesis to obtain the Master of Science Degree in

Biomedical Engineering

Supervisor(s): Doctor João Pedro Estrela Rodrigues Conde
Doctor Ricardo Jaime Pereira Rosário dos Santos

Examination Committee

Chairperson: Doctor Maria Margarida Fonseca Rodrigues Diogo
Supervisor: Doctor João Pedro Estrela Rodrigues Conde
Member off the Committee: Doctor Verónica Cristina Baião Martins Romão

November 2019

"Perhaps life is just that... a dream and a fear." – Joseph Conrad

To my mother.

Acknowledgments

To understand the importance of those that pass through our path, even if is to teach us some aspect of value, is priceless. Nevertheless, regarding who is available to help and support our journey during the course of each event, there are not enough words able to transmit a simple and special thank you.

To Professor Joao Pedro Conde, that gave me the opportunity to perform this thesis in INESC MN facilities, making this project available and possible to be developed. I thank all the support, availability, mentorship, patience and optimism no matter the faced results.

To my colleagues and fellow INESC-MN workers, I thank for all the support, good environment, advices and availability to clarify any doubt, regarding microfluidic fabrication processes and techniques. A special thanks to Catarina Caneira for the guidance and mentorship throughout the project development and for the required patience to teach me and to deal with my schedules and availability. To Eduardo Brás for the advices, accessibility and all the clarified doubts. To Andreia Jardim, Ricardo Serrão and Cristiana Domingues, for the support, fellowship and friendship, help and amazing week throughout the Zweibruecken summer school.

I would like to thank my closest friends that were tireless and eased this period of my life, so, thank you Ana Rita Monteiro, Ana Rodrigues, Joana Mendes, Cláudia Martins, Cláudia Duarte and Margarida Araújo. To Rute Palma that was there when I was the most stressed, mind clouded, thanks for all the love, strength and dedication, without which I would not had the ability to face some obstacles along this path. To Sónia Rosa for the endless support and for never doubting my capacities, a big thank you.

To my family, especially to my mother and father, Ana Maria Pereira and José Domingos, that always supported my dreams and what I wanted to achieved. To my mother for all the strength, motherhood and friendship, for being increasingly tireless and as nervous as I, to accomplish this goal. To my brother Pedro Domingos for let me rest my mind and have some fun.

Resumo

A captura e deteção direta de bacterias é uma das grandes metas em meios terapêuticos. Uma das razões que levam à procura deste tipo de estratégias é o aumento acelerado da incidência na temática Resistência a antibióticos, devido ao descontrolo na prescrição e ao incorreto uso dos mesmos. Os métodos de diagnóstico convencionais são considerados dispendiosos em termos de tempo e custo, sendo que na maioria dos casos, são baseados em cultura de células ou na amplificação do seu material genético. Na microfluídica, há a oportunidade de miniaturizar e replicar processos biológicos, prometendo o desenvolvimento de sistemas low-cost, com elevada sensibilidade, facilidade de transporte e rápidos na aquisição de resultados. No desenvolvimento deste projecto, há a tentativa de criação de um *chip* baseado em microfluídica, que consiga capturar e detetar diretamente células bacterianas de *Staphylococcus aureus*, usando um sistema baseado em *beads* porosas.

Micro-canais de PDMS foram a base do sistema microfluídico, fabricados usando técnicas de soft-litografia e selados contra uma membrana do mesmo material. Aptameros foram adquiridos para formarem uma *sandwich* de captura e deteção, onde se recorreu a uma biotina para imobilizar e um fluoróforo para se poder detetar. Diferentes tipos de beads foram testadas e uma selecionada para testar a capacidade de ligação dos aptameros. Pigmentos distintos foram usados para avaliar se a viabilidade celular teria sido comprometida de alguma forma. Um estudo final foi realizado para avaliar a sensibilidade que as beads no canal teriam para capturar fisicamente as células.

Palavras-Chave: Sistema microfluídico, *beads*, *Staphyloccus aureus,* aptameros, deteção, captura.

Abstract

Direct capture and detection of bacterial cells is one of the aimed goals in the therapeutics field. One of the reasons behind this search is the increasingly incidence of Antibiotic Resistance, occurring due to an uncontrolled antibiotic prescription and incorrect use of this drug. Conventional diagnostic methods are cost and time consuming since, in the majority of the cases, rely on cultures and amplification approaches. In microfluidics there is the opportunity to miniaturize and mimic biological processes, promising the development of systems low-cost, with high sensitivity, ease of transport and time saving. In the development of this project, a microfluidic chip to perform direct capture and detection of *Staphylococcus aureus* was to be achieved using a porous bead-based system.

PDMS microchannels were the basis of the microfluidic system, fabricated using a soft-lithography technique and sealed against a PDMS membrane. Aptamers were acquired to be used as probes in order to perform a capture-detection sandwich, resourcing a biotin to allow immobilization and a fluorophore to detect. Different bead types were tested and one selected to assess the aptamers binding efficacy. Distinct dyes were used in the matter of evaluating if cellular viability was somehow compromised. A final assessment was established regarding the sensibility of physically capturing cells using solely the microfluidic chip packed with beads.

Keywords: Microfluidic system, beads, *Staphyloccus aureus,* aptamers, detection, capture.

Contents

List of Tables

List of Figures

Abbreviations and Acronyms

AR – Antibiotic Resistance

A.a. – Amino acids

Ab/s – Antibody/ies

Biotin-FITC – Biotin, fluorescein isothiocyanate conjugate

DNA – Deoxyribonucleic acid

DWL – Direct write laser

Fc – Framework region

Fab – Antigen binding site

HCL – Hydrochloric acid

MRSA – Methicillin-resistant *Staphylococcus aureus*

MEMS – Microelectro-mechanical systems

PDMS – Polydimethylsiloxane

PGMEA – Propylene glycol methyl ether acetate

PBS – Phosphate buffered saline

PEG – Polyethylene glycol

PCR – Polymerase chain reaction

qPCR – real-time Polymerase chain reaction

RNA – Ribonucleic acid

rRNA – ribosomal Ribonucleic acid

RT-qPCR – reverse transcriptase real-time Polymerase chain reaction

UV – Ultra-violet

VRE – vancomycin-resistant *enterococci*

Strep-FITC – Streptavidin, fluorescein isothiocyanate conjugate

Tris-HCL – Trisaminomethane Hydrochloride

Chapter 1

Introduction

This project focus on the direct capture and detection of bacterial cells in a microfluidic chip. Throughout the first chapter it is exposed the motivation that brought out the development of the project, adding the main concepts necessary to fully understand the themes addressed. On section 1.2 is reviewed the definition of Prokaryotic cells, describing the interest features of Bacteria, followed by its impact on Human health, along section 1.3. The Microfluidic approach of the project is brought up on section 1.4, explaining the main characteristics of the field and the fabrication processes. Other features used during the workflow are detailed on section 1.5 and on the last section, there is the exposure of the project's goal.

1.1 Motivation

Antibiotic Resistance (AR) is based on the capacity of bacteria to undercome the effect of antibiotics, one of the biggest discoveries of Medicine that end up saving countless lives. Nevertheless, during the last years, its overuse, only contributed for what can be called "the disease of the century" [1]. AR is a reality and a crisis that only continues to evolve, due to the lack of alternative treatments, but most of all due to the uncontrolled usage of this drug. Bacterial infections that were once treated with antibiotics are now able to persist by means of these pathogens evolution.[2]

Besides the overuse of antibiotics, another main problem is the misconception of its use [1]. Studies have shown that there is a high insurgence of antibiotic treatments being miscarried and incorrectly performed, which only contributes to increasing the odds of bacterial strains appearance able to resist antibiotics action. For instance, there are antibiotics being prescribed as treatment for viruses, flues or common colds, which is clearly a negligent practice [3]. When, antibiotics are being correctly prescribed but fail to treat the intend occurrence, there is the need to understand why, what to do next and what should have been done in the first place.

In the Hospital Emergence, exists the intention of knowing if a patient is somehow affected by a bacterial resistant pathogen, so that the right procedure can be set in motion. Although the urge in establishing the main source of the patient disease, the current practices are expensive and time

consuming [4]. The idea of having a mechanism able of avoiding the negative aspects of nowadays approaches is enticing and also the main reason behind a vast range of studies.

The Microfluidic field has the potential to miniaturize several procedures avoiding large consumption of reagents and other materials involved on these processes. Even the more complex approaches can be scaled down. Microfluidics brings advantages, like cost and time efficiency adding the fact to be possible of using as a device, bringing ease to the user and means of transportation. This field can bring another view, perspective and innovative features to Antibiotic Resistance thematic and somehow be the tool to overcome some of the disadvantages of the current practices. [5]

1.2 Prokaryotes

The cell is the fundamental unit of life but due to evolution, not all cells are the same, having within themselves, different sizes, shapes, structures and functions. There are two major cell categories, prokaryotic and eukaryotic cells. Although some basic functions of all cells remain the same in a simpler level of action, these two present the higher deviation in their presented features, being this marked by the organization of the cell's genetic material. [6]

Regarding this project, the focus goes to prokaryotic cells topic. In this cell type, the genetic information is not structured and stored inside a nucleus, contrary to what is possible to found on a eukaryotic cell. Prokaryotic cells are characterized by one single compound, surrounded by a plasmatic membrane and the Deoxyribonucleic acid (DNA) is inside forming one unique, circular chromosome on a section named nucleoid (Figure 1.1). [6][7]

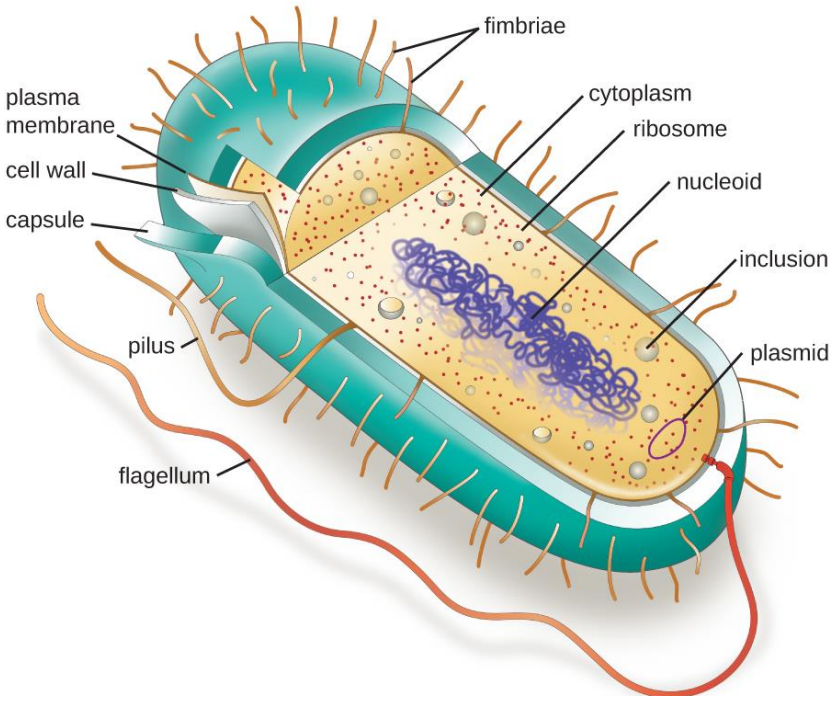

Figure 1.1 Schematic of a Prokaryotic cell with representation of its components. Adapted from the literature [7].

Besides the elucidated major component, prokaryotic cells have other structures that characterize their particularities. Ribosomes play a role on synthetizing proteins and due to the fact of having a simpler organization, prokaryotic cells have their own mechanisms of protection and motion. To protect the thin membrane that encapsulates the cell's inside, prokaryotes also have a cell wall and a capsule, which confer protection and support. The cell wall is rigid, most of the times composed of peptidoglycans and is responsible for the cell's shape, protects its interior and prevents it to burst upon water's entrance; the capsule, made of polysaccharides, prevents the cell from drying out and in some cases allows protection against the host immune system. In order to perform its motion, some prokaryotic cells have on their surface, a flagellum and on the surface, is possible to found pilus that play a role on the attachment to other cells and surfaces (Figure 1.1). [7]

1.2.1 Bacteria

The main group of Prokaryotes is composed by two of the three main domain system representative of the Phylogenetic Tree of life. Besides Eukaryotes, the remaining domain, Bacteria's (Eubacteria) and Archaea's (Archeabacteria) domains characterize Prokaryotes (Figure 1.2). The Phylogenetic Tree of Life is representative of the evolution across organisms and the relation they have with each other. The resemblance was primarily referred by Woese et al., and is based on differences and similarities of the nucleotides sequence on the cell ribosomal Ribonucleic acid (rRNA). [8][9]

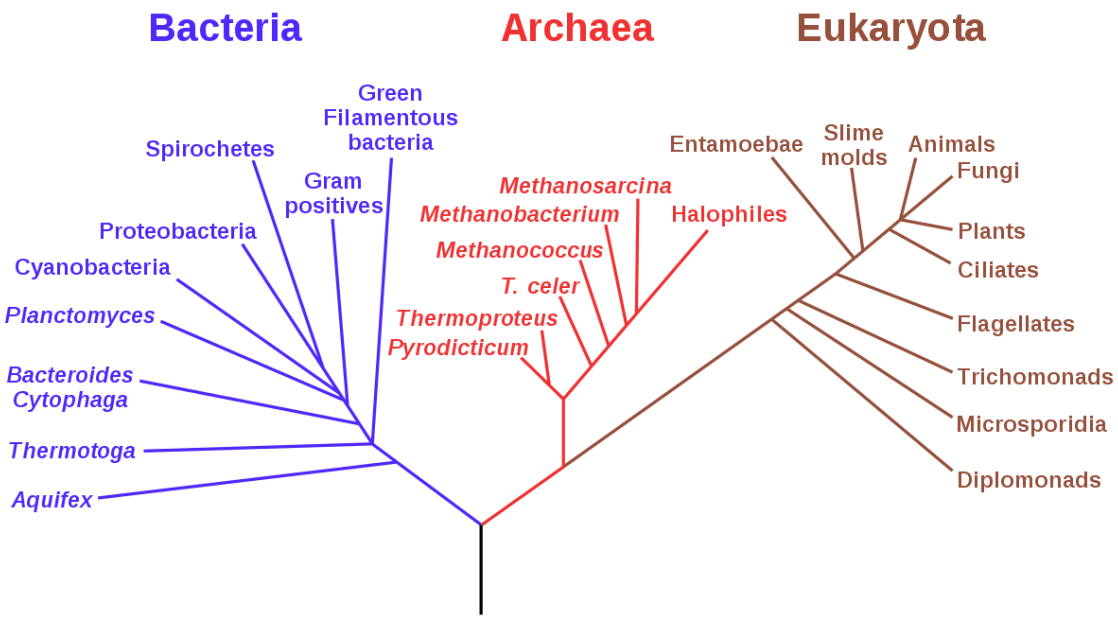

Figure 4.2 Schematic of the Phylogenetic Tree of Life, representing the three main domains: Bacteria, Archaea and Eukaryota domains . Adapted from the literature. [8]

On the present project development, the interest goes to the Bacteria domain, where is placed, bacterial species that can be considered pathogens and compromise human's health like *Staphylococcus aureus* species, detailed in section 1.3.4.

1.3 Bacteria vs Human health

There are different types of interaction between bacteria and its host. This interaction can be characterized according to the effect that emerges on the host. Commensal bacteria are defined by not help or harm the other organism, when living in it. They're usual found, on areas that commonly contact with the exterior or residing on epithelial surfaces. Other type of bacteria, are the ones that somehow help the host by getting some usufruct in return, building a relation of mutual assistance. An example of a mutualistic relationship is for instance, bacteria, which feed up of microbes that are harmful to the host. Last but not the least, the dangerous type of bacteria is the pathogenic one. Pathogenic bacteria act as a parasite and survive at the expenses of the host's health. [10]

On the human body, is usual to found commensal bacteria on the skin, the armpit area or the perineum and mutualistic bacteria can be found on the inside's mouth, for example. The problem is reached, when a bacterium becomes harmful, inducing infections and jeopardizing the human's immunity system. [10][11]

1.3.1 Bacterial infections and diseases

As mentioned above, even though human flora is rich in bacteria, having a very diversified microbiota, there are innumerous opportunistic bacterial pathogens, that take advantages when a person's defenses is somehow weaken or are able to break through those same defenses [10]. Besides this type, when harmful, bacteria can also be consider primary pathogens and likely agents of disease. Nevertheless, it is important to mention that most pathogenic bacteria cause infections, not meaning that the patient has a disease. The capacity of the pathogen to be considered a disease responsible is directly related to the its degree of virulence. Also, each bacterial type as its way of infection and behavior in the host's organism, being this referred as pathogenesis and includes the active role of how bacteria infect, lodge, grow and survive. [12]

Virulence factors are related to the capacity of inducing disease or symptoms related, but should never be considered as common straight actuators specific to each bacteria [12]. The referred factors always depend on how the host reacts to their exposure, for instance, bacteria can release certain toxins or have mechanisms that allow them to survive phagocytosis, but its virulence is assign to how the host responds and which outcome it has to face [13]. Nevertheless, those pathogens aim to multiply and survive without killing its host, in the majority of the cases, since their survival also depends on it. In spite of this, there is a large spectrum of bacteria type, functions, pathogenesis and evolution, which are prone to be more aggressive, to cause disease and to threat the infected organism subsistence [14]. Table 1.1 displays some selected bacteria types that have a negative influence in human health, along with some symptoms and diseases outcomes that urge from their action on the immune system.

Table 1.1 Some bacteria types that negatively influence human's health, symptoms and mechanism of transmittion. [15][16][17][18][19][20][21]

Species		***Transmission***	***Disease***
Chlamydia	*C. pneumoniae*	Respiratory droplets	Atypical pneumonea
	C. trachomatis	Sexually transmitted	Trachoma, Urethritis, Pelvic inflammatory disease , Epididymitis, Prostatitis, among other
Escherichia Coli		Gut flora and in urinary tract. Proliferating in the Gastrointestinal tract	Diarrhea, Urinary tract infections, pneumonia, sepsis, among other
Haemophilus influenzae		Droplet contact, Human flora of upper respiratory tract	Bacterial meningitis, Upper respiratory tract infections, Pneumonia, bronchitis, among other
Pseudomonas aeruginosa		Infects damaged tissues, infects people with immunodeficiency.	Pneumonia, Urinary tract infection, Burn wound infection, Sepsis, among other
Salmonella typhi		Fecal-oral route, through food or wate	Fever, abdominal pain, chronic carrier state, among other
Staphylococcus aureus		Human flora on mucosae in anterior nares, skin and vagina among other, entering through wound	Skin infections, sepsis, Osteomyelitis, Toxinoses, Staphylococcal food poisoning
Streptococcus	*S. pneumoniae*	Respiratory droplets Human flora in nasopharynx	Acute bacterial pneumonia and meningitis, Sepsis, among other
	S. viridans	Oral flora, penetration through abrasions	Subacute bacterial endocarditis, Dental cavities, among other

1.3.2 Antibiotics

Antibiotics are considered one of the biggest discoveries that came across Medicine's history. In the majority of human existence, infectious diseases threatened its health and well-being [22]. Antibiotics arrived to change that path of the history's course. Although common beliefs place the introduction of antibiotics side-by-side to the beginning of the nominated "antibiotic era" [23], the truth is evidences of tetracycline, an antibiotic derived from *Streptomyces aureofaciens*, were reported to be

found in archeological remains dating 350-550 CE [24]. This antibiotic is commonly used to treat infections from the respiratory track, caused by specific pathogens [25]. The discovered traces of tetracycline in ancient human bones, were stated to have been sourced from food exposure that was fermented upon contaminated soils containing bacteria of the *Streptomyces* genus. There were other examples of cases pre-antibiotic era, reported to have used antibiotic and antimicrobial derivatives [24]. Nevertheless, the names Paul Ehrlich and Alexander Flaming appear as foundation pillars of antibiotic's discovery age [23].

Ehrlich "magic bullets" had a major contribution in the beginning of the epoch. Based on the fact of synthetic dyes be able to stain microbes with specificity, targeting them without, neither interfering with the host's cells nor be harmful. This discovery was the entering path to the search and study of drug's effects on diseases, opening the gates to the discovery and identification of innumerous antibiotics. [23][26]

Across its studies on *Staphylococci* properties, Fleming encountered a contaminated bacterial culture that had destroyed some colonies. This occurrence led to the accidental discovery of *penicillin*, the revolutionary antibacterial on the path of Medicine's history. Although it took years of Fleming's studies in order to *penicillin's* have the mentioned importance, years later, from its research on, Howard Florey and Ernst Boris Chain, accomplished the drug's mass production. [23][27]

Between 1950 and 1970, the majority of antibiotic classes were discovered. In his initial findings Fleming alerted that an overuse of the drug would end up leading to its resistance by pathogens. After the refereed golden era of antibiotic new classes discovery, there were not others to be found, solely modifications of already existent ones, which gave space to resistance emergence and rise.[23][28]

1.3.3 Antibiotic Resistance

Antibiotic Resistance is the designation attributed to the phenomenon of infectious pathogens to overcome the effect of drugs that were design to kill them in first instance, developing the ability to resist antibiotic's action. As all organisms, also bacteria are prone to evolve in order to adapt to the surrounding environment, developing different mechanisms to sustain life and allow the species proliferation. [3][13][28]

As mentioned in section 1.3.2, the lack of new emergent antibiotic classes, gave room to bacteria adapt against these drugs. This adaptation can be based in distinct mechanisms, such as the manifestation of a mutation conferring the bacteria certain abilities, a modification that might have occurred due to an enzyme's action or a formation of a barrier acting as a shield, protecting the pathogen. Even the mechanisms of action can vary by destroying the antibiotic, expelling the drug from the cell, of simply resist to it [29]. Nevertheless, as evolutionary organisms is not unusual this ability to adapt. The problem is antibiotic resistance has been having an increasingly higher incidence the past few years, existing more and more species that persist the drugs usage, on a rate that overcomes the

natural evolutionary adaptability. This speeded up raising is converting antibiotic resistance in a true crisis, which can lead to the re-emergence of harmful bacteria, that were once considered trivialized upon antibiotic use. [28][30]

There are distinct causes that contributed to the continuous escalation of this crisis. Besides antibiotic use lead to an inevitable resistance emergence, adding the fact of the drug not be considered a wise investment due to its commercial low cost and short need of time needed, the problem resides in the management of its use. The “cake” slices with higher impact in the thematic, are related to antibiotics overuse and misconception. These two factors played and still play the alarming role on the crisis emergence. It is natural to assume that the use of antibiotics contributes to its resistance, by eliminating certain bacteria and those who survive proliferate as result of natural selection, but when this use is uncontrolled, the resistance reaches critical levels [3][28]. Studies have shown high numbers of antibiotic prescriptions, much more than should be expected. There are also countries where does not exist boundaried regulations for antibiotic acquisition. On this topic, can also be inserted, antibiotic’s unappropriated prescription and consumption, being both causes interlinked. For instance, there are records of antibiotics being used to treat flues or colds. Studies have also shown that there still is an incorrect prescription of antibiotics even in developed countries. This is being caused by lack of awareness on the theme of antibiotic resistance and on when and how should antibiotics be used, by the general population and even between health professionals. Awareness propagandas are increasingly more visible, trying to teach and alert in which concerns the abuse and correct employment of antibiotics. [28][31][32]

The excessive use of the drug in agriculture, to avoid infections and support the corps growth, also contributes to the increased occurrence of this crisis. [33]

1.3.4 Staphylococcus aureus

Staphylococcus aureus (SA) is a Gram-positive bacteria type and is characterized by being round and spherical (cocci). SA is a species that belongs to the *staphylococci* group and is commonly found in the surrounding environment. Cataloged as a human pathogen, being the main responsible for several infections that end up compromising human health, can be also seen as part of the normal bacterial flora on the human species, colonizing without disease. [20][34]

Human normal flora containing SA, includes the skin and some mucous membranes, nevertheless when entering into the blood stream, can be the main agent taking responsibility for innumerous infections, for instance, urinary tract infections, gastroenteritis or meningitis, since produces a wide variety of virulence factors [20]. The symptoms caused by *S. aureus* depend on its mechanism of action, in which is able to block the host’s immune system, produce biofilms or antiphagocytic capsules to protect itself, among other. The production of capsules around the bacterium helps prevent the phagocytosis by macrophages and leukocytes. Different strains produce different toxins that can cause a myriad of disease from mild to life threatening. [35][36]

The normal course to treat Staphylococcus aureus infections is the use of penicillin, but from section 1.3.3 it was learned bacteria can evolve, adapt and resist antibiotic action, and the same happened with S. *aureus*. Methicillin-resistant *Staphylococcus aureus* (MRSA) is able to resist a wide range of antibiotic's action, it developed a resistance to methicillin due to a mutation occurred on a penicillin-binding protein allowing the bacteria not to bind to the drug [37]. This mutation was characterized by the addiction of thmecA gene sequence in S. *aureus* genes, that lowered the affinity of the organism connection to beta-lactam antibiotics, such as *penicillin* [38]. MRSA infections can cause meningitis, pneumonia, infections on the skin, infective endocarditis, among others, being a leading cause of infections acquired in a hospital environment. It is also associated to morbidity, mortality and high spent costs due to the rate of incidence,treatments and means use to identify the bacteria. [37]

This is the main reason why a good assessment of which is the causer agent of the infection or disease, is necessary to set. Besides the clinical and physical evaluation, analysis to blood and others samples from the patient, must be performed and the use of techniques that allow to identify the bacteria that induced the symptoms series. The entire assessment avoids costs and time spent on ineffective medicines, which can jeopardize even more the health of the infected.

1.3.5 Detect and Identify bacteria: State of the art

As mentioned, there are various organisms characterized as multi-drug resistant, having the ability to survive to antibiotics or other antibacterial drugs action, related to the emergent crisis of antibiotic resistance. Thus, a higher importance is given in trying to identify these organisms, to set the correct procedure, avoiding ineffective treatments that can be time and cost consuming. Nowadays, routine cultures are performed, from blood, sputum and urine. The samples are collected and cultured, allowing bacteria to growth and expressing their featured proteins. From that, a possible profile can be obtained in order to identify the pathogen/s present in the sample. Nevertheless, the need to culture the cells is a time burdening, considered an essential counter back in the patient's course treatment. This protein expression assembly is considered to be unique and thus, is in the middle of bacterial identification. The use of polymerase chain reaction (PCR) in order to amplify the DNA samples can also be used to identify a bacteria type and genus. Although it overcomes the time consumption issue from the cultured approaches, its sensitivity is not as ideal. Across this section is detailed phenotypical and genomically-based tests, that are used to achieve the goal of bacteria identification. [4][39][40]

Biochemical testing

From clinical samples, the culture can be performed using an agar-based media in order to support the pathogen's growth. Other culture medias can be used to attend certain bacteria needs and even antimicrobials can be added to eliminate the presence of commensal bacteria, that are not aimed to be identified. From the culture is possible to assess a wide range of features that allow its identification. The use of pH indicators to access the culture acidification after sugar had been provided; targeting specific enzymes that are part of the amino acid metabolism or even hydrolase enzymes.

Multiple kit tests are commercially available to perform different biochemical tests and these have a positive impact on the identification, on a couple of hours. This type of testing as the disadvantage of lack sensitivity. [39][40]

Chromogenic or Fluorogenic medias

Chromogenic or Fluorogenic medias can be used as a substrate to culture the samples in analysis. Upon the presence of specific expressed bacterial enzymes, it changes color or acquires fluorescence. This is a high specificity test, due to the fact that the used substrate needs to be specific to color in the enzyme's presence. It is a test performed when exists a suspicion of what is the pathogen that is trying to be identified. Can be used with antimicrobial selective drugs as well, to eliminate the presence of commensal bacterial or non-target ones. Is widely used to lower the options of the identification process, since it only will stain upon the expression of certain proteins that are specie's characteristic. These medias are commonly used in screening for multi-drug resistant bacteria, as the already mentioned MRSA or vancomycin-resistant *enterococci* (VRE). As the remaining cultured-based techniques, the use of methods that include these media types are also time consuming, due to the need of culturing the bacteria in order to have enzymatic expression. [39][40]

Fluorescence *In Situ* Hybridization

It works by allowing the detection of present genes of interest. It uses synthetic labeled probes of DNA or ribonucleic acid (RNA) with fluorescent dyes that intend to be complementary to what is being targeted. The Hybridization occurs if the probes indeed complement the target sequence. The dye works as signalization for the hybrid. This technique as challenges related to the small size of the sequences to be targeted. It has the disadvantages of being limited on sensitivity and specificity matters, adding the fact of being a time-consuming approach. [39][40]

PCR Techniques

PCR is an amplification technique that increases the detection ability of the target bacteria among others. Characterized as a genetic approach it is keen to detect one genome copy in a short period of time. PCR techniques are of relevance when looking for specific resistance mechanisms. Pointing out, on these approaches is inserted Quantitative real-time polymerase chain reaction (qPCR) and reverse transcriptase real-time PCR (RT-qPCR), a gold standard for gene expression analysis. Regarding qPCR, the amplified DNA is detected in real time throughout the reaction process using a DNA probe labeled with a fluorescent molecule performing a specific detection. If the intended detection is upon RNA evaluation, this molecule is set on a reverse transcription step, converting it into cDNA, before the sequence be amplified, characterizing the RT-qPCR technique, that besides detecting allows a sample quantification. Both methods rely on nucleic acid denaturation and polymerization. The probe acts like the complementary double stranded DNA to allow the detection. When using the correct probes, these two approaches are highly specific and sensitive in the matter of bacterial pathogens identification. [39][40]

Microarrays

A lab-on-a-chip multiplex approach, that analysis large amounts of probes to target multiple organisms using highly efficient screening methods. The detection of different organisms can be acquainted and resistance assessments can also be made in order to identify closely different species. It is a technique that has become widely used, existing different types of microarrays analysis. To the matter of pathogenic bacteria identification hereby referred, DNA, protein and antibodies microarrays, can be used. In this technology, multiple hybridizations assay are performed. Using a solid surface (array), the probes can be immobilized and afterwards incubated with complementary dyed strands of the intended target. Regarding DNA microarrays, the probes are characterized as being a single-stranded molecule of DNA or RNA, where their sequence is previously known. The molecule to be targeted is firstly amplified resourcing PCR technique. DNA microarrays have the advantageous capacity of being multiplex in the mean of diversified samples. Protein microarray approach is used with the attachment of proteins dyed labelled to the solid surface. This intends to detect protein activity from the bacterial pathogen and use this detection as means of identification. As for the antibody microarray, it acts on the same basis, but fixes the antibodies to perform an antigen detection. [40][41]

1.4 Microfluidics

Microfluidics is an emergent field that retracts the science behind the fabrication of small devices aiming to deal with fluids in a micro or nanoscale. Resourcing microfabrication, it is possible to mimic several procedures that are otherwise complex, time and material consuming. During the past years, Microtechnology has become increasingly appealing and scale miniaturization is being already used in many fields like mechanics, electronics, lab researches, to access food quality or in the emergent field of Medicine, and has a vast range of applications and flexibility in what is intend to be achieved.[5]

Being multifaceted, there was the need of Microtechnology to be qualified according to its aim. It was in the 1980s that the field of Microelectro-mechanical systems (MEMS) began to emerge, but only later, in the 1990s, medical, biological and even chemical applications took their place in the field. Through fluidic manipulation under artificial conditions, where there is a scaled down to the range of micrometers. Microfluidics studies "… flows that are simple or complex, mono- or multiphasic...", according to Patrick Tabeling, on the "Introduction to Microfluidics" published by Oxford Press. [42][43][44]

Microfluidics presents innumerous advantages that make its use suitable for a vast range of applications. Besides MEMS, there are also perks in the fields of electrical sensors and Lab on a chip technology. Through its use it is possible to have a restrict control in the consumption of reagents, samples and materials needed on those applications. Adding to low-cost fabrication, it should also be easier for the user in terms of employment and transportation. For analyses and assays, adds the advantage of low time consumption face other techniques [5][42][45]. Although the listed advantages, there is an important step on the choice of materials to be applied. Silicon is appealing due to its thermal

conductivity, giving the possibility of adapting this technology to already existent ones, on the semi-conductor industry. Glass in also on the table due to its optical transparency and to its surface be chemical imbalanced [46]. Nevertheless, there is a higher interest in the use of polymers and elastomers due to its savings in cost and fabrication time. One of these examples, to highlight, a very important material in the Microfluidic field is polydimethylsiloxane (PDMS), that when adding a curing agent is able to be transformed in an elastomer by applying a certain temperature allowing PDMS to polymerize. Other advantages that can substitute features appearing in several materials, are PDMS features in having optical transparence (wavelengths: 300-2200nm), in behaving as a thermal and electrical insulator and although being impermeable to water, this can be changed resourcing surface modifications. PDMS is also suitable to be fabricated with integration of pumps and valves, one of the highlights of the Microfluidic field. [47][48]

1.4.1 Microfabrication[1]

The fabrication of a miniaturized device can be described in several steps but there are also several approaches that can be used as fabrication methods. During the development of this project the focus goes to photolithography and soft-lithography. Photolithography technique results in a hard-mask that can be used as a reusable mold to perform the soft-lithography technique and fabricate multiple PDMS structures. The hard-mask used in the course of this project was already available from the project developed by Doctor Inês Iria, and so, it is only explained the steps of the technique used.

The first point of action in a hard mask fabrication is to create a bi-dimensional design of the microfluidic structure using an appropriate software (e.g. Auto-CAD). In it, the main features for the structure dimension are established. Follows the mask fabrication, were glass substrates are washed accordingly and dried with compressed air. An aluminum layer is deposited on the substrate by a sputtering technique, followed by spin-coating of a positive photoresist. Using direct write laser (DWL) lithography equipment, the design performed on the software is transferred onto the photoresist layer that after exposure is soluble and can be washed out through a developer solution. Removing the design sections of the photoresist, exposes the aluminum layer that can be etched, which leads to its pealing, creating the mask with the desired dimensional features. (Figure 1.3) Although the mask has the appearance of the structures created on the software, in order to perform a soft-lithography technique achieving the same conditions, is necessary to fabricate a mold from the hard-mask to be engraved on the PDMS structure. Using a cleaned silicon substrate, a negative photoresist is spin-coated on it, followed by a pre-exposure baking. The initial fabricated hard-mask is then placed, facing-down, on top of the silicon substrate and an exposure is performed, resourcing Ultra-violet (UV) light. After baking the exposed substrate, a development, using a Propylene glycol methyl ether acetate (PGMEA) solution, allows the exposure of the regions non-affected by the UV light, creating a master mold (SU-8 mold) that will allows the design structure to be engraved on the PDMS fabrication process. (Figure 1.4)

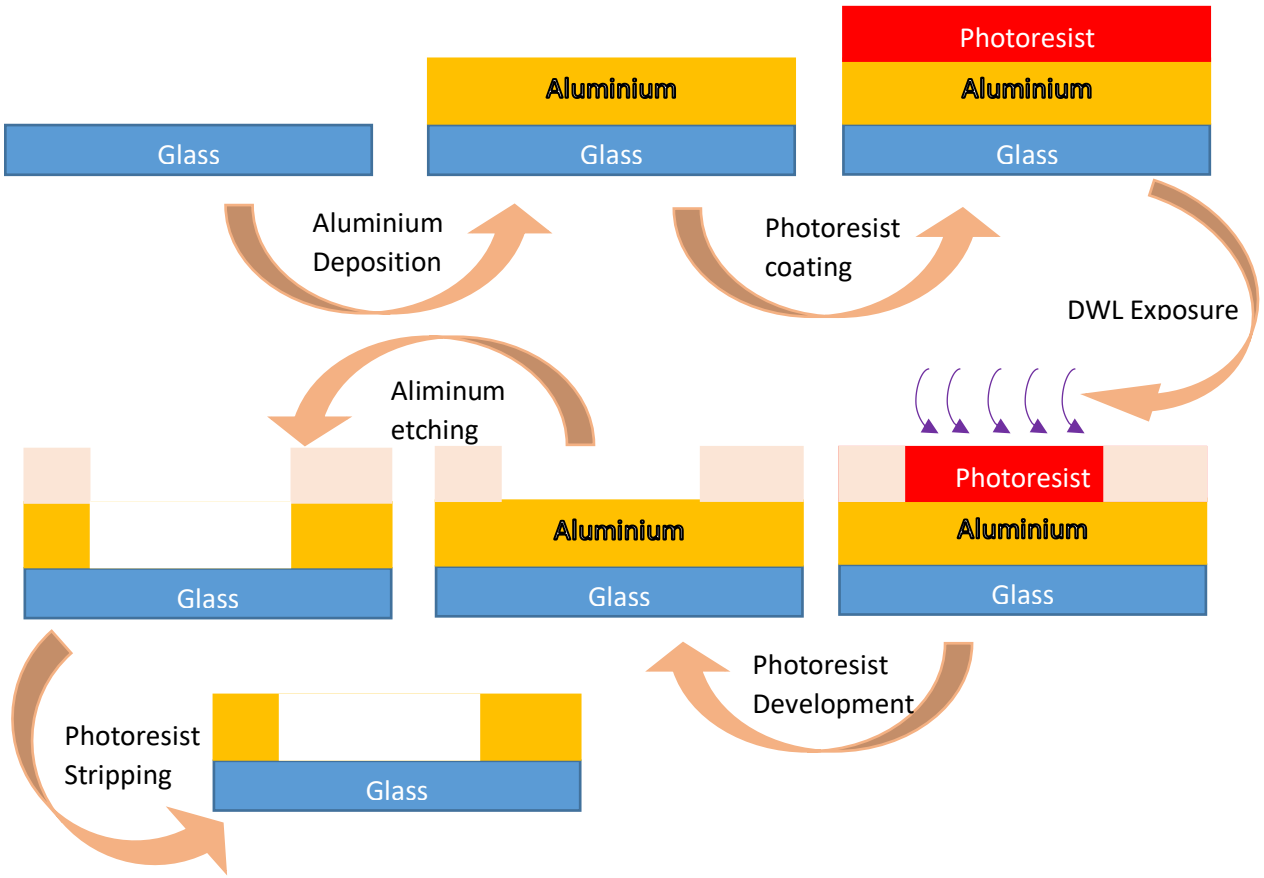

Figure 1.3 Schematic of the Hard mask fabrication. Dimentions not at scale.

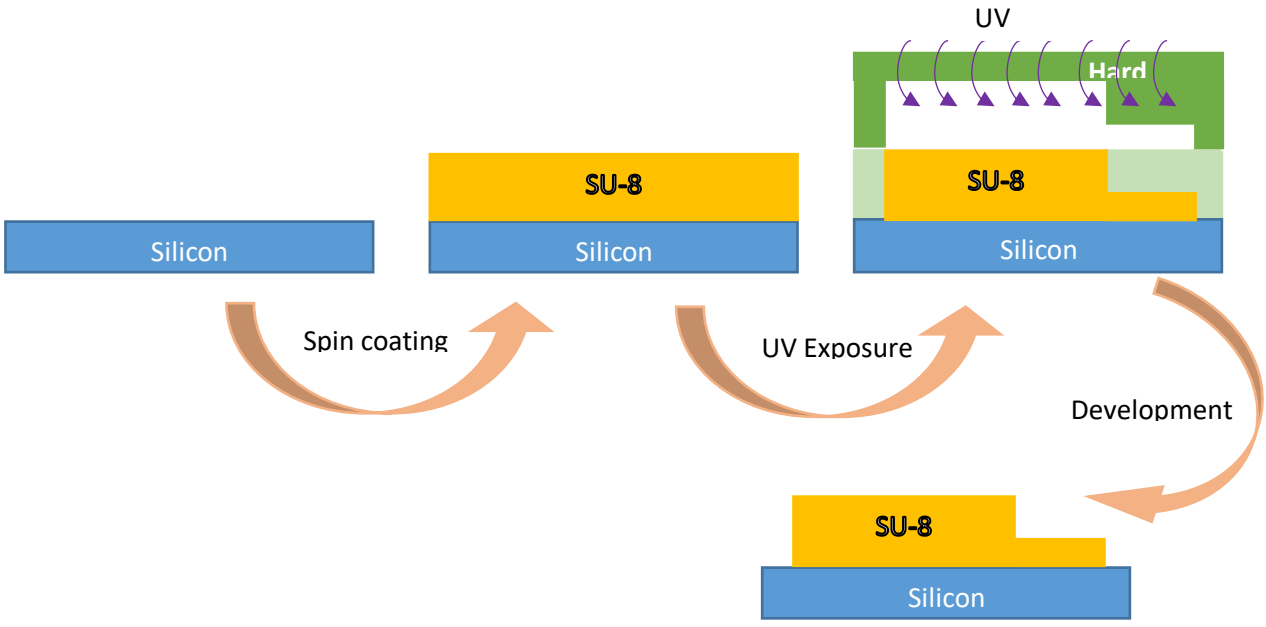

Figure 1.4 SU-8 mold fabrication. Dimentions not at scale.

Regarding the soft-lithography technique, the PDMS prototyping is addressed on section 2.1 and detailed on a closer look. Nevertheless, PDMS when mixed with a curing agent and heated up to a

temperature of 70ºC, transforms into an elastomer, as already mentioned. Using the mixture in the SU-8 master mold, will allow the engraving of the structures on the PDMS that hardens with the temperature treatment.

1' The content displayed on this section was based on information obtained in INESC-MN facilities and by observing the techniques being performed.

1.4.2 Microfluidics in Bacterial detection

Microfluidic devices are becoming popular in distinct themes, like experimental cellular biology, where is inserted the thematic of this project development [49]. In this section are specified microfluidic applications addressed to the topic of bacterial detection. Although being a relatively new field of research and clinical applications, the truth is microfluidics devices are exponentially being inserted in what concerns medical diagnostics, targeting single diseases or pathogens detection [50]. Nevertheless, the efforts point out a future use of these devices to perform a multiplex system in screening and detection. Bacterial detection is one of the aimed approaches, given the rising rates of infections and infectious diseases incidence, not excluding the exponential crises of antibiotic resistance. As stated on section 1.3.5, conventional diagnostic methods, are costly and time consuming, adding to the fact that the majority relies on amplification approaches.

Current techniques in the field of microfluidics, base their detection into two distinct methods. Detection by immune-sensing, where a probe acts to target a specific molecule characteristic of a certain bacteria. In this case a probe can be selected and can be used to perform the bound antibody-antigen or aptamer-target. Another method is based on the detection resourcing nucleic-acid identification, other specific type of targets. Nevertheless, both methods are approaches that work as a bacterial detection-based sensor, which resource specific targets exclusive from what is intended to be detect [51]. The use of probes, such as antibodies or aptamers as an agent of detection can also be used as means of capture and immobilization of the intend target, creating a "sandwich" ('capture molecule'-'target'-'detection molecule'), like the known ELISA approach. Regarding mechanisms to perform the detection, there is a vast range that included optical, electrical or electro-chemical impedance, cantilever, quartz crystalline microbalance,surface plasmon resonance (SPR), and magnetoresistivity, in means of the immune-sensing and resource to PCR or RT-PCR can be used if the intention is the amplification of target nucleotides, increasing the signal to detect [52]. The use of fluorescence probes is shown to be very appealing due to the high specificity, which can be performed adding the promising sensibility of these methods [53]. Xiang et al. reported a microfluidic system for detection of *Escherichia coli* using laser-optical fiber fluorescence detection and Meagher et al. detailed an integrated microfluidic platform fluorescence-based detection of Shiga toxin I (*Shigella dysenteriae*) and Staphylococcal enterotoxin B (*Staphylococcus aureus*) [54]. Electrical-based methods of detection are also appealing in what concerns ease-to-fabricate features, for instance Boehm et al. elucidates the presence of *Escherichia coli* in suspension by measuring its impedance [51]. Innovative new approaches are also keen to

emerge. Terekhov et al. combined the use of a droplet system with FACS detection technique to develop a single-cell activity selection in the matter of cell screening, common to a “Single-cell microscopy of suspension cultures using a microfluidics-assisted cell screening platform”, reported by Okumus et al. [55][56]. Figure 1.5 displays a summarized list of bacterial detection methods on microfluidics.

Analyte	Detection method	Material	Limit of detection
Escherichia coli O157:H7	Fluorescence	PDMS	0.3 ng/μL
Escherichia coli O157:H7	Fluorescence	PDMS	0.02 μg/mL
Helicobacter pylori	Fluorescence	PDMS	0.1 μg/mL
Shiga toxin I	Fluorescence	Glass	500 pM
Staphylococcal enterotoxin B	Fluorescence	Glass	300 pM
Escherichia coli	Electrical (impedance)	Silicon	10^4 CFU/mL
Escherichia coli, *Proteus mirabilis*, *Pseudomonas aeruginosa*, Enterococococcus spp., and the Klebsiella–Enterobacter group	Electrochemical (amperometric)	Au on plastic	Not specified
Plasmodium falciparum	Optical	Mylar/PMMA	10 ng/mL

Figure 1.5 Summarized list of bacterial detection methods on microfluidics. Adapted from the literature [51]

Some approaches of the development of this project were based on Yi-Chung C. et al. that reported a “Rapid single cell detection of Staphylococcus aureus by aptamer-conjugated gold nanoparticles.” [66]

1.5 Antibodies and Aptamers

Antibodies

Antibodies (Abs) are molecules that belong to a family of globular proteins, nominated immunoglobins considered heterodimeric proteins. This class is characterized by having two chain pairs, heavy and light and can also be divided and classified into different domains, variable and constant. Antibodies naturally belong to the Human’s immune system and act as a defense against pathogenic agents. These proteins type are characterized by having a Y shape that acts as an advantage to be used as a detection mechanism. Its variable domain can recognize and bind to specific proteins present in the pathogens surface membrane, called antigens a domain composed by different amino acids (a.a.). Since the Human body as a wide range of a.a., the number of possible variable domain sequences is extremely high. Complementary determining regions that highly vary and four framework regions (Fc) yet characterize this domain. The complementary regions are present on the heavy chain and bind to other complementary regions from the light chain, creating the antigen-binding site (Fab). Regarding the constant domain, it specifies effector functions upon the Abs bound, once are characterized as a secreted adaptation of B-cells receptors, but differ on having this hydrophilic sequence able to perform

secretion. On heavy chains, the constant regions can be distinguished by classes: IgM, IgA, IgG, IgD and IgE. The last three are considered monomers, but IgA is a dimer and IgM a pentamer. Since constant domains of the heavy chain are variable, antibodies can allow to vary in its effector function without changing antigen specificity and the contrary effect is also possible to be observed. (Figure 1.6) [57][58][59][60]

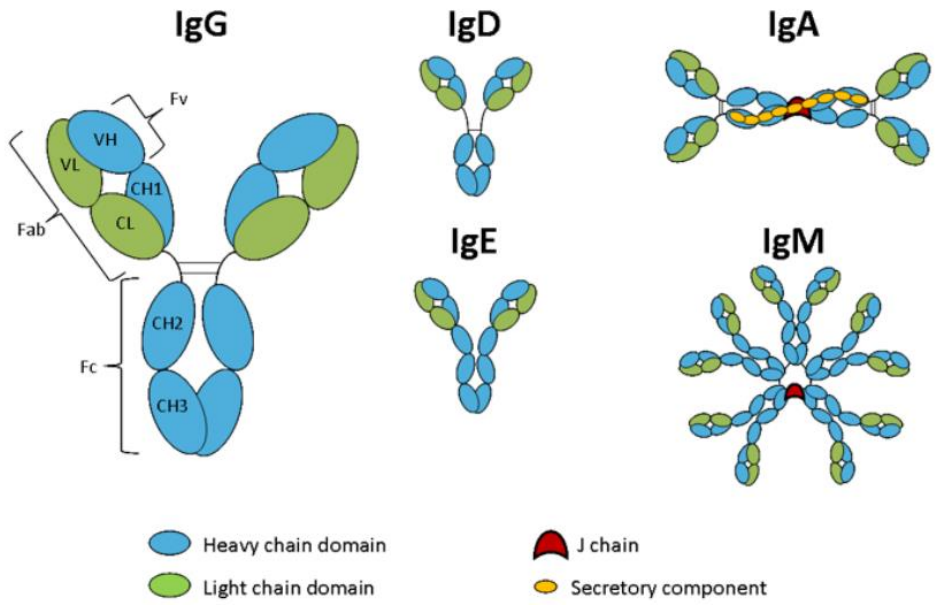

Figure 1.6 Immunoglobins structural features and different classes. Adapted from the literature. [58]

Regarding IgG, it can be divided into IgG1-4 subclasses and is considered the antibody with the highest abundance in the human body, being an attractive protein to be used on therapeutic approaches [59]. Besides this advantage, antibodies can also be used in capture and detection assays of pathogenic agents, such as cells or even toxins and thus, are considered to have an increasingly interest in the thematic addressed in the development of this project.

Aptamers

Aptamers are sequences of nucleotides, that are able to target specific molecules and can be considered as single or double strands of DNA or RNA. Aptamers are part of a new approach in the therapeutic field, where nucleotides are used as functioning not only to store genetic information but also as enzymatic catalysis or even to bind to other molecules, proteins and cells acting similarly featured to the antibody-antigen interaction [58]. Thus, are passible to be used as to replace antibody's functions on the therapeutic field, overcoming some of the challenges that are being faced, and also, used as mean to capture and detect pathogenic agents. Aptamers also have a high specificity to its target, which due to their three-dimensional structure perform the bound resourcing non-covalent interactions. This referred structure is not equated to RNA or DNA, is another stable conformation that

nucleotides can accomplish, nominated G-quadruplex. The final appearance of this secondary structure is dependent of the nucleotide sequence, and thus various complexes can be formed. Upon folding, aptamer's three dimensional structure creates a specific conformation that promotes a ligand also specific binding. The created complex is based on non-covalent interactions, which rely on the base sequence and the spatial arrangement of those nucleotides. Regarding the targeting, aptamers are selected using the SELEX method that synthesizes random sequences of oligonucleotides and the target molecule, cell or protein is added to the sum of those sequences. After an incubation period, the bound sequences can be separated from the remaining and a PCR is performed for the nucleotide sequences, which are double stranded at that point. After the first round, multiple cycles are performed to acquire higher specificity, after denaturing the sequences in the beginning of each cycle, where the target molecule can be used in lower concentrations to attend the goal of specificity. It is important to point out, that the initial sequences are randomized and so, the final aptamer achieved can have higher binding affinities if certain modifications are set, changing the sequence, but since the modification sequence was not in the initial pool, the resultant aptamer differed .[58][61][62]

1.5.1 *Head to head:* Advantages and Disadvantages

Table 1.2 details advantages and disadvantages of both antibodies and aptamers elucidating, which should the preferable choice regarding that propriety. As is possible to observe, aptamers are highly advantageous regarding an innumerous range of characteristics. Although having less affinity to targets, studies have shown that aptamers are prone to be keen to high affinity as well and thus, aptamers were the chosen and acquired molecule in order to develop this project.

Table 1.2 Advantages and disadvantages of using Antibodies and Aptamers.[58][62][63]

Property	Antibody	Aptamer	Advantageous for - Observation
Development time	~4 to 6 months	~1 to 3 months	Aptamer
Acquisition process	Can only be produced against a target that provokes an immune system in the initial animal model. Need to be humanized antibodies to suppress the immunological response.	Acquisition using a sequence library through SELEX process. Chemical synthesis.	Aptamer – Aptamer Is synthetized in Vitro and can be selected against non-immunogenic compounds.
Toxicity	May induce an immune response in the body due to the presence of Fc region.	Higher tendency to be non-toxic and non-immunogenic.	Aptamer – Antibodies need to be humanized antibodies

			to suppress the immunological response
Stability	Prone to temperatures and pH changes; If denatured the process is irreversible	Can be used in non-physiological means. If denatured the process is reversible	Aptamer
Modifications	Typically conjugated with one detection molecule	Easy to be modified. Different molecules can be added.	Aptamer
Cost	More expensive	Less expensive	Aptamer
Production	Hard to perform large scale production	Chemical acquisition allows large scale production	Aptamer – Antibodies are difficult to maintain homogeneity from batch-to-batch. Tests are necessary for each batch in therapeutics
Affinity	High affinity to targets	Affinity depends on the SELEX process	Antibodies
Specificity	Highly specific	Less specific	Antibodies – Have a higher specificity to its target. Aptamers are randomized oligosequences.

1.6 Objectives: Project development

The objective of this project is the development of a microfluidic device capable of direct capture and detect bacterial cells from the bacterium model *Staphylococcus aureus* (SA) resourcing microbeads to increase the immobilization area. The capture aims to function due to the integration on the used beads, in the microfluidic chip, of labeled aptamers that in other approach are used as a detection tool together with fluorescence and imaging techniques.

Chapter 2

Materials and Methods

This chapter focuses in describing the entire set of materials and methods used along the project development. The protocols followed on the performed assays and the techniques for the microfabrication processes are here to be present. Figure 2.1 describes how Chapter 2 is organized, being also representative of the active workflow performed, that goes from a structure fabrication until the assay results analysis.

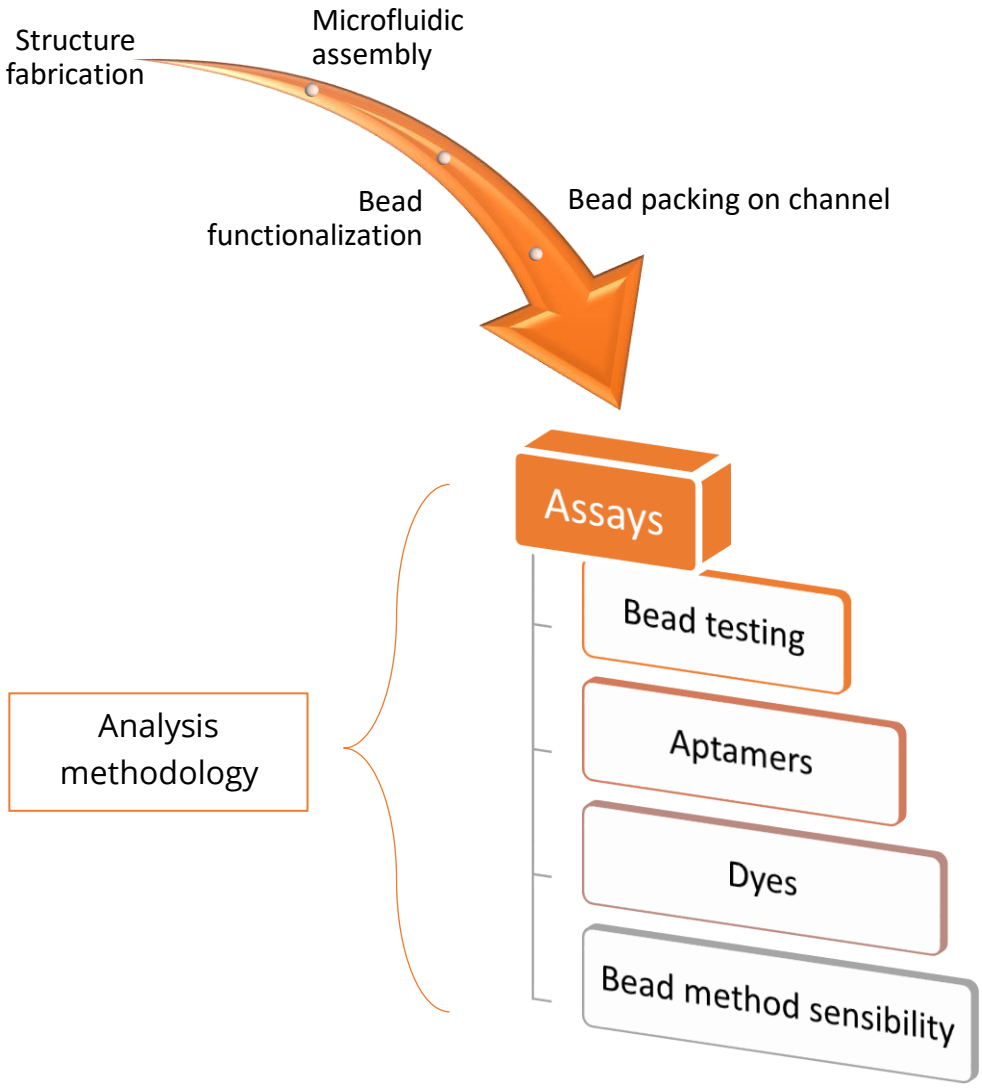

Figure 2.1 Schematic of Chapter 2 layout and representation of the technical workflow.

2.1 Microfabrication: Soft Lithography

Along this section, it will be described the steps that involve the fabrication of the Polydimethylsiloxane (PDMS) structures by a soft lithography technique. In order to perform these structures, it was used a mold with simple columns engraved on it. The mold was already available for usage, so the theoretical fabrication process of the technique is described on section 1.4.1. Although, the hard-mask and master mold fabrication were not performed during the course of the development of this work, the concepts behind the techniques are important to understand how the final structure is achieved. Nevertheless, the information regarding the entire process was acquired by observing PhD-student Pedro Monteiro during the fabrication of SU-8 mold, who explained the described process. The steps to fabricate this mold, used in the project development are here elucidated, although simplified (Figure 2.2).

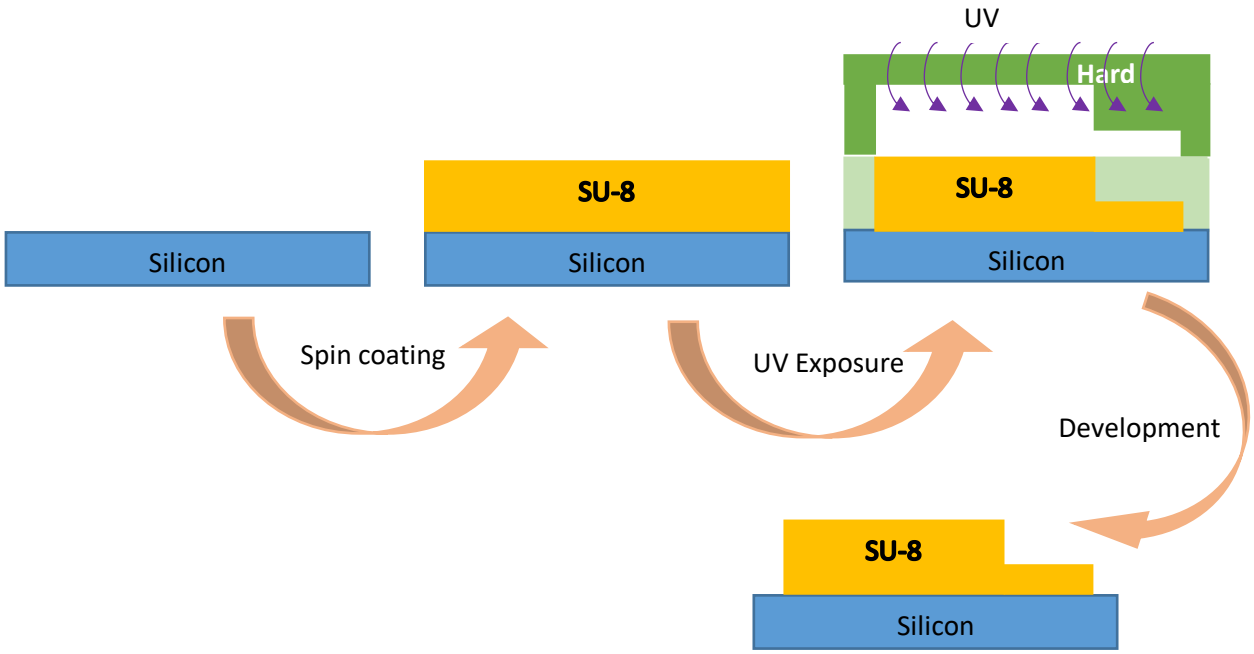

Figure 2.2 Simplified schematic of the SU-8 mold fabrication. Dimentions not at scale.

It is from the point, illustrated on, that was possible to fabricate the used work structure resourcing Soft Lithography techniques. The complete and prior fabrication to the SU-8 mold refers that different mold layers (SU-8 or hard mask) need to be performed sequentially. For instance, in the case here illustrated, the spin coating, UV exposure and development processes, were needed to be done twice in order to have the intended last design, inasmuch as there is two layers with distinct heights (Figure 2.3).

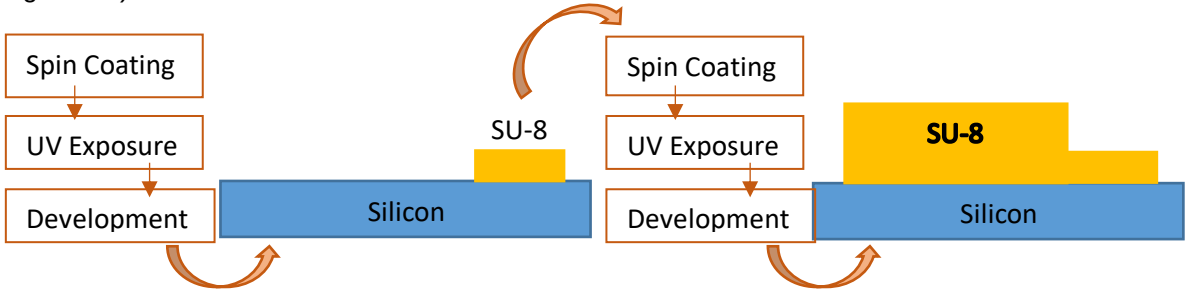

Figure 2.3 Two round process related to the SU-8 mold fabrication. Dimentions not at scale.

2.1.1 Reagents, Materials and Equipment

Table 2.1 Details of the components used in the perfomed microfabrication processes. Blue section: reagents; Orange section: materials; Pink Section: equipment

Name and features	Abbreviation	Purchase details
Polydimethylsiloxane	PDMS	Sylgard 184 silicon elastomer kit (Dow Corning)
Curing agent	-	Sylgard 184 silicon elastomer kit (Dow Corning)
Silicon wafer - 150 mm diameter	-	University Wafer (South Boston, MA/USA)
17 Gauge Rounded syringes tips	17Ga	Instech Laboratories, Inc. (Plymouth Meeting, PA/USA)
20 Gauge Rounded syringes tips	20Ga	Instech Laboratories, Inc. (Plymouth Meeting, PA/USA)
Expanded oxygen plasma cleaner PDC-002-CE	-	Harrick Plasma (Ithaca, NY/USA)
Oven loading model 100-800	-	Memmert (Schwabach, DE)
Spin coater	-	Laurel Corp. (North Wales, PA/USA)
Vacuum desiccator	-	Bel-Art Products (South Wayre, NJ/USA)

2.1.2 Protocol

To fabricate the elastomer it was necessary to mix the PDMS base and the curing agent from the elastomer kit, on a ratio of 10:1. The mixture should have an opaque white color with a bubbly consistence. Ready to be gazed-out, the mixture was left on the Vacuum desiccator during 45 minutes. The pre-polymer was then ready to cured and should be poured in the Petry dish that had the SU8 mold, already available, that contained the columns were the assays were to be performed. An extra attention should be taken into consideration, of not leaving bubbles on the PDMS mixture, which can appear due to the pouring action. Next, the Petry dish was left in the oven, during 90 minutes at an average temperature of 70ºC. Cured, the PDMS structure was cut down and the inlets and outlets were open

with different size needles. For the inlet, 20Ga syringe tips were used and for the outlet, 17Ga ones. With the performed holes, it was possible to flow solutions inside the column, so, the remaining step was to seal the channels.

The structure was sealed against a 500 µm PDMS membrane, where the pre-polymer preparation was proceeded equally as above. Once having it, the mixture was poured onto a silicon wafer and spin coated at 250 rpm during 25 seconds. This is the suitable program to achieve the desired thickness. The PDMS was then ready to be cured and the wafer was left on the oven, during 90 minutes at 70ºC, previously identical. From the wafer, several membranes could be cut down with shape and size able to cover the fabricated structure.

To seal the structure against the membrane, both needed to be oxidize, which was possible to achieve with the use of a plasma cleaner during 60 seconds at medium power. After the removal from the equipment, the structure was placed on the membrane and Si-O-Si covalent bonds were created. The plasma treatment allowed the sealing and it marked the end of the fabrication process. It is of relevance to point out that on this stage, the remaining surface of the PDMS is yet oxidized, and a rest period of 24 hours should be regarded before the structure use. (Figure 2.4 and 2.5)

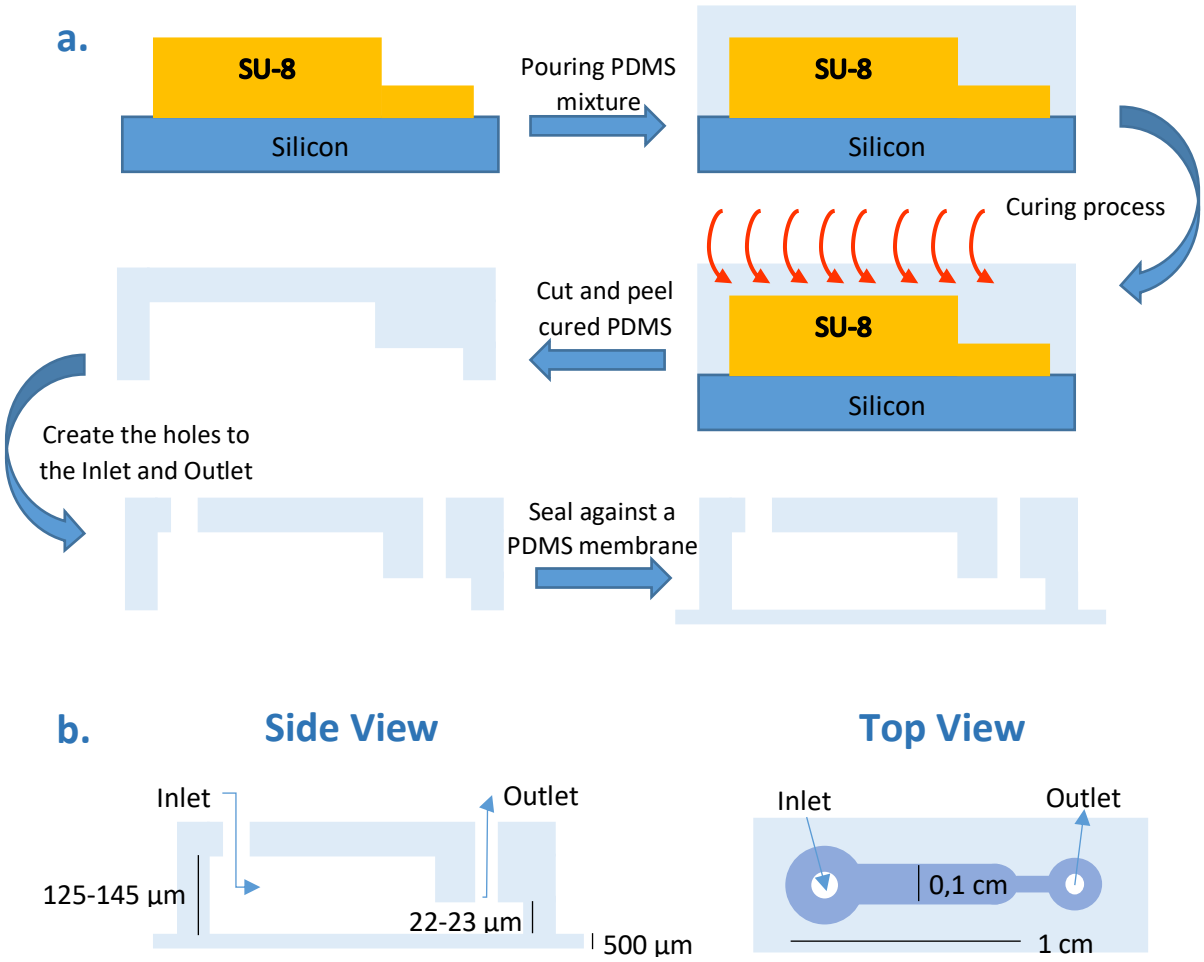

Figure 2.4 a. Schematic of the Soft Lithography technique fabrication: PDMS structure. b. Side and top view of the final design with the channel dimentions. Dimentions not at scale.

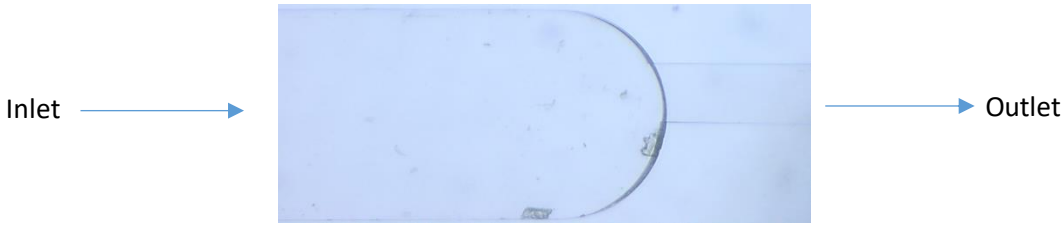

Figure 2.5 Experimental image from the PDMS channel.

2.2 Microfluidic handling

2.2.1 Reagents, Materials and Equipment

Table 2.2 Details on the components used on the microfluic handling. Blue section: reagents; Orange section: materials; Pink Section: equipment

Name and features	Abbreviation	Purchase details
Milli Q water	-	18 MΩ CM, Millipore
PDMS structure	-	Fabricated at INESC-MN
90 Polyethylene tubing	90 Tube	BTPE-90, Instech Laboratories, Inc. (Plymouth Meeting, PA/USA)
Metallic adaptors	-	SC20/15, Instech Laboratories, Inc. (Plymouth Meeting, PA/USA)
Insulin Syringe – 1mL	-	U-100 Luer-Lock, Codan (Lensahn, DE)
20 Gauge Rounded syringes tips	20Ga	Instech Laboratories, Inc. (Plymouth Meeting, PA/USA)
Microscope Color Camera	-	CCD color camera XC30, Olympus (Shinjuku, Tokyo, JP)
Fluorescence Microscope	Olympus	Inverted Fluorescence Microscope CKX41, Olympus (Shinjuku, Tokyo, JP)
Pumping System	-	4000 microsyringe pum, New Era Pump Systems, Inc. (Farmingdale, NY/USA)

2.2.2 Microfluidic preparation

Assembling all that was needed to perform an assay in a microfluidic device, passed through creating a circuit to allow the fluid flow. To attend that, 1mL insulin syringes were filled with Milli-Q water and fixed on the pumping system. This system allows to push or to pull the solution inside the column, creating, respectively, a positive or negative pressure on it. For the assays that were performed, only the pulling option was required and that is the reason why Milli-Q water was used in the syringes, as it never got inside the microfluidic structure. 20Ga syringe tip were the syringe tips used, connected to the syringes itself and to the 90 Polyethylene tubing, that continued the assembling process. On the 90-

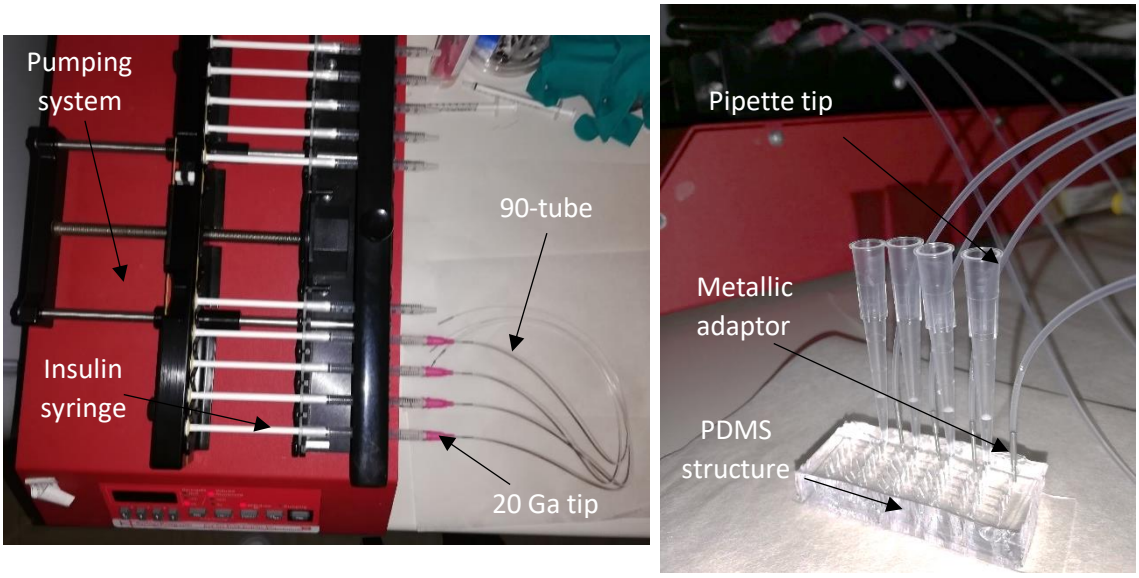

Figure 2.6 Microfluidic assembly with used components .

tube free end, metallic adaptors, suitable for microfluidic handling, were attached. These adaptors were what was going to connect the described pumping system to the microfluidic structure, fabricated according section 2.1, by means of its insertion on the outlet of the channel. On the inlet, a pipette tip is placed, that should contain the desired solution to flow. (Figure 2.6)

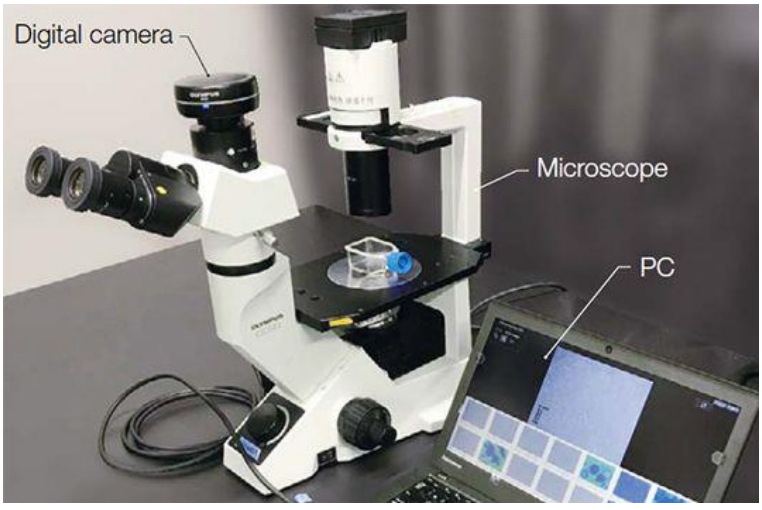

Figure 2.7 Inverted Fluorescence Microscope CKX41 incorporated with a color digital camera. Image adapted from the website company. [64]

For the assay measurements, Olympus microscope was used to capture the images to allow its signal analysis. The microscope has a color digital camera incorporated suitable for bright field acquisition and has the necessary functions to acquire fluorescent signals, both needed in the development of the project. (Figure 2.7)

2.3 Beads

Table 2.3 Details on the components used on the Beads handling. Blue section: reagents; Pink Section: equipment

Name and features	Abbreviation	Purchase details
Phosphate buffered saline	PBS	P4417, Sigma-Aldrich, (USA)
Polyethylene glycol 8000	PEG 8000	8000 MW, Sigma-Aldrich (USA)
Absolut Ethanol	-	Sigma-Aldrich, (USA)
Ethanol 96%	-	Sigma-Aldrich, (USA)
Trisaminomethane Hydrochloride	Tris-HCL	Sigma-Aldrich, (USA)
Hydrochloric acid	HCL	Sigma-Aldrich, (USA)
Biotin, fluorescein isothiocyanate conjugate	Biotin-FITC	Sigma-Aldrich, (USA)
Streptavidin	-	S476, Sigma-Aldrich, (USA)
Streptavidin, fluorescein isothiocyanate conjugate	Strep -FITC	Thermo Fisher
Microfluidic Pumping System	-	Assembly on 2.2.2 section
Microscope Color Camera	-	CCD color camera XC30, Olympus (Shinjuku, Tokyo, JP)

2.3.1 Reagents, Materials and Equipment

Table 2.4 Beads and details used in the entire project development.

Name and features	Abbreviation	Purchase details
NHS-Sepharose® Beads ~ 90 µm	-	NHS-activated Sepharose Fast Flow Beads, GE Healthcare
Q-Sepharose® Beads ~ 90 µm	-	Q-Sepharose Fast Flow Beads, 17051001, GE Healthcare
Spherical silica® beads 45-75 µm	SiO_2 beads	Spherical flash silica beads, 97728-U Supelco Analytical (Bellefonte, PA)
Spherical $\boldsymbol{C_{18}}$ silica® beads 45-75 µm	C_{18} beads	Spherical C_{18} bonded flash silica, 97727-U Supelco Analytical (Bellefonte, PA)
Spherical $\boldsymbol{NH_2}$ silica beads 45 - 75 µm	NH_2 beads	Spherical silica® beads modified and available at INESC-MN
Phenyl Sepharose® beads ~ 90 µm	-	Phenyl Sepharose® Fast Flow beads, GE Healthcare

From the purchased material, the different beads stocks have their own treatment and storage in order to be possible to handle on the microfluidic device. Commercially beads are supplied in an ethanol solution or on form of dry stock solutions, according to its characteristics. NHS-Sepharose®, Q-Sepharose® and Spherical silica® beads were prepared in a stock solution of 20% ethanol being necessary to vortex that solution to allow its homogeneity. Afterwards, a specific volume of that stock was added to a PEG 8000 20% solution in a proportion of 1:4, as working concentration. Spherical C_{18} silica beads solution was already available, nevertheless, its preparation protocol differs due to their high hydrophobicity. That solution was achieved by weight 10 mg of the dry stock solution and add 600 µL of PEG 20% and 2 µL of Triton X-100, followed by vortexing the mixture several times until the solution becomes homogeneous. Spherical NH_2 silica beads solution was also already available and from that stock, a dilution of 1:4 was performed with a PEG 8000 20% solution. NH_2 silica beads were obtained by functionalizing Spherical silica® beads resulting in a positively charged surface.

2.3.2 NHS-Sepharose® Beads conjugation with streptavidin

It is of relevance to mention that this protocol was based on common Succinimidyl Ester (NHS Ester) flurophores kit protocols and the changes applied to it were due to the optimization performed by PhD-student Catarina Caneira, that was assisting and supervising the conjugation procedure.

To prepare 100 µL of streptavidin functionalized NHS-Sepharose® Beads, 300 µL of absolute Ethanol were added to 200 µL of the beads storage. After the flushing by pipette action and a rough centrifugation followed a 450 rpm centrifugation during 10 minutes, aiming to sediment the beads and remove the supernatant. To perform the conjugation, it was necessary to activate the NHS groups with HCL at 4ºC, 15x the Beads volume (1500 µL). A new centrifugation and supernatant removal were performed and at this stage, it was added what was intended to bind on a 1:1 ratio.

100 µL of 1mg/mL streptavidin were added to the concentrated beads and the solution was incubated during 3 hours at 750 rpm velocity agitation. After this period, it was necessary to block the groups that were not functionalized but remained active. Aiming that, the solution was centrifuged, the supernatant removed, 0.1 molar of tris-HCL was added, 10x the beads volume (1000 µL) and kept in the same agitation conditions for 2 hours.

The final approach was to perform washing steps, alternating between a pH basic and a pH acid solutions, which is described on Figure 2.8.

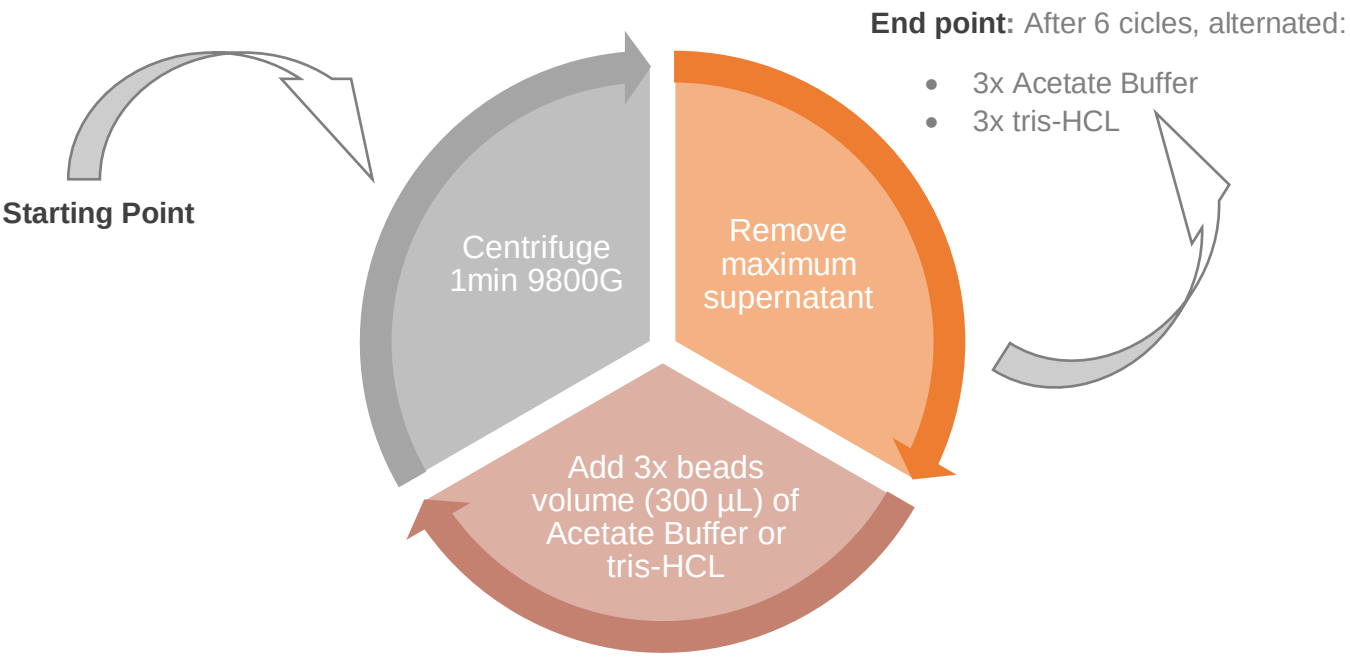

Figure 2.8 Schematic of the washing steps cycle necessary to perform in order to block the activated groups that were not functionalized.

After the washing steps, 100 µL of 20% Ethanol was added to the NHS-Sepharose®, conjugated streptavidin beads and storaged at 4ºC.

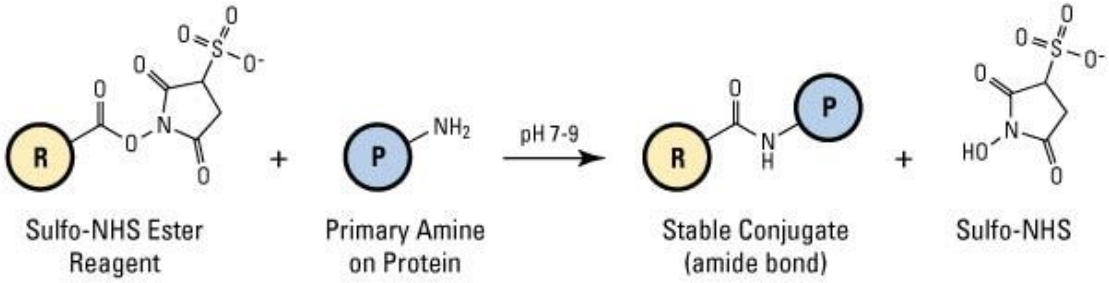

Figure 2.9 Addition of an Ester to a Protein. Adapted from the literature. [65]

This conjugation is a variant of the reaction type showed on Figure 2.9 that traduces the bound of an ester and a protein.

2.3.3 Beads packing

In the present work, beads were packed using the pulling option of the pumping system. With this method, the beads solution was placed on the inlet of the microfluidic channel, resourcing a pipette tip. In the entire project development, a volume of 20 µL of beads solution, was used, regardless the bead type that was intended to pack. Although the volume was kept constant, the dilution and medium was independent for each type, which is related to their characteristics. (Table 2.5)

Table 2.5 Bead individual preparation from each stock.

Bead Type	Bead medium stock	Dilution from stock	Washing step
SiO_2	20% Ethanol	6 µL+14 µL PEG	20 µL PBS
C_{18}	PEG 20%	3 µL + 17 µL PEG	20 µL PBS
Q-Sepharose®	20% Ethanol	3 µL + 17 µL PEG	20 µL PBS
NHS-Sepharose®	20% Ethanol	5 µL + 15 µL PEG	20 µL PBS
NH_2	20% Ethanol	5 µL + 15 µL PEG	20 µL PBS
Phenyl Sepharose	PEG 20%	5 µL + 15 µL PEG	20 µL PBS

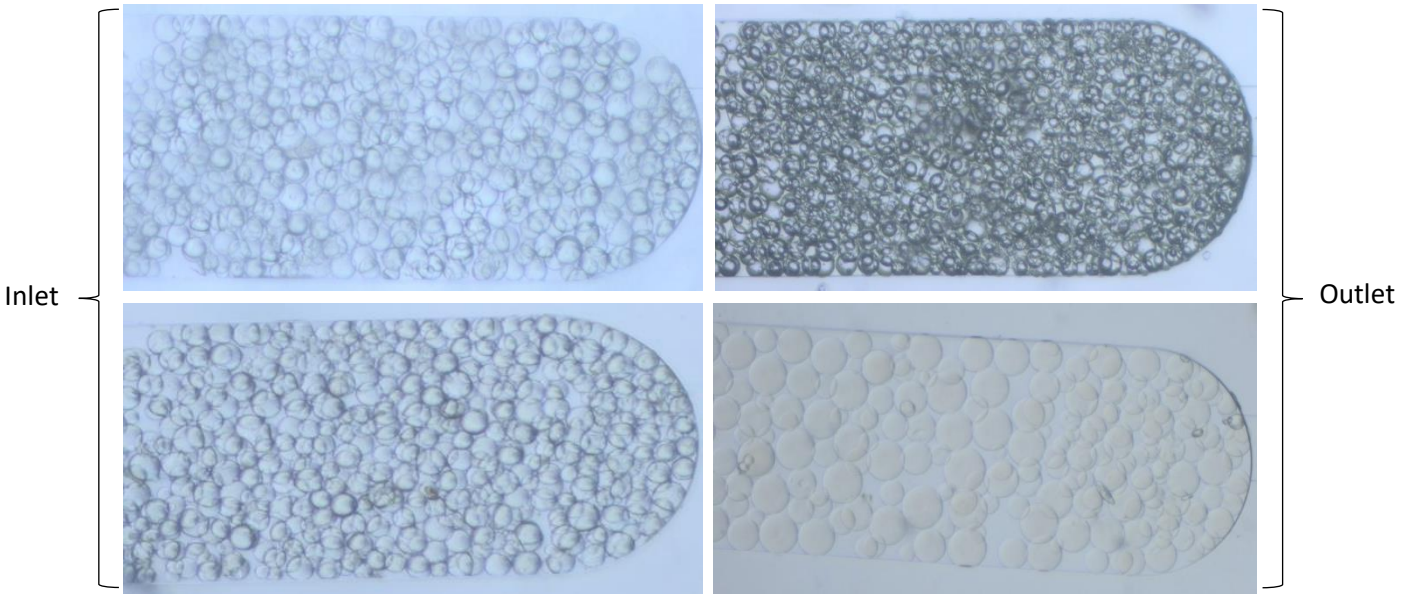

Figure 2.10 Packed beads on column. Top Left: Spherical silica® beads Top Right: Spherical C_{18} Silica®; Bottom Left: Spherical NH_2 silica® beads; Bottom Right: Phenyl Sepharose® beads.. All the experimental images were acquired in Olympus Microscope CHX41, exposure time: 50ms, gain: 0 dB, magnification:10x.

Within the different beads, the packing protocol had always the same features. The pumping system was set to pull at 5.5 µL/min flow rate, during approximately, 3 minutes, allowing keep a volume margin to avoid air entering the column. Regarding the washing step, 20 µL of PBS were flowed with the same features as the packing process. Figure 2.10 displays an example of four packed bead types.

2.4 *Staphylococcus aureus* assays

In this section is described the protocol assays that used a *Staphylococcus aureus* solution. For each method, are elucidated, the used solution features, as initial OD stock concentration, working concentration and the different materials and reagents. The solutions were provided by PhD student Catarina Caneira, that grow the bacterium in Laboratório de Análises facility from Instituto Superior Técnico, Lisbon University.

2.4.1 Test on Beads assay

Name and features	Abbreviation	Purchase details and features
Staphylococcus aureus stock solution	SA solution	0.20 OD ~ $1.6 * 10^8$ cells/mL
Phosphate buffered saline	PBS	P4417, Sigma-Aldrich, (USA)
Microfluidic Pumping System	-	Assembly on 2.2.2 section
Microscope Color Camera	-	CCD color camera XC30, Olympus (Shinjuku, Tokyo, JP)

Table 2.6 Details on the material used in the test on beads assay. Blue section: Reagents; Pink section: Equipment

After the bead type, aimed to test, had been packed in the column, the SA stock solution was concentrated in order to work with a 10 OD (~ $8 * 10^9$ cells/mL) solution. To achieve this high concentration, five Eppendorfs® were filled with 1000 µL of SA's stock, and centrifuge at a 9800G's speed during 10 minutes. After this process, the supernatant was removed from four of the Eppendorfs® and a 930 µL volume from the last. The process continued by flushing that volume across the five tubes to collect the pellets on the bottom of each Eppendorf®. On the last one, it was added PBS until it reached a 100 µL volume. This way, the stock solution was concentrated 5x first and 10x then, to achieved the desired 10 OD solution.

Ready, the SA solution was flowed through the column at 2.5 µL/min during 20 minutes and visual acquisition was achieved using Olympus microscope Color camera, at minutes 0, 10 and 20 of the assay.

2.4.2 Aptamers – SA61 and SA17 assays

SA17 and SA61 are named according the intended function as capture and detection aptamers, respectively. When purchased, in addition to their DNA sequence an extra element was requested to be added to each one, in order to be possible to either function as a detection or capture aptamer. Table 2.7 has the specific DNA sequence of SA17 and SA61 and their additional features. According to the literature, these two aptamers were the ones that showed the best results in binding to *Staphylococcus aureus* cells, among a list of 96 different oligosequences tested. Besides the binding results, SA17 and SA61 presented a low Kd of 3.03nM and 9.9nM, respectively, what re-forced the reasons behind their choice to the development of the presented project. Adding that, it was also available, the aptamers tridimensional structure upon folding (Figure 2.11) [66]

Table 2.7 Features of the acquired aptamers. The detection aptamer is entitled as SA61 and the capture one as SA17

Aptamer Nomination - Function	Purchase details	Oligosequence 3'-5'	5' Modification
SA61 - Detection	STAB Vida, (Portugal)	TCCCTACGGCGCTAACCTCCCAACCGCTC CACCCTGCCTCCGCCTCGCCACCGTGCTACAAC	Spacer C12 + Atto 430LS
SA17 - Capture	STAB Vida, (Portugal)	TCCCTACGGCGCTAACCCCCCCAGTCCGTCCT CCCAGCCTCACACCGCCACCGTGCTACAAC	Spacer C12 + Biotin

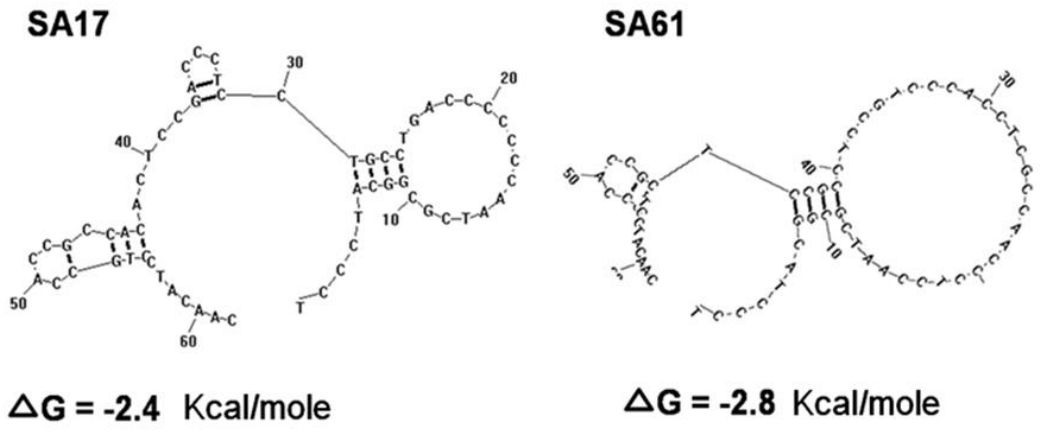

Figure 2.11 Tridimentional structure of SA61 and SA17 upon folding and respective Gibbs free energy. Adpted from literature. [66]

Regarding Atto 430 LS, according to its product information, it has a large Stokes-Shift (114 nm) and is a hydrophilic molecule with an appealing water solubility. It is excited efficiently between 400 - 460 nm, being its maximum at 436 nm with emition on the green, having its peak at 545 nm. In the florescent measurements, the suitable filter to be used is the Blue one. (Figure 2.12)

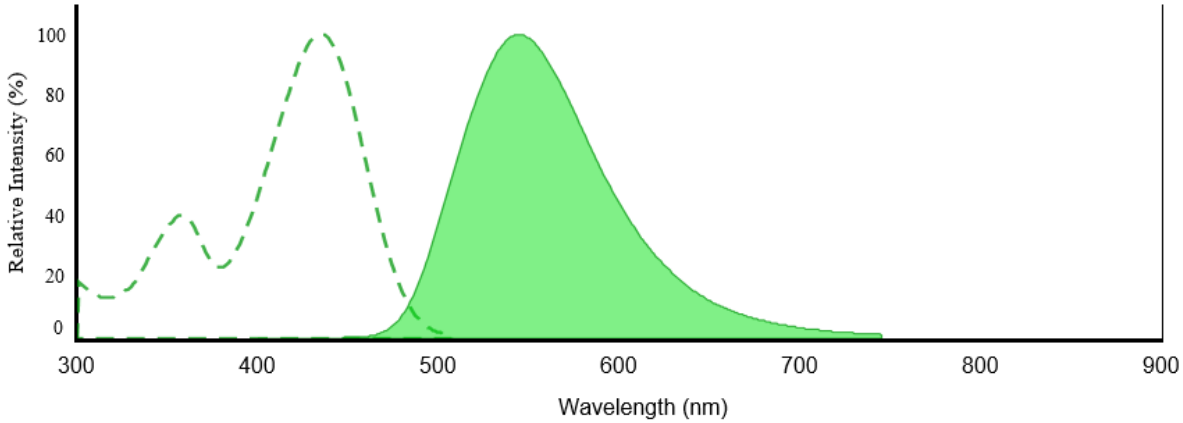

Figure 2.12 Excitation/emission spectrum of Atto 430LS fluorophore.

The aptamers stock arrived freeze dried and to prepare the solution to storage, was necessary to follow the information sheet details from the purchased company. The stock was flushed multiple times in 1xTE buffer (10mM Tris, 1mM EDTA, pH8.0), with volume to perform a 100 µM stock solution, which was divided into PCR Eppendorf's (20 µL volume) and storage in the freezer.

SA61 assay protocols

Table 2.8 Details on the material used in the SA61 assays. Blue section: Reagents; Pink section: Equipment

Name and features	Abbreviation	Purchase details and features
Staphylococcus aureus solution	SA solution	0.20 OD ~ $1.6 * 10^8$ cells/mL
Phosphate buffered saline	PBS	P4417, Sigma-Aldrich, (USA)
SA61 aptamer	-	Table 2.7
Folding Buffer	-	30 mM KPi, 100 nM KCl, pH=6.7
Microfluidic Pumping System	-	Assembly on 2.2.2 section
Microscope Color Camera	-	CCD color camera XC30, Olympus (Shinjuku, Tokyo, JP)

Fluorescence Microscope	Olympus	Inverted Fluorescence Microscope CKX41, Olympus (Shinjuku, Tokyo, JP)
Block Heating System	-	QBD2 Dry Block Heating System, Grant, (UK)

In this assay different protocols were followed in order to test the binding efficacy of the detection aptamer and upon succeeding, which would be the folding and incubation approach that better suited the aimed goal. Every time it was intended to be used, SA61 was diluted to a 2 µM working concentration using the folding Buffer. To follow the dilution, two different folding protocols were used in the assay. (Figure 2.13)

Folding Protocol 1 – Controled temperature drop	Folding Protocol 2 – Fast tempertature drop
1. Using the heating plate at 95ºC and in a water-bath the solution was left there for 2 minutes. 2. Measuring the water temperature, it was performed a controlled temperature dropping, with colder water, until it reached 37ºC. 3. Left at 37 ºC during 15 minutes.	1. Using the block heating at 95ºC, the solution was left there for 10 minutes. 2. Left 30 minutes on ice.

Figure 2.13 Protocols for Aptamer Folding.

Besides the folding protocols, also the incubation between the aptamer and SA cells was tested with two different approaches. The SA initial solution was concentrated in order to test a 4 OD solution. First, outside the column, the cells alongside the SA61 solution were incubated 30 minutes at 750 rpm and flowed, on the packet column, at 2.5 µL/min during 20 minutes following by a washing step of 3 minutes at 5.5 µL/min with PBS. The other type of incubation was achieved inside the column, sequentially, where the SA solution was flowed first using the same concentration at a 2.5 µL/min flow rate during 20 minutes followed by SA61 solution at 1 µL/min during 15 minutes, ending the flowing process by washing the column with identical features as the first protocol. Regarding the acquisition, given the stated Atto 430LS properties, for the various approaches, Bright Field and Blue filter florescence acquisitions were atchieved resourcing Olympus microscope equipment.

SA17 conjugation

Table 2.9 Details on the material used in the SA17 assays. Blue section: Reagents; Pink section: Equipment

Name and features	Abbreviation	Purchase details and features
Staphylococcus aureus solution	SA solution	0.20 OD ~ $1.6 * 10^8$ cells/mL
Phosphate buffered saline	PBS	P4417, Sigma-Aldrich, (USA)
SA17 aptamer	-	Table 2.7
Streptavidin, fluorescein isothiocyanate conjugate	Strep -FITC	Thermo Fisher
Q-Sepharose® Beads ~ 90 µm	-	Q-Sepharose Fast Flow Beads, 17051001, GE Healthcare
Microfluidic Pumping System	-	Assembly on 2.2.2 section
Microscope Color Camera	-	CCD color camera XC30, Olympus (Shinjuku, Tokyo, JP)
Fluorescence Microscope	Olympus	Inverted Fluorescence Microscope CKX41, Olympus (Shinjuku, Tokyo, JP)

Although SA17 is characterized as the capture aptamer, the truth is, it was also feasible of using as having detection proprieties. Due to the existent biotin in the 5'-end of its DNA sequence, this aptamer easily connects to other features by a streptavidin bound (affinity coupling). Having this ability, the aptamer was conjugated with a Streptavidin, fluorescein isothiocyanate conjugate (Strep-FITC). To this end, a final solution with a 2 µM concentration for each component, SA17 and Strep-FITC, was achieved by adding one component to the other, in solution and incubate at 750 rpm during 15 minutes. In order to test the binding efficacy of the procedure, a channel was packed with Q-Sepharose® beads, that due to its positively charged surface, have a high affinity to DNA. The final solution was flowed at 1 µL/min during 15 minutes with an ending washing step at 5.5 µL/min with PBS, during 3 minutes. Since FITC is a fluorophore that has excitation/emission spectrum peak wavelengths of approximately 495 nm/519

nm, it will emit on the green color and this acquisition should be possible using the Blue Olympus florescence microscope filter. (Figure 2.14)

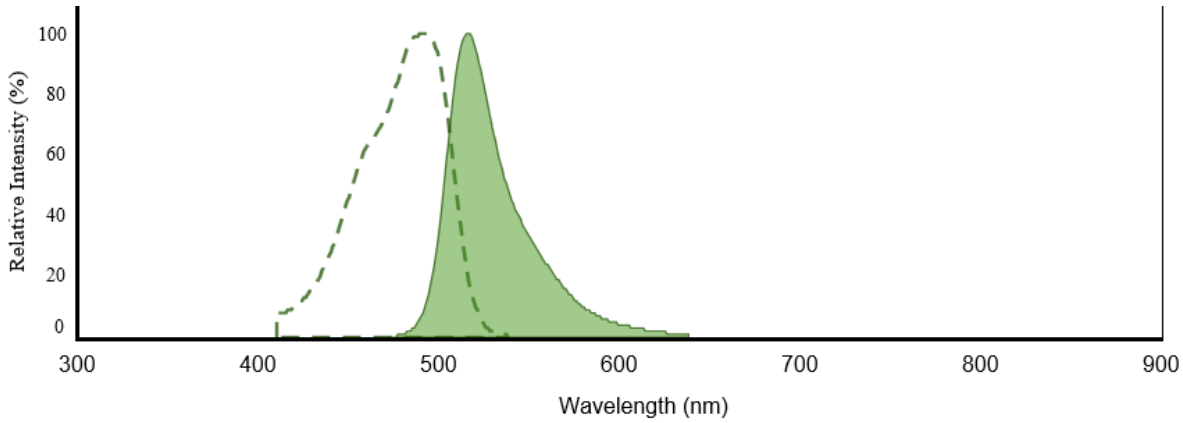

Figure 2.14 Excitation/emission spectrum of FITC fluorophore.

2.4.3 Dyes – *Staphylococcus aureus* viability

On the course of the development of this project, there was the need to use specific dyes that summon other properties of interest. In this section it will be detailed those dyes characteristics and how they were used in the performed assays. A specific viability test assay took motion in order to assess the cellular integrity of *Staphylococcus aureus cells.* With that aim, two different dyes were selected to perform an alive/dead cell test. EvaGreen™ and Hoechst 33342 gathered certain features that shown to be useful in the mentioned assessment. (Table 2.10)

Table 2.10 Details on Hoechst 33342 and EvaGreen™ dyes.

	Hoechst 33342	**EvaGreen™**
Purchase Details	62249, TherniFisher, (USA)	EvaGreen™ , 31000, Biotium Inc., (USA)
Purchase Concentration	20 mM	20X (25 µM) in water
DNA binding type	minor groove–binding DNA stain with AT selectivity	Intercalates the DNA
Excitation/Emission Peak	361/497 nm	500/530 nm (when bound to DNA)

Characteristics	Excited on UV, emitting on Blue; Fluoresces upon binding; Can cross cells membrane.	Excited on Blue, emotting on Green; Fluorescec upon binding; Cannot cross cells membrane

Hoechst 33342 is able to stain every cell, regardless of its viability, having the ability to cross an intact cellular membranes, by other words can be used as an accountant for the total number of cells in solution. EvaGreen™, however, is not passible of crossing a viable cell membrane. This dye fluoresces when bound to ssDNA and its action is only allowed upon the membrane disruption thus, acts as a compromised cell stain. Adding to this alive/dead staining approach, the dyes have a different excitation/emission spectrum (Figure 2.15). This presents an advantage by means of distinct color staining. Hoechst 33342 measurement acquisition is based on the use of UV Olympus florescence microscope filter, emitting on the blue color, on the other hand EvaGreen™ needs the use of the Blue filter to be excited which results visually on a green staining.

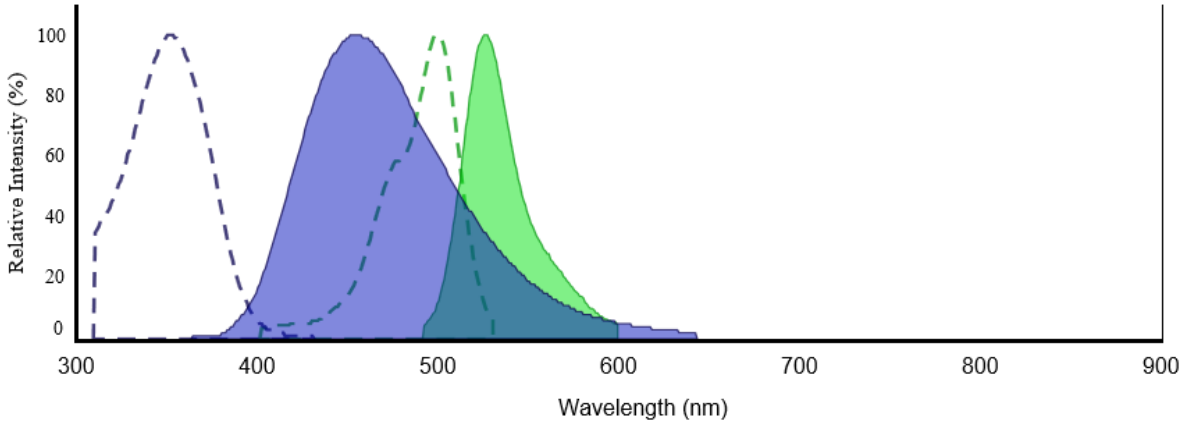

Figure 2.15 Excitation/emission spectrum of Hoechst 33342 (Blue) and EvaGreen™ (Green) dyes.

Although their emission curves overlap from wavelengths 490-600nm, the excitation occurs on different wavelengths so, using the right filters allows the distinction between their emission signal.

Table 2.11 Protocol details of Hoechst 33342 and EvaGreen™ dyes use.

Protocol type	Protocol Features	Flow Rate	Time
Incubation outside channel	750rpm agitation of Dye(s) + SA solution during 30 minutes. When together, EvaGreen™ is added first to the solution.	2.5 µL/min	20 minutes
Incubation inside channel	1-Flowed alone; 2-together in a mixture; or 3-sequentially, flowing EvaGreen™ first	1 µL/min	15 minutes

Regarding the assay, different approaches and concentrations were used along the project development. Nevertheless, the used protocol features were similar to those performed on the aptamers assay. Both dyes were used simultaneously, alone, incubated outside the channel with SA cells and inside the column after the SA solution had been flowed at 5.5 µl/min during 20 minutes. Table 2.11 assemblies times, features and flow rates used in each situation. A final washing step was always required at 5.5 µl/min with PBS during 3 minutes.

2.4.4 Sensitivity beads method assay

Table 2.12 Details on the material used Beads sensitivity assay. Blue section: Reagents; Pink section: Equipment

Name and features	Abbreviation	Purchase details and features
Staphylococcus aureus solution	SA solution	1 OD ~ $8 * 10^8$ cells/mL
Phosphate buffered saline	PBS	P4417, Sigma-Aldrich, (USA)
Spherical silica® beads 45-75 µm	SiO_2 beads	Spherical flash silica beads, 97728-U Supelco Analytical (Bellefonte, PA)
Q-Sepharose® Beads ~ 90 µm	-	Q-Sepharose Fast Flow Beads, 17051001, GE Healthcare
Microfluidic Pumping System	-	Assembly on 2.2.2 section
Microscope Color Camera	-	CCD color camera XC30, Olympus (Shinjuku, Tokyo, JP)
Fluorescence Microscope	Olympus	Inverted Fluorescence Microscope CKX41, Olympus (Shinjuku, Tokyo, JP)

This assay intend to assess the beads sensibility of physical capturing *Staphyloccocus cells*. The protocol features to attend this matter are similar to those performed on the alredy described assays. The column was packed with either Q-Sepharose® or Spherical silica® beads at 5.5 µL/min during 3 minutes, followed by a PBS washing step with the same time and flow rate. With the packed channels, different SA solution concetrations were flowed trought it at 2.5 µL/min during 20 minutes. The tested concentrations are displayed on table 2.13 resultant from an intial SA stock solution of 1OD

(~$8 * 10^8$ cells/mL). The stock solution was once again provided by PhD student Catarina Caneira, grown on Laboratório de Análises facility from Instituto Superior Técnico, Lisbon University and its concentration differs from the previous stocks used in order to perform simple dilutions and thus, avoiding extra centrifugation steps that can damage the cells. Hoechst 33342 was then flowed at 1 µL/min during 15 minutes, using a 2.5 µg/mL solution to allow cellular detection, followed by the recurrent PBS washing step.

Table 2.13 Tested SA solution concentrations in cells/mL.

cells/mL
~ $4*10^8$
~ $2*10^8$
~ $8*10^7$
~ $4*10^7$
~$4*10^6$
~ $4*10^5$
~ $8*10^3$

2.5 Analysis Methodology

To analyze the channel images, different approaches were taken into consideration. Nevertheless, the entire analysis set was performed resourcing ImageJ software and for the results presentation, Origin 2020 software.

2.5.1 Bright Field Measurements

Existing the need to perform an analysis across different colored images, two types of ImageJ tools were selected. Grayscale measurements assess the change in color intensity translated to shades of gray across a defined region. In this case, a middle line crossing the inside's channel was defined to measure the changes across the column. (Figure 2.16 a.) The second approach uses ROI manager tool from the software to output a mean Bright Field intensity value of certain sectional area. This analsys consisted in selecting a oval shape form inside the column and a squared one outside (background). (Figure 2.16 b.) Afterwards, the absolute value from the channel was achieved by subtracting the measurments acquired from the selected channel region by the background average intensity.

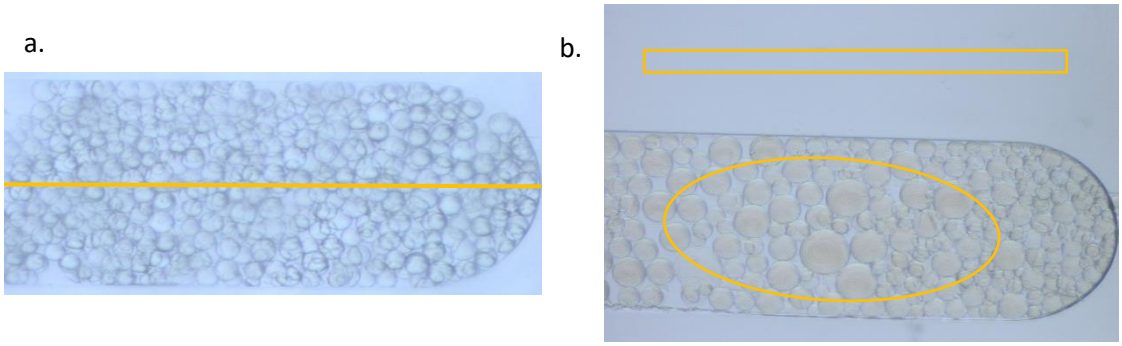

Figure 2.16 Section used for signal measurements in ImageJ software: a. Grayscale analysis; b. Mean RGB signal intensity.

2.5.2 Fluorescence Measurements

An identical aproach to figure 2.16b was carried to perform fluorescence measurments. ImageJ allows the splinter of the images into the three color channels: red, green and blue. In the majority of the assays, the fluorophores used, when excited, colored on green, so, that was the channel used to perform the measurments. This way, the albsolut value for the mean fluorescence intensity was achieved by, once again subtracting the selected region inside the column by the background signal. (Figure 2.16 b.) In some specific cases, different fluorescence signals were expected in distinct sites of the channel. In those cases, two regions were selected inside and compared to one another.

Besides this, there was one fluorophore used that when excited, colored on the blue and in this situation the measurments were acquired in both green and blue channel of ImageJ software, due to the existance of signal in each one. Nevertheless, to compare to other results, the green channel measurments had a higher role.

Chapter 3

Results and Discussion

This chapter focuses in describing the work of the performed assays, along with the results obtained. Each analysis is always based on two replicas for each experiment, although only one will be visually displayed.

The capture and detection of *Staphylococcus aureus* cells was to be achieved using two different aptamers, each one aimed for each function, creating an aptamer sandwich. In spite of the aimed method, an initial approach was carried out, where different bead types were tried in order to understand if they could have any sort of advantage in the SA capture possible to be used alongside the aptamers or by means of test their binding efficacy. On Figure 3.1 is represented how this chapter is structured and what is intended to be tested upon each set of results obtained, being this schematically elucidated in the beginning of each section.

Guideline 1

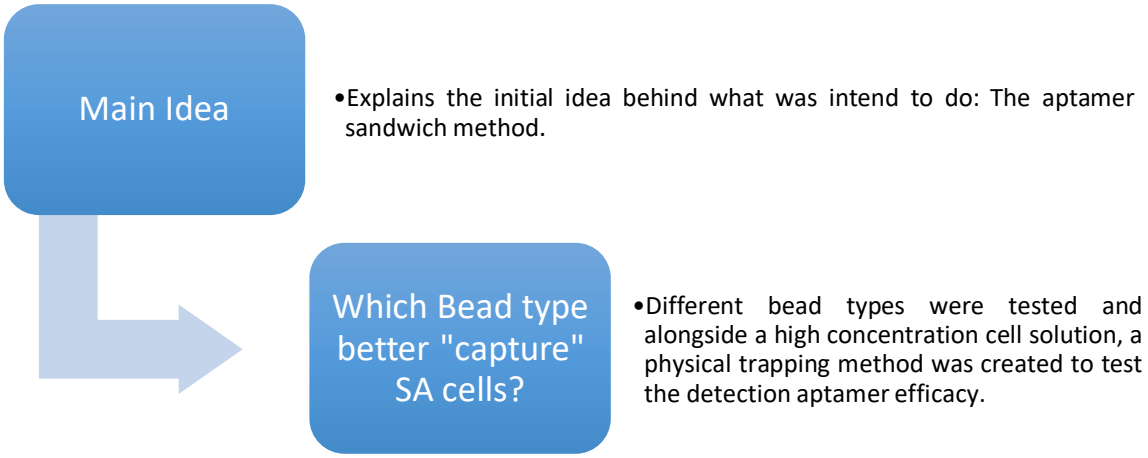

Figure 3.1 Schematic of the first guideline

3.1 Aptamer Sandwich Method – Main Idea

The theory behind the microfluidic chip here assigned, to perform a direct capture and detection of bacterial cells, was set aiming to use the simple column, which its process fabrication was described in section 2. This initial main idea was divided into two phases.

In a first step, the “naked” channel was to be packed with beads aiming to enhance the surface area, increasing the probability of capture. These being NHS-activated Sepharose Fast Flow beads that were functionalized with streptavidin, according to section 2.3.2 of the second Chapter. The capture aptamer (SA17) has a biotin bind to it, at the end of the DNA sequence and since the interaction Streptavidin-Biotin easily occurs due to the strong attraction between these two components, flowing SA17 through the channel means to have NHS-Sepharose® Beads conjugated with the capture aptamer. The following step would be then, flow a SA solution and allow the cells to be kept in the beads by means of the SA17 interaction.

In the second phase, the aim was to detect what have been captured by the conjugated Sepharose-SA17 Beads. Aiming that, the detection aptamer (SA61) that has a fluorescent molecule (Atto 430LS), in the end of its sequence, can be flowed through the channel and bind to the cells that have been captured at first instance, creating a sandwich between the cell and both aptamers (Figure 3.2).

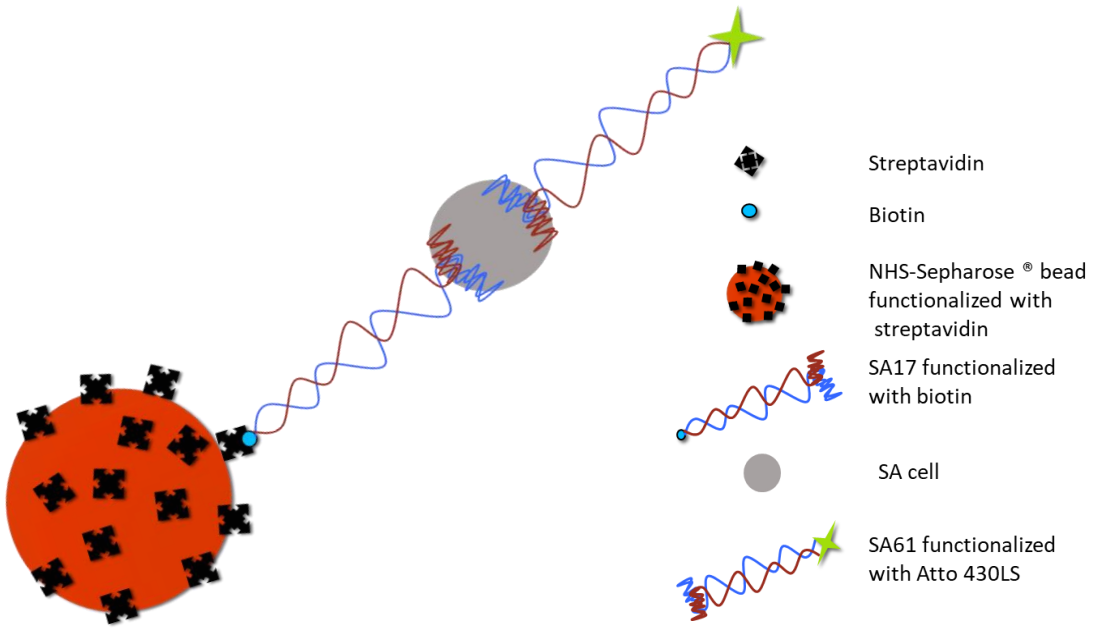

Figure 3.2 Ilustration of the initial aimed idea.

With resource to microscopic fluorescent techniques, the emission of Atto 430LS, could then be measured after its excitation with posterior signal acquisition.

3.2 Beads test assay

Four different bead types were tested, aiming to understand if there was one that could influence, positively, the capture of SA cells. Nevertheless, it was intended to select a bead type from those options in order to use it to test if the aptamers were binding to the cells. Table 3.1 exposes the used beads and the features that were being explored in order to attend the announced goal.

Table 3.1 Features of the used Beads in the assay. Type of Matrix and surface characteristic.

Bead Type	Matrix	Surface Feature
$\boldsymbol{SiO_2}$	Silica	Hydrophilic
$\boldsymbol{NH_2}$	Silica	Positive
$\boldsymbol{C_{18}}$	Silica	Hydrophobic
Phenyl Sepharose	Agarose	Hydrophobic

Each bead type was packed according to the method described on section 2.3.3 with a 5.5 µL/min flow rate, followed by a washing step with PSB at the same velocity. After the packing, a 10OD ~ $8 * 10^9$ cells/mL *Staphylococcus aureus* solution was flowed at 2.5 µL/min during 20 minutes. Using microscope Olympus camera, images of the column were acquire, at different time points, kept consistent along the entire assay. The acquisition was set at minutes 0, 10 and 20 of the cell solution flowing step. Afterwards the images were analyzed using two distinct approaches, both resourcing ImageJ software, as detailed on section 2.5.1.

Regarding the grayscale analysis, lower values correspond to higher cell density. *Staphylococcus aureus* presence on the column, that alongside the beads, tend to darkener the area, mainly due to the solution's high concentration, which is correspondent to lower scale values.

3.2.1 SiO_2 beads

Regarding SiO_2 beads experiment (Figure 3.3), a silica's hydrophilic bead type, at minute 10 (Figure 3.3) it was possible to observe a decreasing of the grayscale signal in the first part of the channel,

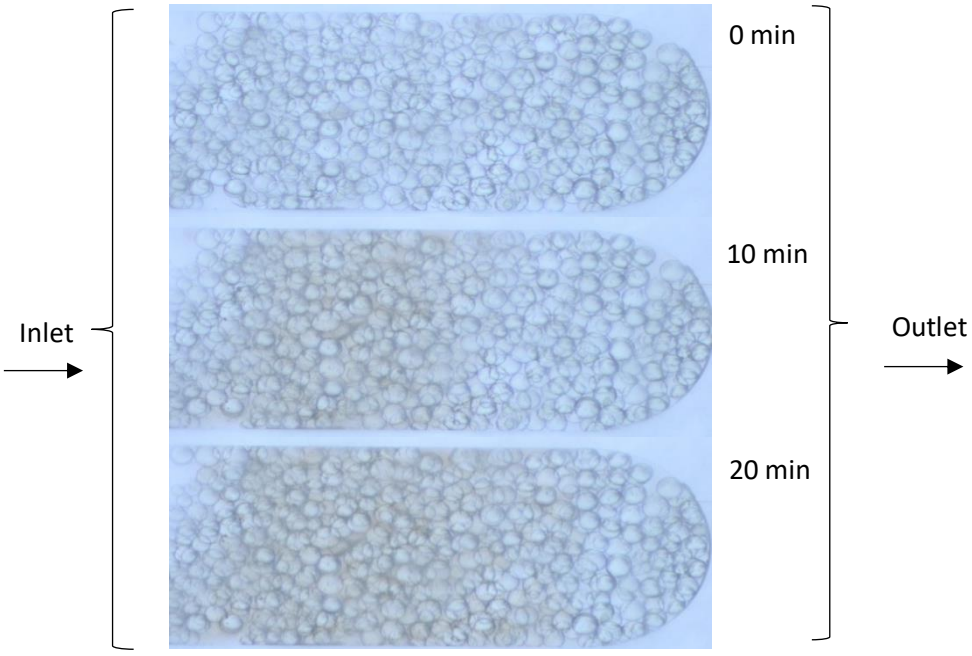

Figure 3.3 Experimental image from the SiO_2 beads assay at 0, 10 and 20 minute time points. Channel with Spherical silica ® beads and a 10 OD ~ $8 * 10^9$ cells/mL Staphylococcus aureus solution. All the experimental images were acquired in Olympus Microscope CHX41, exposure time: 50ms, gain: 0 dB, magnification:10x.

up to the 1000^{th} pixel, where the values appeared as being very close to the ones found on minute zero. The lower signal, in comparison to zero, was correspondent to the cellular progression on this area of the channel. The viability of this statement increases when looking at grayscale values on minute 20. From the beginning of the channel to pixel 700, the grayscale values were quite similar compared to the same region at minute 10, having slightly increased the cellular concentration. From pixel 700 to 1250, while at minute 10 the grayscale values decreased until being similar to those from the control (up to pixel 1000), at minute 20 the cell concentration was noticeably higher. Figure 3.4 values are decreasing on that time point more gradually and linearly, reaching, once again, grayscale values similar to those of the control (zero minutes), around pixel 1250.

It was possible to ascertain that over time the cells progressed in the channel but slowly and at a slow rate, since the pixel range showing the presence of concentrated cellular content from minute zero to 10, was clearly higher than what was seen on the progression that went from minute 10 to 20. There was some cell retention and accumulation on the beads, but this may be an amplified effect related to the high cell concentration passing through the channel, which led to a trapping effect between beads and cell aggregates that eventually were being formed.

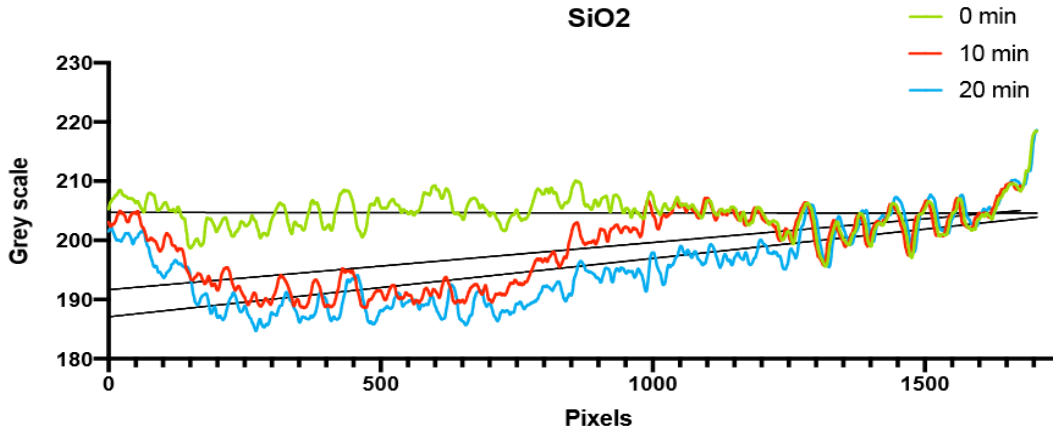

Figure 3.4 Grayscale signal measured accross the column middle line (measured in pixels) at 0, 10 and 20 minute time points. (Aquisition: Olympus Microscope CHX41, exposure time: 50ms, gain: 0 dB, magnification:10x.)

3.2.2 NH_2 beads

NH_2 beads are positively charged beads made of silica. Upon the experiments with SA cells (Figure 3.5), it was observed that the grayscale decreased considerably the values when comparing time points zero and 10, sourcing the analysis of figure 3.6. There was a significant existence of cells crossing and the presence of cellular content was shown to be increasing until pixel 900, having afterwards decreased until the end of the channel. At minute 20, the cellular concentration increased as it was expected and the grayscale values decreased to support that fact. The difference between the middle and end of the experiment was notice to be a homogeneous event. From the experimental images (Figure 3.5) was possible to understand that the cells advance through the channel was notorious, occurring a darkening of the structure, from time point 10 to 20. Although there was cellular

content along the entire column, the trapping was higher until its center, existing a breaking effect that avoided the cell solution to flow properly. (Figure 3.6)

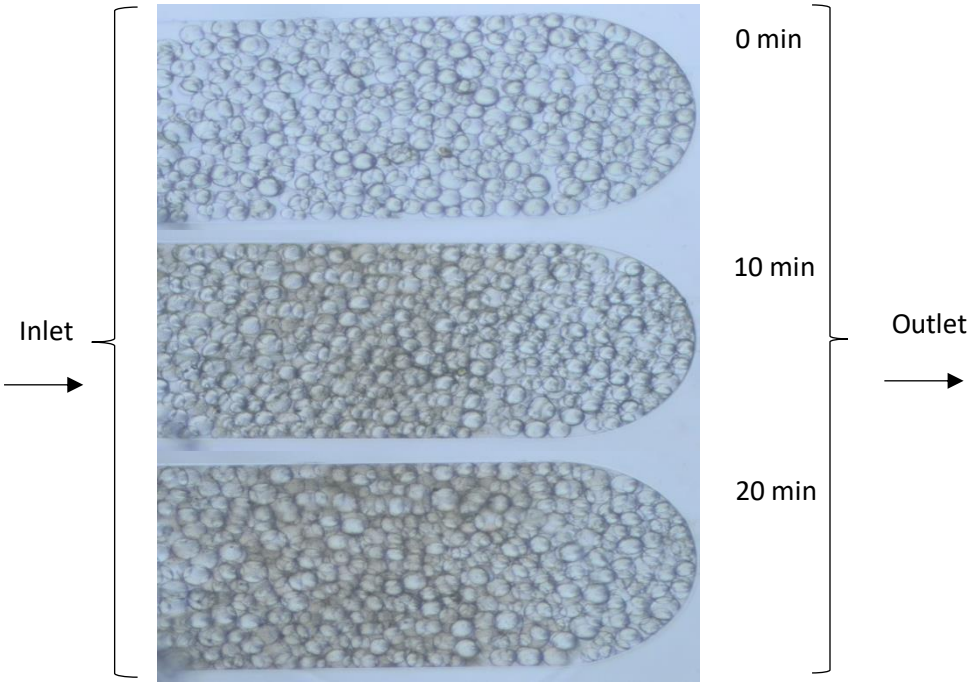

Figure 3.5 Experimental image from the NH_2 beads assay at 0, 10 and 20 minute time points. Channel with NH_2 modified Spherical silica ® beads and a 10 OD ~ $8 * 10^9$ cells/mL Staphylococcus aureus solution. All the experimental images were acquired in Olympus Microscope CHX41, exposure time: 50ms, gain: 0 dB,

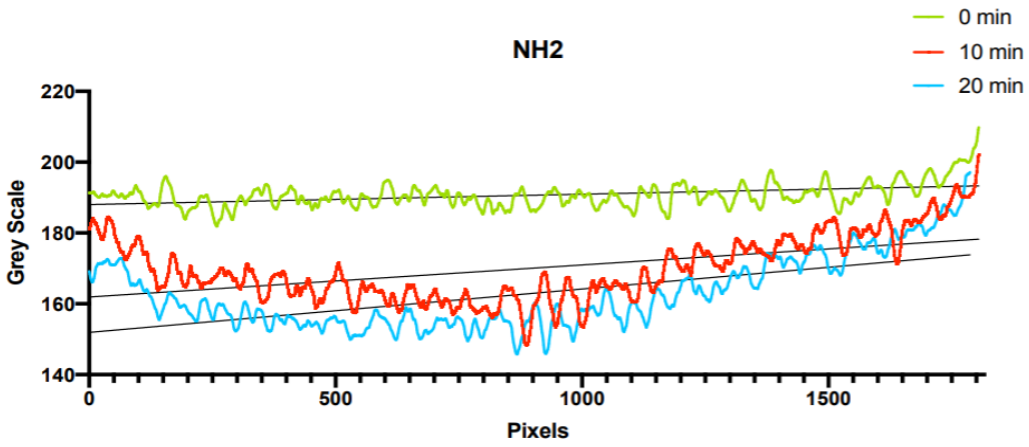

Figure 3.6 Grayscale signal measured accross the column middle line (measured in pixels) at 0, 10 and 20 minute time points. (Aquisition: Olympus Microscope CHX41, exposure time: 50ms, gain: 0 dB, magnification:10x.)

3.2.3 C_{18} beads

C_{18} beads, with a hydrophobic surface and a silica matrix are the tested beads where existed the greatest discrepancy of the results, visually and in terms of grayscale values. C_{18} beads are quite small and overlapped each other in the same location. This factor adding to the flowed high cell concentrations and the beads hydrophobic surface, seemed to bring some complications on the cells flow. (Figure 3.7 and 3.8)

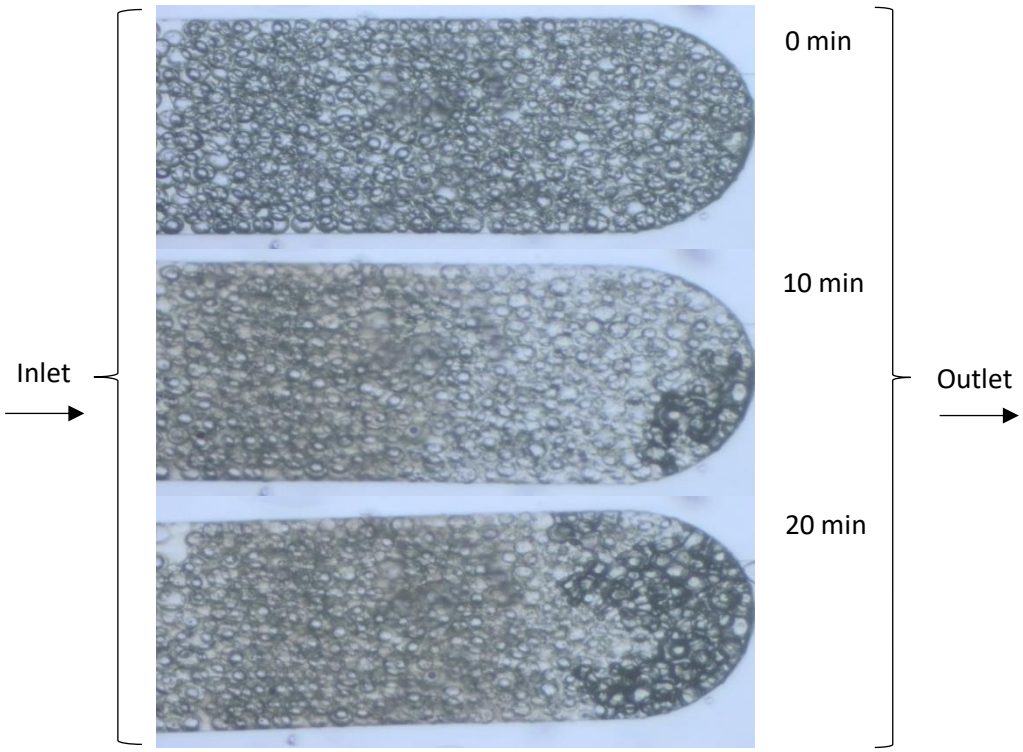

Figure 3.7 Experimental image from the C_{18} beads assay at 0, 10 and 20 minute time points. Channel with Spherical C_{18} silica® beads and a 10 OD~ $8 * 10^9$ cells/mL Staphylococcus aureus solution. All the experimental images were acquired in Olympus Microscope CHX41, exposure time: 50ms, gain: 0 dB, magnification:10x.

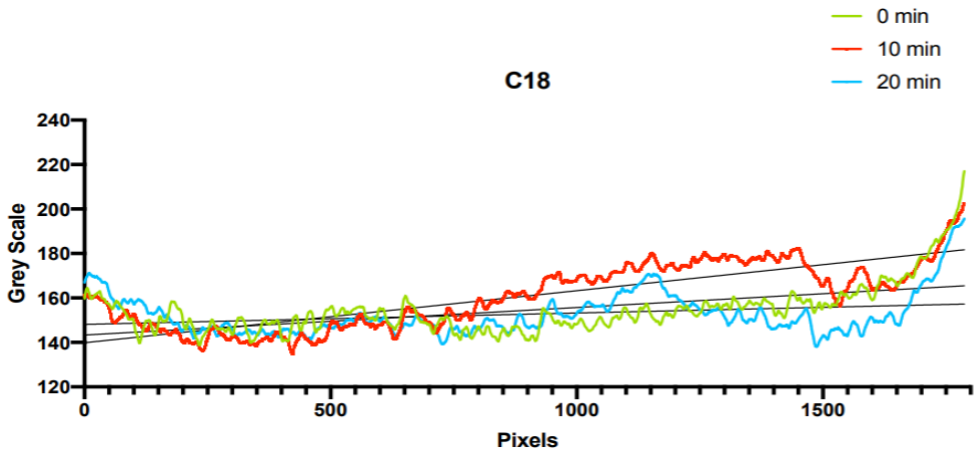

Figure 3.8 Grayscale signal measured accross the column middle line (measured in pixels) at 0, 10 and 20 minute time points. (Aquisition: Olympus Microscope CHX41, exposure time: 50ms, gain: 0 dB, magnification:10x.)

Air bubbles presence, the distinct bead color and the difficulty to flow the highly concentrated cell solution, were the origin of C_{18} results discrepancy. Nevertheless, in order to choose the bead type to be used in the following assay, there was also the analysis of the mean bright field signal intensity and the fact that Phenyl-Sepharose® beads took part on this study. Although having a different matrix, they also have a hydrophobic surface, which was taken in consideration side-by-side with C_{18} visual support (Figure 3.7).

3.2.4 Phenyl-Sepharose®

Phenyl-Sepharose® beads were chosen to be part of the Bead test assay, for having a different matrix: Agarose. The intention was to use agarose beads during the aptamer sandwich method. The use of silica beads was set on the table in order to test the aptamers binding efficacy and so, it was of interest to test an agarose bead type alongside silica's, to understand its physical capability on capturing cells. Right after the visual acquisition of this experiment (Figure 3.9), was possible to observe that even with a high concentrated cell solution, the cellular content was able to flow without side backs throughout the channel crossing the packed beads. Although it can be seen some cellular content on the column, the grayscale values were regular and linear across its path. Even when comparing both minutes 10 and 20 values from the graphic, they showed no relevant difference between them, occurring only a very smooth decrease from one to another (equated to a slight increase in the cell concentration). (Figure 3.10)

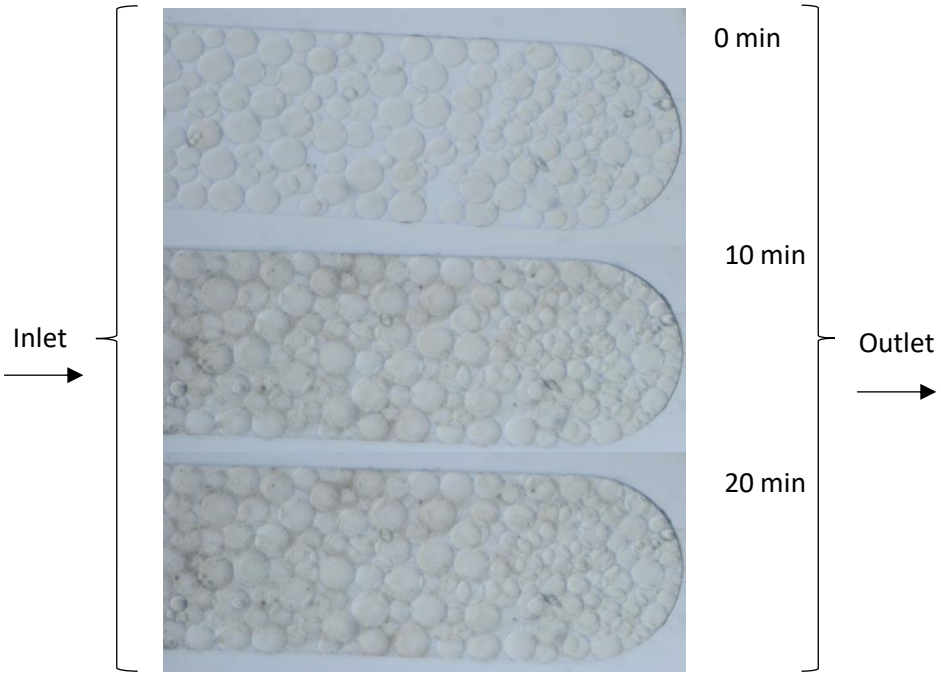

Figure 3.9 Experimental image from the Phenyl Sepharose® beads assay at 0, 10 and 20 minute time points. Channel with Phenyl Sepharose® beads and a 10 OD ~ $8 * 10^9$ cells/mL Staphylococcus aureus solution. All the experimental images were acquired in Olympus Microscope CHX41, exposure time: 50ms, gain: 0 dB, magnification:10x.

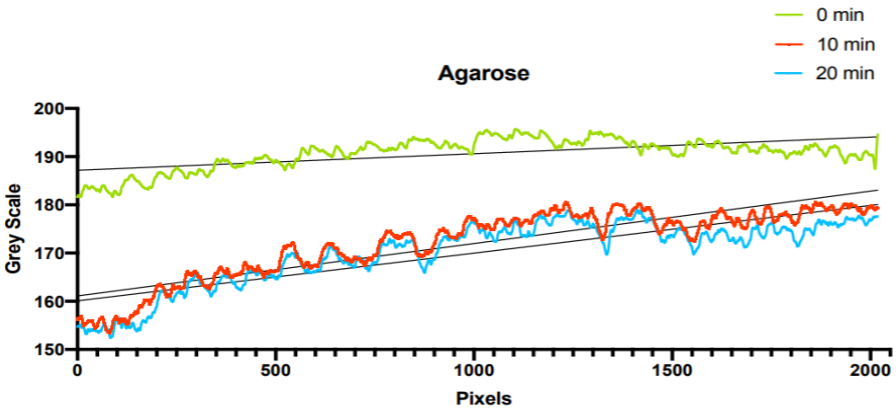

Figura 3.10 Grayscale signal measured accross the column middle line (measured in pixels) at 0, 10 and 20 minute time points. (Aquisition: Olympus Microscope CHX41, exposure time: 50ms, gain: 0 dB, magnification:10x.)

3.2.5 Mean Bright Field Intensity signal analysis

Regarding the analysis using ROI manage tool from ImageJ software, the sum of all four experiments was displayed on figure 3.11 and some conclusions were able to be taken. This analysis was taken into consideration in order to support the results from the grayscale approach. From it, was notorious that C_{18} beads registered the higher signal, nevertheless, it also shown the higher discrepancy between its replicas. Regarding SiO_2 and NH_2, hydrophilic and positive beads, respectively, also had shown good signals with coherence across the double experiment, which support the already analyzed grayscale results. Phenyl-Sepharose® beads have shown the least appealing signal values as their previous analysis.

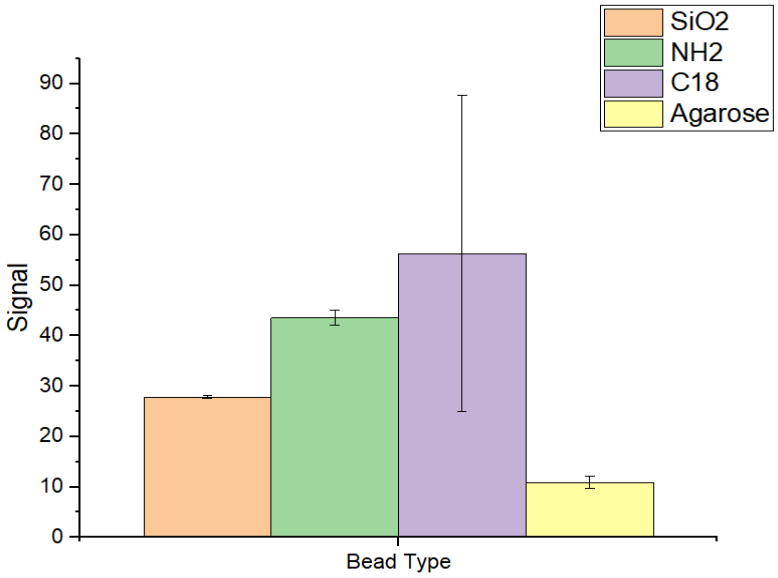

Figure 3.11 Mean bright field intensity signal measured on a section of the column from each bead at the end of the experiment. (Aquisition: Olympus Microscope CHX41, exposure time: 50ms, gain: 0 dB, magnification:10x.)

3.2.6 Bead selection

C_{18} beads both grayscale and mean bright field intensity signal had dubious results. Besides the non-coherence across the measurements, the truth is, during the multiple attempts of performing this experiment, several side backs were encountered. Air entering the channel was the main problem, due to the beads hydrophobicity and the high cell concentration, there were complications in flowing the solution properly. To avoid this situation, C_{18} beads were excluded from the selection. The discrepancy of the results, the reason why this selection was performed in a first instance (test the aptamer efficacy) and the troubles that the bead use brought up to the experiment performance, heavily weighted on the balance to not had been the one selected.

The grayscale analysis from SiO_2 bead test had quite positive results in which concerns the physical trapping of *staphylococcus aureus* cells. Although showing a progression of the cellular content across the flowing time, the truth is SiO_2 beads were able to sustain SA cells in part of the column, slowing down its passage. Adding to this, the visual darker effect, which occurred due to the high cell concentration, was another advantage taken into consideration that could be used on, when testing the detection aptamer's binding efficacy, in which is inserted the aim of this selection. For instance, if it is known that SA cells have higher presence in one side of the channel, the fluorescence on that site is expected to also be increased, gauging this way the binding of the aptamer.

Apart from these, NH_2 beads also showed intention to sustain cellular content across the column, supporting this statement by its grayscale results. Although having a positive outcome, the trapping effect by NH_2 beads was less accentuated when compared to the action of SiO_2 beads, tending to allow SA cells to flow with less retention.

Nevertheless, regarding the bright field signal analysis, both of the above bead types have shown good results among the all set tested. Although NH_2 beads presented a higher signal, SiO_2 beads were selected to continue the development of this project. Positively charged beads, like NH_2, can present an advantage in the *staphylococcus aureus* attraction, due to the cell surface properties, but they also would have influence near the flow of the aptamer since is a DNA sequence and this side back was to be avoided.

Guideline 2

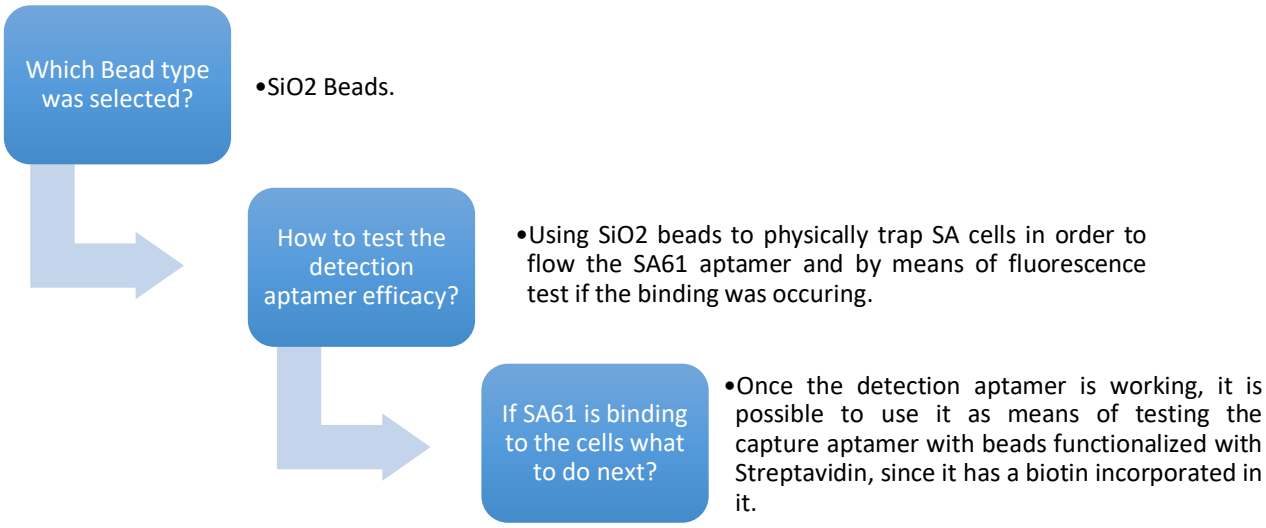

Figure 3.12 Schematic of the second guideline

3.3 SA61 binding efficacy

After choosing the best bead type to use and according to the results obtained in the previous section, it was possible to perform an essay where SA61 binding efficacy was tested. The idea of having a strategy capable of concentrating the cells in the channel was an optimal path to assess the detection aptamer efficacy.

It is of relevance to point out that the choice of using a high concentration cell solution was to have the guarantee that SA cells were being kept in the channel. The results of the Beads assay have shown that a higher congeries could be observed in a specific site of the column. The main idea of the initial workflow approach, was then, to use those results as an advantage to test SA61 binding ability. Has it had been shown in the methods chapter (2.4.2), SA61 was tested using two different protocols of DNA folding and incubation. Being this said, there are four main types of results, one for each Folding/Incubation protocol (Figure 3.13).

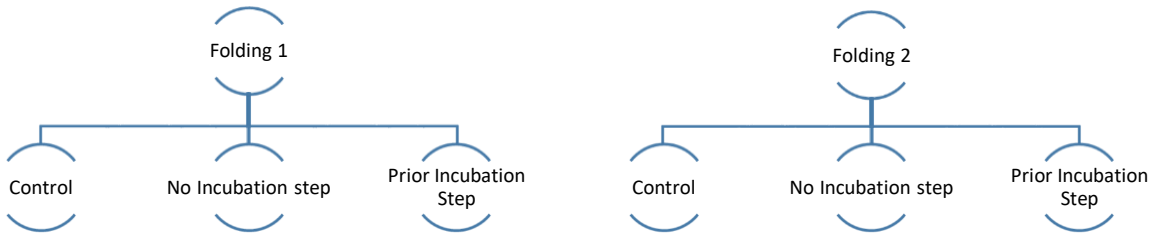

Figure 3.13 Schematic of the four different protocols used along the SA61 assay

Regarding SA61's folding technique, the cooling down of the solution was performed in one hand, resourcing a rapid and drastic dropping of the temperature, placing the Eppendorf® in water with ice blocks after it had been 10 minutes at 95ºC. In the other hand, the folding was performed gradually, controlling the temperature dropping until it reached 37ºC where it was maintained during 15 minutes. In this last approach, the solution was heated initially until 95ºC but only kept at it during 2 minutes, before beginning the cooling down process. As for the incubation step, the adding of the SA cells to the SA61 solution was set to be prior the flowing through the column, where the mix was 30 minutes under agitation at 750rpm, for each of the folding protocols. Both solutions were also flowed sequentially though the channel, for the same folding protocols. (Figure 3.14)

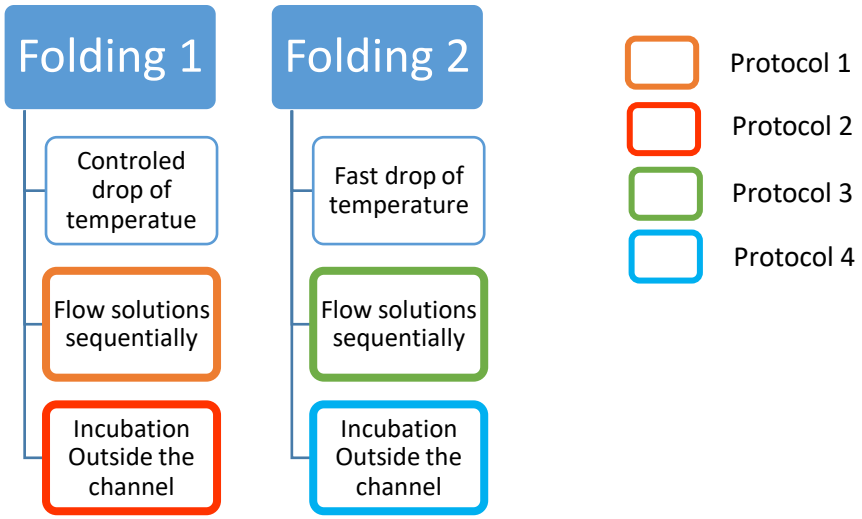

Figure 3.14 Schematic of the diferent protocol and atributed nomination.

3.3.1 Q Sepharose® Beads

To understand if the fluorescent molecule that was conjugated with the aptamer was correctly bound to it, an assay was performed where Q-Sepharose® beads were packed on the column. These are positively charged beads, which attract molecules with negative charges, for instance, DNA. Being the aptamer, no more than a specific DNA sequence, flowing it through this bead type should concentrate SA61 and consequently function as tool to obtain a higher output signal when measuring the excited signal. Using a 2µM as SA61 working concentration, it was flowed at 1 µL/min during 15 minutes followed by a washing step with PBS at 5.5 µL/min during 3 minutes. The analysis of the measured signal by ROI manager tool from ImageJ software was obtained using the software's green channel, due to Atto 430 LS properties, resourcing the images acquired at 500ms, 1s and 2s exposure times and throughout different time points: before SA61 flow, after it and upon the washing step. (Figure 3.15 and 3.16).

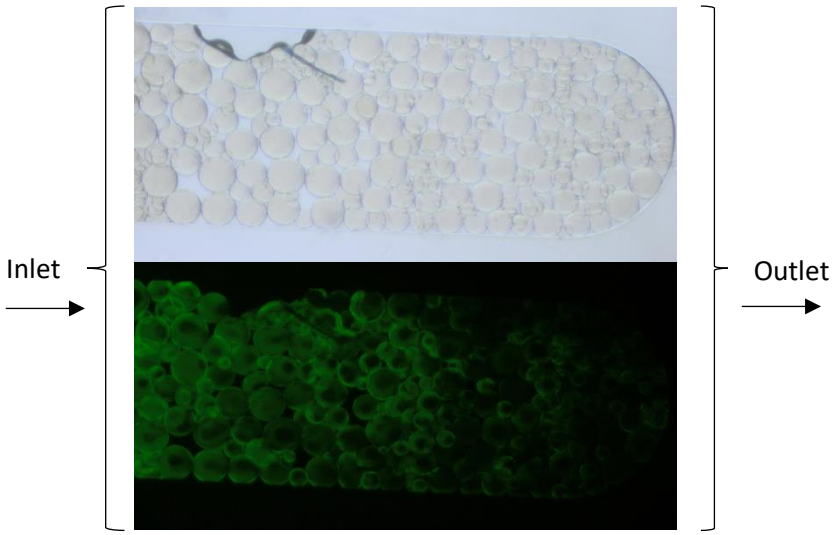

Figura 3.15 Experimental image from the Q-Sepharose assay after the washing step. Channel with Q-Sepharose® beads and a 2 µM SA61 solution. All the experimental images were acquired in Olympus Microscope CHX41, exposure time: 50ms – colored image; 2s – Fluorescence use, Filter: Blue, gain: 0 dB, magnification:10x.

From the analysis of figure 3.16 was possible to state the correct functioning of SA61 as a detection tool, since the DNA negative charge was being kept by the Q-Sepharose® positively charged surface and Atto 430LS molecule was emitting fluorescence after being excited, using the blue filter. In between the exposure times the represented proportion, also meant the assay was well carried.

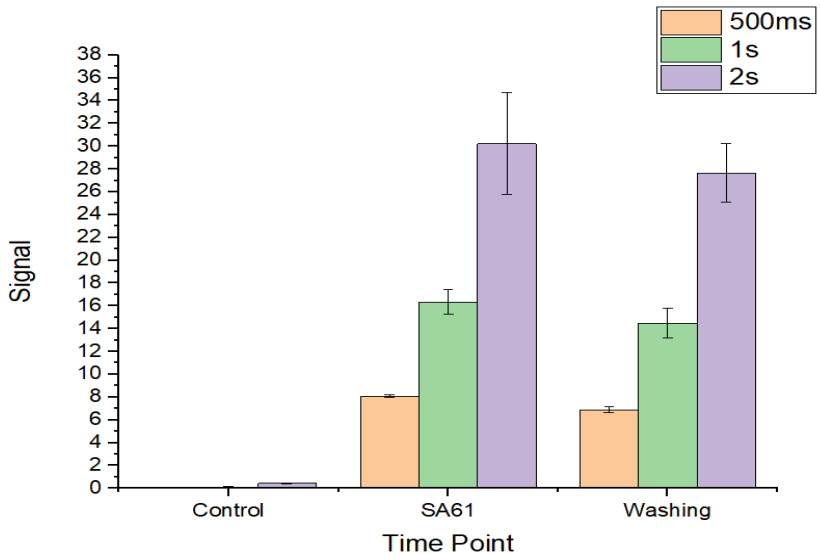

Figure 3.16 Mean Fluorescence Intensity measured on a section of the column of each time point.. (Aquisition: Olympus Microscope CHX41, exposure time: 500ms, 1s and 2s, gain: 0 dB, magnification:10x.)Microscope CHX41, exposure time: 50ms – colored image; 2s – Fluorescence use, Filter: Blue, gain: 0 dB, magnification:10x.

3.3.2 SA61 assay

The protocol followed on this assay was previously described on section 2.4.2 of the second Chapter. The signal analysis of the images was set, once more, to be on the beads column and outside

in order to take the background signal, but also, it was established the difference between the highly concentrated cells site, that visual appeared has a darker zone, and the remaining. This way, a higher signal was expected to be measured there, in comparison to the rest of the column.

The experimental image of all four protocols (Figure 3.17) have not showed any relevant fluorescence in the entire set. The images are correspondent to the assay's time point after the washing step. As it was possible to retain from the analysis to the signals displayed on the figure 3.17, there was no significant binding of SA61 to the SA cells. The presented values were extremely low and are not what should be expected to obtain from a correct binding of the aptamer, when comparing to the fluorescence signal obtain form the Q-Sepharose® assay. From the literature, it is uncertain how many binding SA61 sites has a *Staphylococcus aureus* singular cell [66]. In spite of it, if only one aptamer would attach to each cell, the concentration needed to obtain the darker zone that appear on the images of figure 3.17, should be enough to output an exponentially higher signal.

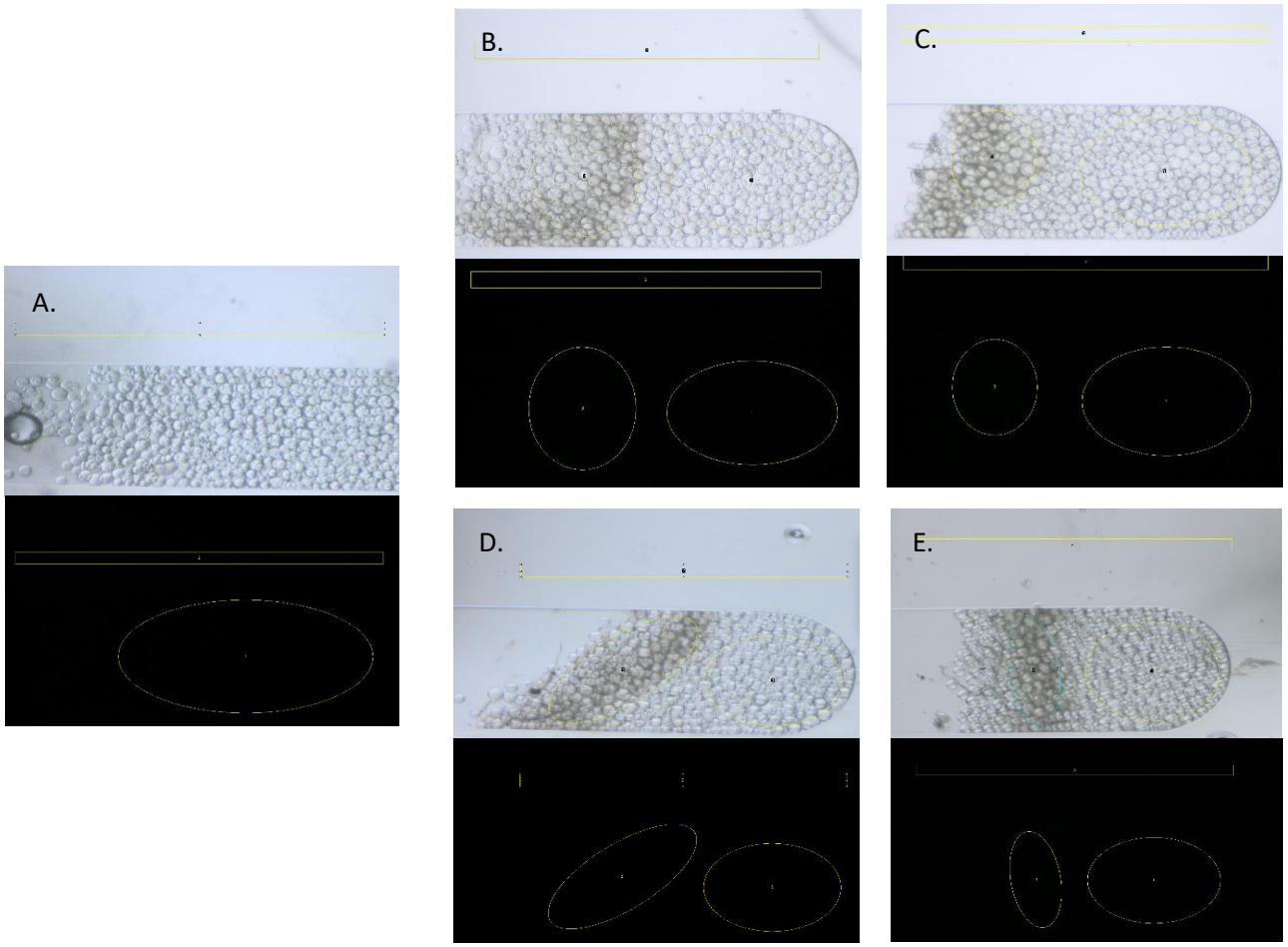

Figure 3.17 Experimental images from the SA61 assay after the washing step. Channels with Spherical silica® beads . A.Control: Only beads; B.Protocol 1; C.Protocol 2; D. Protocol 3; E. Protocol . B-E: Beads, 2µM SA61 solution and a 4OD ~ $3.2 * 10^9$ cells/mL *Staphylococcus aureus soltution. All the experimental images were acquired in Olympus Microscope CHX41, exposure time: 50ms – colored image; 2s – Fluorescence use, Filter: Blue, gain: 0 dB, magnification:10x.*

By analyzing figure 3.18, the signal values were not featured to be labeled as a positive result, however, there was a particularity that was interesting and should be pointed out. Observing the signal difference between the darker and lighter sites of the beads in the channel, it was constant thought all four protocols that the signal measured onto the concentrated cell's zone was slightly higher. This could mean that a small portion of the aptamers could have been being withheld, but not at the cell's concentration proportion.

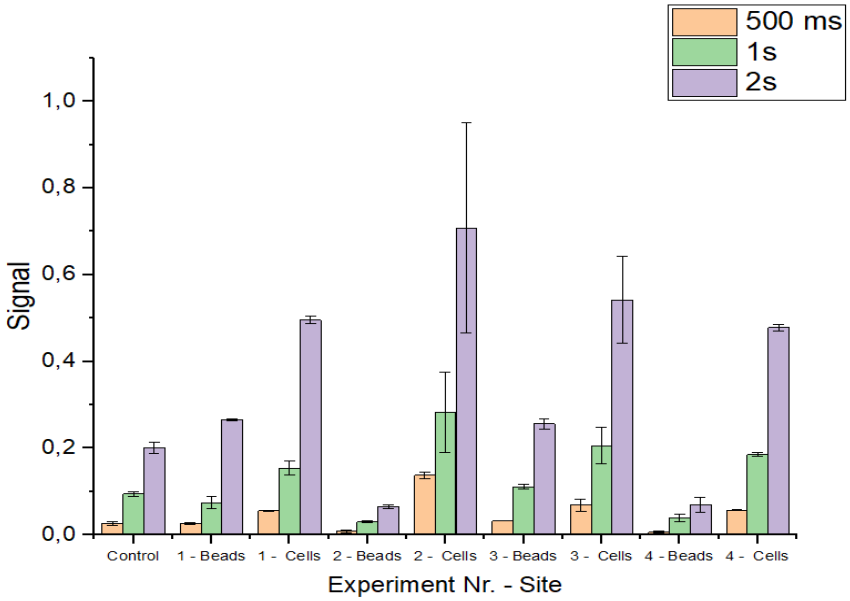

Figure 3.18 Mean fluorescence intensity signal measured on a section of the column after the washing step. Values from protocols 1-4 on the concentrated cell site (Cells) and outside that zone (Beads). (Aquisition: Olympus Microscope CHX41, exposure time: 500ms, 1s and 2s, gain: 0 dB, magnification:10x.)

Considering the information mentioned above, there was the need to perform a trouble shooting of the situation. What could be affecting the binding of the aptamer to the SA cell? Does the aptamer binds to the cell wall? If this is the case, there is the need to understand how the performed protocols affect cell viability not allowing the binding process.

Guideline 3

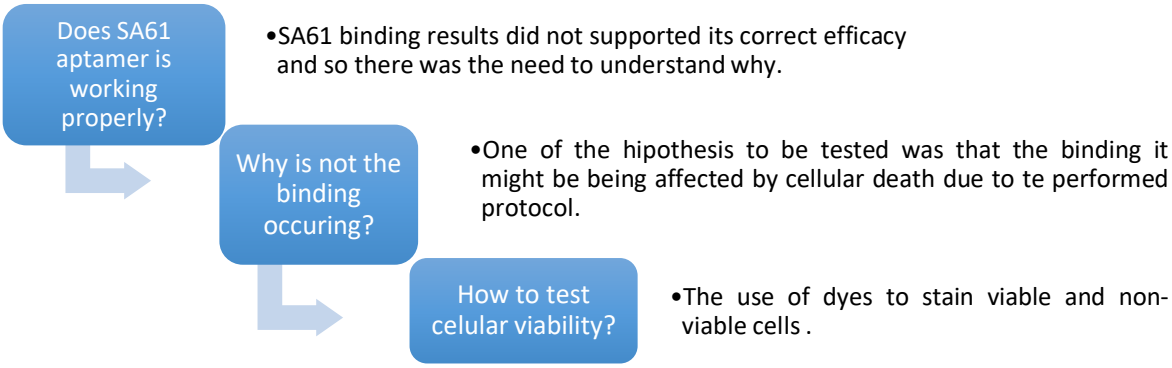

Figure 3.19 Schematic of the third guideline

3.4 Staphylococcus aureus viability

On this section, is described how *Staphylococcus aureus* viability was to be tested in order to understand if the previous protocols were somehow compromising cell wall integrity. These, performed on the assay with SA61 aptamer, had different actions that could have jeopardized SA viability and must be counted in, such as high cell concentration, centrifugation steps, pumping flow rates and the bead's physical characteristics.

To perform this assay, several aspects were taken into consideration, for instance, how should cells be marked and how the information about its viability could be obtain. To this end, two different dyes were used: EvaGreen™ that colors the cell if there is a disruption on the membrane, meaning that the cell is no longer viable; and Hoechst 33342, that can pass through the cell wall even if it is intact, in other words, it will stain all cells (alive or dead). The dyes were used, separately and alongside each other, on a fresh solution – control for alive cells – and on a thermally treated one – control for death cells (Figure 3.20). These controls were performed resourcing Q-Sepharose® beads, always using the same cell concentration (4OD ~ $3{,}2 * 10^8$ cells/mL), 100 nM for EvaGreen and 5 µg/mL for Hoechst 33342. The dead cells control was achieved by submitting the solution to 95ºC during 10 minutes.

Figure 3.20 Schematic on the controls performed during this assay

Has shown on section 2.4.3, Hoechst 33342 and EvaGreen™ are excited by different wavelengths and emit fluorescence in different ones as well. Although emitting in distinct colors, the dyes excitation/emission spectra shows that there is a bandpass where both emit fluorescence simultaneously, on a lower intensity. EvaGreen™ emits only on the green color but Hoechst 33342, has a range that varies between blue (the uppermost) and green. For this reason, when treating the results on ImageJ software, this last dye had a mean fluorescent intensity signal in the green and blue channel of the RGB mean intensity signal. To compare the results of each dye and conclude from there, green channel values were prioritized. That is the reason why, although Hoechst 33342 emits on the blue color, the experimental images here displayed appear colored green, figure 3.21 shows an example of an experimental image posterior to its analysis measurement, where it was splintered into the green and blue channel of ImageJ software.

The experimental images from Alive and Dead cells controls were summed up and divided into categories. Each variant of these controls was acquired using UV and Blue Olympus filters, suited to excite Hoechst 333342 and EvaGreen™, respectively (Figure 3.22). Has mentioned above, these experimental images were analyzed resourcing ImageJ green channel in order to be possible to compare the signal generated by Hoechst 33342 and EvaGreen™ action. The values obtained using ImageJ blue channel, due to Hoechst 33342 interaction, are extremely high in comparison, which could ending up belittling the remaining results.

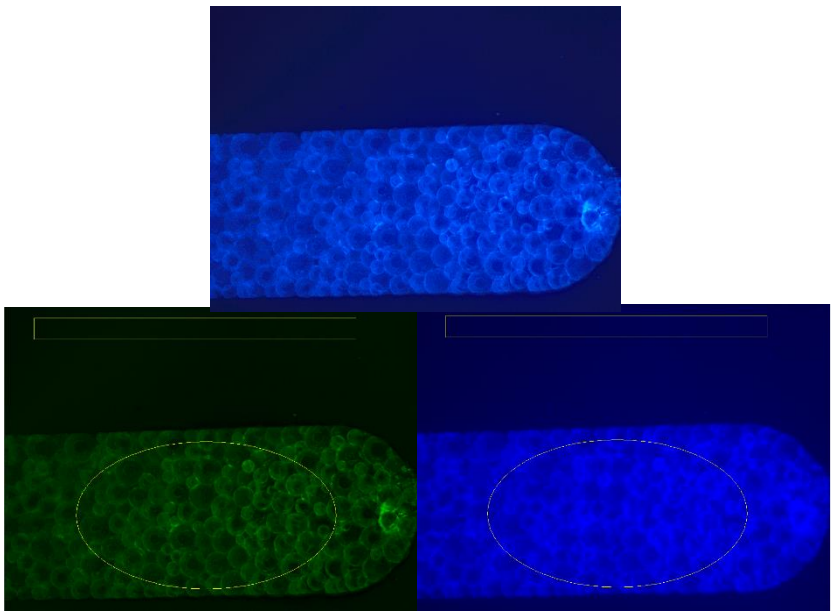

Figure 3.21 Top: Experimental image of an example using UV filter to measure the fluorescence signal. Botton: image slintered into green and blue channel of imageJ software. All the experimental images were acquired in Olympus Microscope CHX41, exposure time: 50ms – for BrightField; 2s – for Fluorescence use, Filters: Blue and UV, gain: 0 dB, magnification:10x.

A closer look to figure 3.22 adding the analysis of figure 3.23 showed that, as foreseen, EvaGreen™ usage alone on the alive cells solution, had not presented a significant fluorescence value. This value, acquired through the blue filter, was traduced on the same range of those obtained from UV filter use, either on the alive or dead cells solutions, which was expected once this last filter should not

be capable of exciting EvaGreen™ dye. Also, there was no Hoechst 33342 signal when exciting using the Blue filter, which went according to its excitation wavelengths. When analyzing the remaining results, the uptake observations were increasingly interesting. Hoechst 33342 showed high signals through UV filter use, as expected, but the difference between the alive and dead cells solution had a considerable

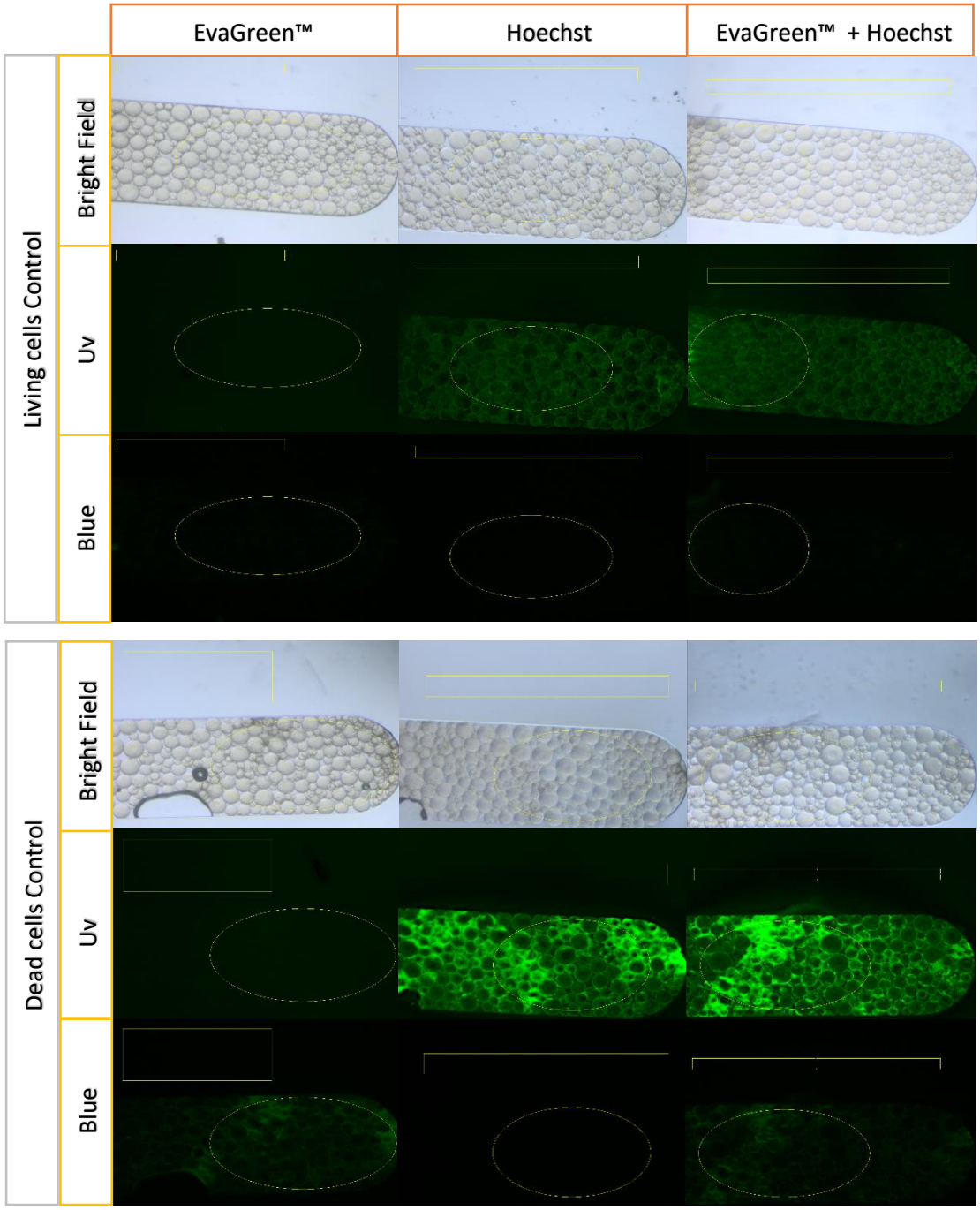

Figure 3.22 Experimental images from the Controls of the Dyes assay after the washing step. Channels with Q-Sepharose® beads. Controls devided into Alive and Dead cells contain a 4OD ~ $3.2 * 10^9$ cells/mL Staphylococcus aureus fresh and thermally treated soltution, respectively. These controls were performed using a 100 nM EvaGreen and 5 µg/mL Hoechst 33342 solutions, isolated and alongside. All the experimental images were acquired in Olympus Microscope CHX41, exposure time: 50ms – for BrightField; 2s – for Fluorescence use, Filters: Blue and UV, gain: 0 dB, magnification:10x.

unconformity. This suggested that although the dye could pass through the cellular membrane, its emission had a higher intensity when the cell was somehow compromised. Regarding EvaGreen™ signal, acquired through its rightful filter, on the thermally treated cells solution, it was passible of being measured. Comparing its intensity, on the same cells condition, Hoechst's presented fluorescence mean values substantially raised. Once, both dyes bound to DNA's, it was also expected them to have similar signals when used separately, which was not verified. Regarding that feature, when analyzing the signals of the dyes when the filter was being correctly employed (i.e. UV and Blue filter to Hoechst 33342 and EvaGreen™, respectively), a constant fluorescent value was observed when comparing the use of an isolated dye to both simultaneously. This occurred on the dead cells control for both filters and on the alive cells control for UV filter (there was no lowering of the expectant Blue filter values on this control), which could suggest a possible binding competition between the dyes.

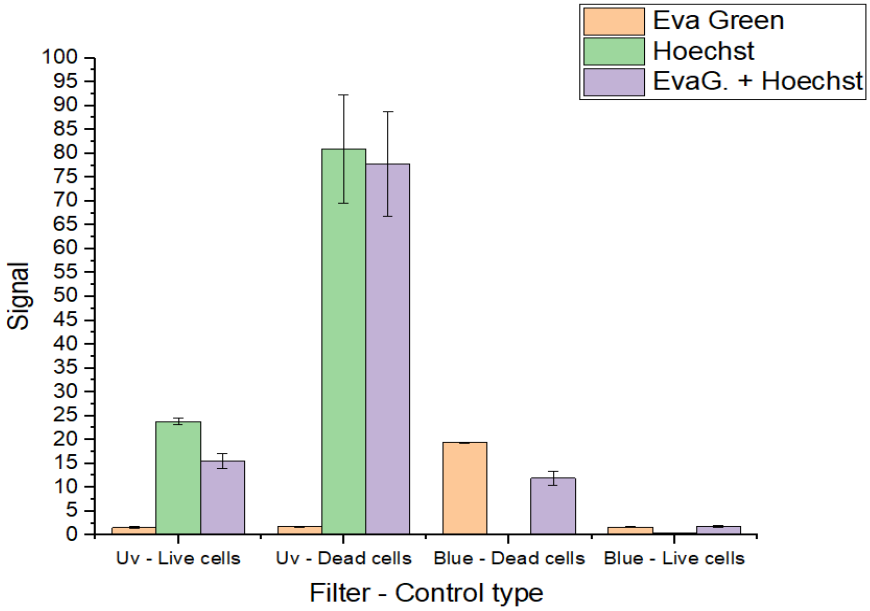

Figure 3.23 Mean fluorescence intensity signal measured on a section of the column after the washing step. Values from the Alive and Dead cells control and their variants, through the use of UV and Blue filters (Aquisition: Olympus Microscope CHX41, exposure time: 2s, gain: 0 dB, magnification:10x.)

Although there was a range of results, that could give origin to further analysis, the focus of this assay was to assess if the protocols used in the previous section were somehow compromising SA's viability. To that end, a column was packed with Spherical silica® beads and a $8 * 10^9$ cells/mL SA solution was flowed through the channel, maintaining the exact features from the controls protocol. After it, both dyes (using the same concentrations as already mentioned) were flowed sequentially, followed by a washing step. Once the experiment with the SiO_2 beads used both dyes, 'EvaG. + Hoechst' values from UV and Blue filter - Alive and Dead cells, were selected from figure 3.23, to analyze that result. Due to the hypothesis of existing a binding competition between the dyes and once, throughout the Spherical silica® beads experiment, EvaGreen™ was flowed first through the column, also "EvaGreen" alive and dead values (Blue Filter) from figure 3.23 were added to the analysis, by means of two straight lines. (Figure 3.25)

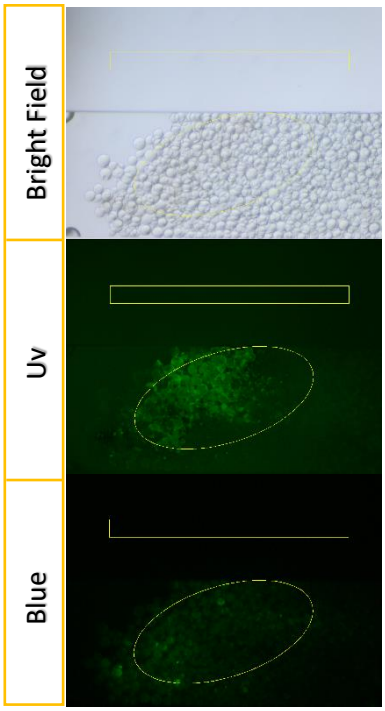

Figure 3.24 Experimental images from the Dyes assay after the washing step. Channels with Spherical silica® beads, a $\sim 8 * 10^9$ cells/mL *Staphylococcus aureus, a 100 nM EvaGreen and 5 µg/mL Hoechst 33342 solutions, flowed sequentially. All the experimental images were acquired in Olympus Microscope CHX41, exposure time: 50ms – for BrightField; 2s – for Fluorescence use, Filters: Blue and UV, gain: 0 dB,*

From figure 3.24 is possible to observe fluorescence by either using UV and Blue filters, which means, SA cells were being affected in the experiment process. Although the experimental image obtained from the use of the UV filter showed evident fluorescence, it was not even similar in intensity to what was observed in Q-Sepharose® controls experiments. Nevertheless, the Blue filter experimental image presented an unexpected fluorescence signal assigned to cellular membrane disruption. From the analysis to figure 3.25, the results were consistent to what was displayed on the experimental images form figure 3.24. The SiO_2 experiment showed UV filter results similar to those from the Alive cell control in this filter. In the other hand, Blue filter values from the assay, support cells were being affected. The value from SiO_2 experiment using the blue filter, was also between the two straight lines, from EvaGreen™ single use controls. The discrepancy between UV and Blue figure 3.25 values, supported the idea of existing a binding competition between the dyes. Once EvaGreen™ was flowed prior to Hoechst 33342, it had time to bind first, while, although in the control both dyes + SA cell solution, EvaGreen™ being added first, the time between that action and the addiction of Hoechst 33342 to the solution was much lower, which ended up engendering a higher signal for Hoechst in the control.

Summing up all the results, what was intended to understand was to test the protocol followed on SA61 assay and conclude if was somehow compromising SA viability, ending up jeopardizing the aptamer binding potential. From the experimental images and analytical results was possible to ascertain that although there was live cellular content posterior to SiO_2 beads experiment, there was also *Staphylococcus aureus* cells being disrupted during the process. This could have happened due to

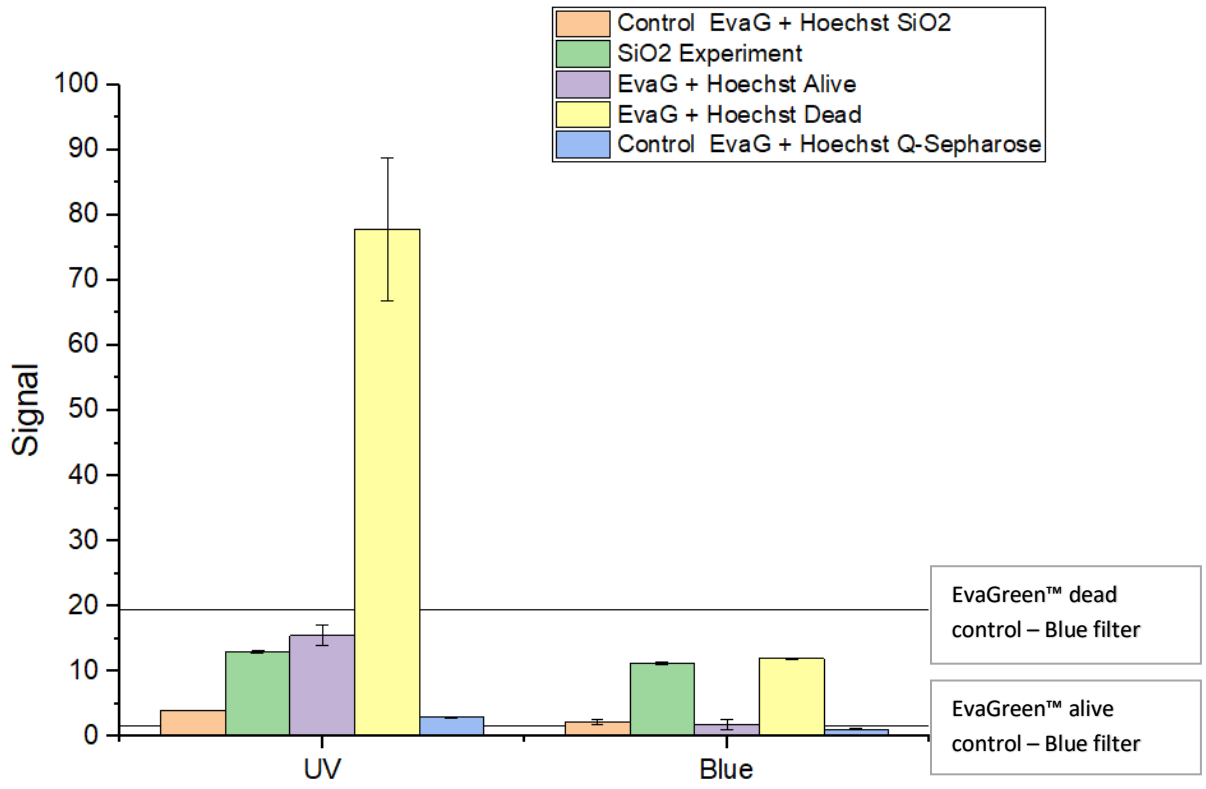

Figure 3.25 Mean flurescence intensity signal measured on a section of the column after the washing step. Values from: the Alive and Dead cells control using both dyes simultaneously; the Spherical silica® bead experiment; and the interaction controls of the dyes in SiO2 and Q-Sepharose bead; through the use of UV and Blue filters; The straight lines correspond to "EvaGreen" alive and dead values (Blue Filter) (Aquisition: Olympus Microscope CHX41, exposure time: 2s, gain: 0 dB, magnification:10x.)

the fact, that cells were highly concentrated, based on centrifugation action that corrupted the cells. In addiction, SiO_2 beads are heavily dense and the applied flow rate against them could also have plaied a role in the cells death. The following approach was to reduce the concentrated SA solution in order to skip centrifugation steps. Beside adjusting SA cellular concentration, from $8 * 10^9$ cells/mL to $4 * 10^8$ cells/mL, also EvaGreen™ an Hoechst 33342 concentrations were reduced in half. Due to the possible binding competition between the dyes, the set of experiments using the new features was followed according figure 3.26.

Q-Sepharose® Beads – Dyes + SA solution incubation outside the column.

1st SiO2 Beads – Flowing EvaGreen™ dye **first** and then Hoechst 33342.

2nd SiO2 Beads – Flowing both dyes **simultaneously** through the column.

Figure 3.26 Schematic of the experiments performed with the new Staphyloccocus aureus concentration.

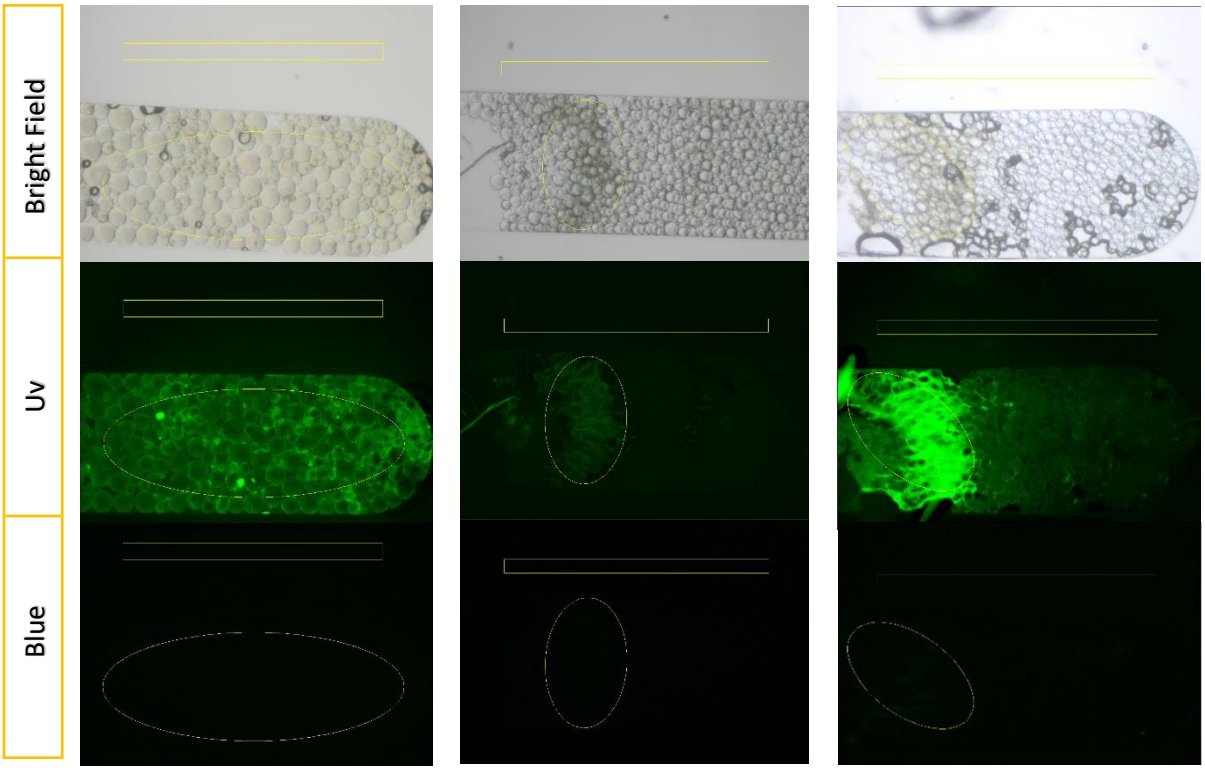

Figure 3.27 Experimental images from the Dyes assay with the new concentration after the washing step. Channels with Q-Sepharose® beads on the left and Spherical silica® beads on the right and middle. All channels with a $4* 10^8$ cells/mL *Staphylococcus aureus solution, a 50 nM EvaGreen and 2,5 µg/mL Hoechst 33342 solutions.Middle and Rigth images refered to the first and second silica beads experiments, respectively. All the experimental images were acquired in Olympus Microscope CHX41, exposure time: 50ms – for BrightField; 2s – for Fluorescence use, Filters: Blue and UV, gain: 0 dB, magnification:10x.*

The experimental images (figure 3.27), showed no relevant fluorescence related to the Blue filter use. Since this filter is associated to EvaGreen™ action, that stains cells with its viability compromised, the results support the cellular integrity conservation. Analyzing the analytical outcome from figure 3.28, this statement could be supported. Blue filter measurements did not demonstrate relevant values across the set of experiments and so, it was possible to conclude that cells were not being considerably affected from the applied protocol features. Regarding UV measurements, there was a substantial difference between both SiO_2 bead protocols. The difference in those two approaches was simply the order of the dyes flow as shown by figure 3.26, which went on behalf of what was already stated, that a binding competition could be the main reason behind the highly different signal results. One the case that EvaGreen™ was flowed first, UV results showed no relevant fluorescence, but when the solution flowed contained both dyes, Hoechst 33342 emitted a considerable higher signal. Nevertheless, with the new established SA solution concentration, the cellular integrity was being kept and SA61 aptamer could once more be tested in order to access its binding efficacy.

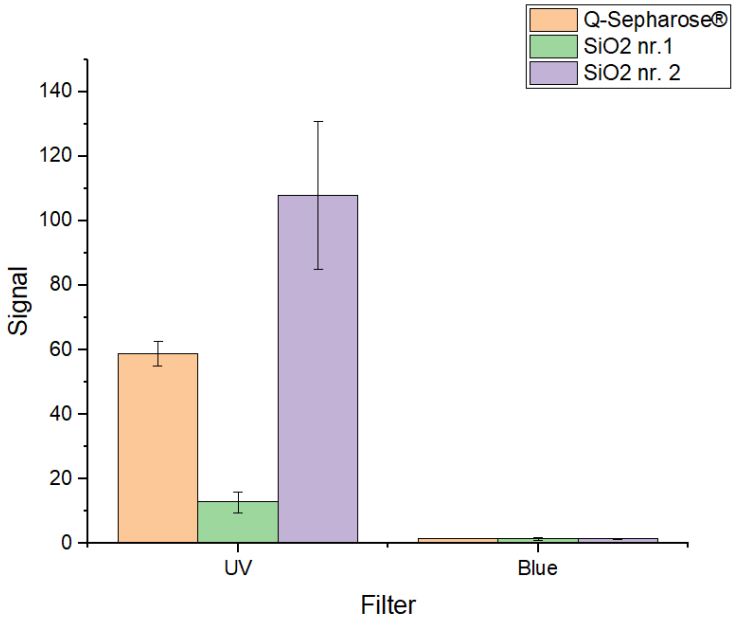

Figure 3.28 Mean fluorescence intensity signal measured on a section of the column after the washing step. Values from a $4 * 10^8$ cells/mL *SA solution on Q-Sepharose® beads and Spherical silica® beads; Hoechst 33342 and EvaGreen™ were used simultaneously on Q-Sepharose® and* SiO_2 *nr.2 experiments and sequentially on* SiO_2 *nr.1. (Aquisition: Olympus Microscope CHX41, exposure time: 2s, gain: 0 dB,*

Guideline 4

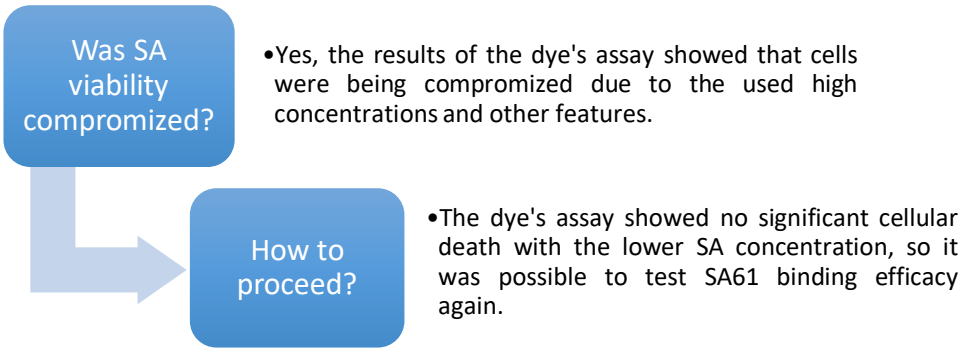

Figure 3.29 Schematic of the fourth guideline

3.5 SA61 binding efficacy - new protocol features

The results in the previous section have shown that the use of centrifugation steps was always keen to burst some cells, but a high cell concentration solution flowing at a certain velocity against the SiO_2 beads was the main factor for the signal measured, representative of cellular death. Using a lower concentration, as approach to avoid this type of result was proven to be the solution to outrun the setback supported, by section 3.4 final measurements.

One from the four protocols flowed across section 3.3, was selected to retry the tests onto the binding efficacy of SA61 aptamer, with a redefinition of the SA solution concentration. Besides this uptake on the protocol features, it was added an extra step at the end of the assay. Flowing Hoechst 33342, should confirm the cellular content presence on the beads column, serving as assurance.

To perform the assay Spherical silica® bead were packed and a $4 * 10^8$ cells/mL SA cells solution, previously incubated at 750 rpm with a 2 µM SA61 solution during 30 minutes, was flowed through the channel at 2.5 µL/min during 20 minutes, followed by a washing step with PBS. Afterwards, a 2.5 µg/mL was flowed at 1 µL/min during 15 minutes ending with the recurrent washing step. Both time points signal were acquired using Blue and UV filters from Olympus microscope, but due to the properties of each fluorophore (Atto 430LS and Hoechst 33342), the experimental images displayed on figure 3.30 are related to the Blue filter measurements for the first time point (after SA61) and the UV filter for the second one (after Hoechst 33342). The analysis was based on the mean signal intensity of the darker zone caused by the *Staphyloccocus aureus* concentration site and a further zone of the channel with lower cellular agglomeration. From the experimental images and analyzing figure 3.31, after SA61 time point there was no significant fluorescence or difference between both sites, where the beginning is related to the darker zone and the end referred to the second region. If the aptamer would have bind SA cells, there should have been an expected variation on the fluorescence mean signal

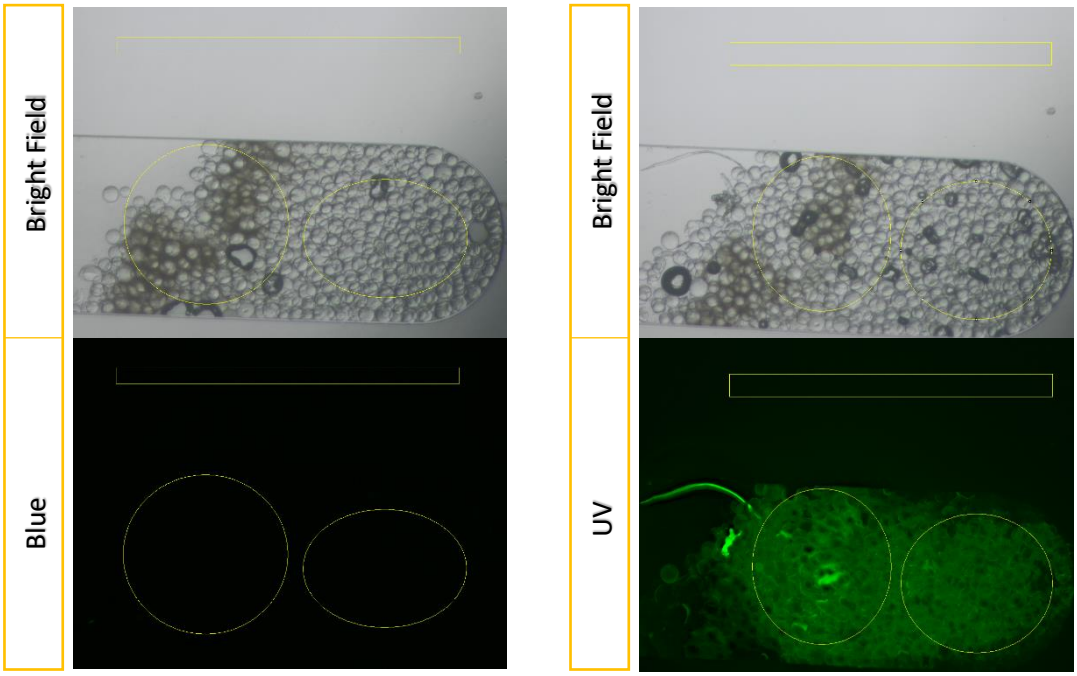

Figure 3.30 Experimental images from SA61 assay with new protocol features, after the washing step. Channels with Spherical silica® beads and a $4 * 10^8$ cells/mL *Staphylococcus aureus solution. Left: First time point – after a 2 µM SA61 solution Right: Second time point – after a 2.5 µm/mL Hoechst 33342 solution. All the experimental images were acquired in Olympus Microscope CHX41, exposure time: 50ms – for BrightField; 2s – for Fluorescence use, Filters: Blue and UV, gain: 0 dB, magnification:10x.*

intensity between both sites and clearly a signal emission, which is not observed neither on the visual nor analytical results. From the UV signal displayed on figure 3.31, the mentioned difference between both sites was evident. Being this said, the use of Hoechst 33342 supported the existence of cellular content in the column in spite the lack of efficacy in SA61 binding ability.

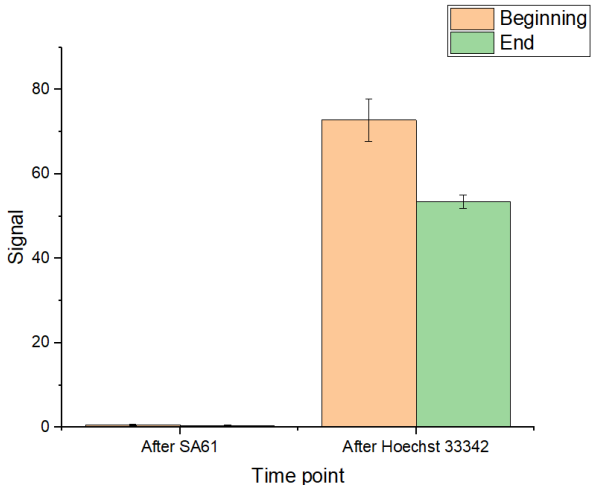

Figure 3.31 Mean fluorescence intensity signal measured on a section of the column after the washing step. Values from a $4 * 10^8$ cells/mL *SA solution on Spherical silica® beads; First time point – After SA61 solution – is related to the Blue filter acquisition and the secont time point – After Hoechst 33342 – related to the UV. The Beginning and End labels are refereed to the different measured sites in the column. (Aquisition: Olympus Microscope CHX41, exposure time: 2s, gain: 0 dB, magnification:10x.)*

Since SA61 aptamer was not working as a detection tool, the following approach was to modify the capture aptamer (SA17) in order to function as a detection aptamer as well.

Guideline 5

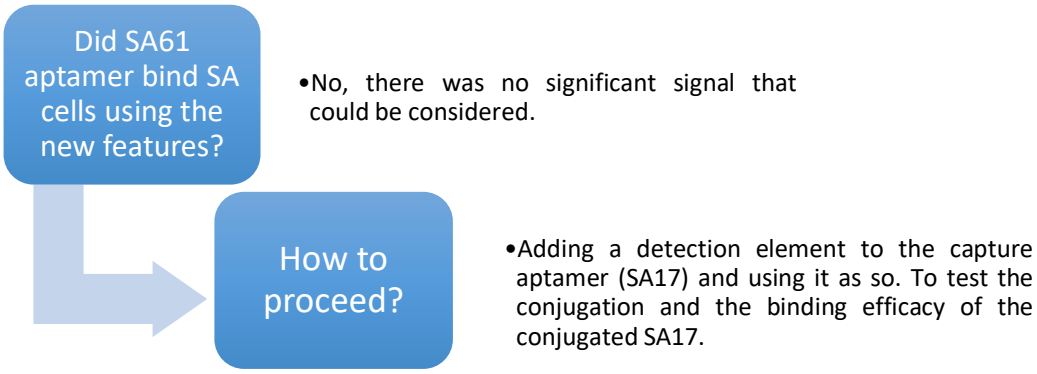

Figure 3.32 Schematic of the fifth guideline.

3.6 SA17 as a detection aptamer

The failure of using SA61 as a detection aptamer propel the search of an alternative, as so, the strategy was to use SA17, the capture aptamer, as a mean for both functions. Converting this aptamer (suitable to function as a detection tool) was proceeded by adding to it, a molecule of streptavidin-FITC. SA17 aptamer has a biotin incorporated in the end of the DNA sequence and the bound biotin-streptavidin has an extremely high efficacy rate.

The efficiency of the conjugation was tested using Q-sepharose® beads, able to attract DNA's negative charge. The fluorescence of FITC was measured using the blue filter to promote the excitation

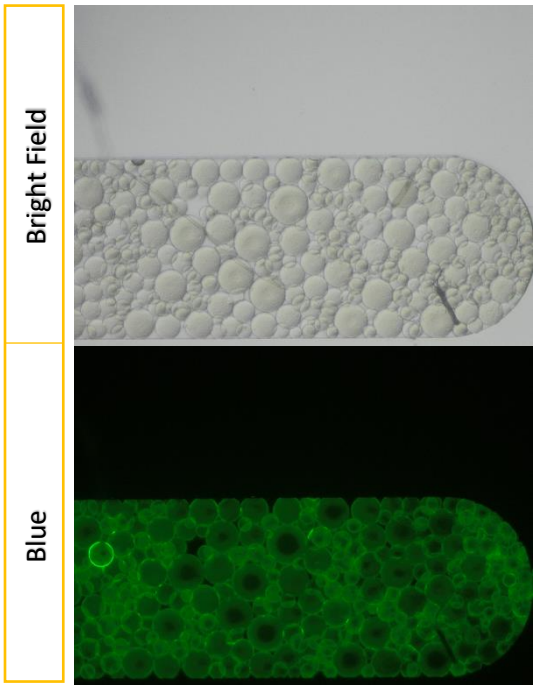

Figure 3.33 Experimental images from SA17 conjugation efficacy test, after the washing step. Channels with Q-Sepharose® beads and a 2 µM SA17-streptavidin-FITC solution. All the experimental images were acquired in Olympus Microscope CHX41, exposure time: 50ms – for BrightField; 2s – for Fluorescence use, Filter: Blue, gain: 0 dB, magnification:10x.

of the molecule. FITC emits on the green, as shown on the assay experimental images illustrated on figure 3.33, which could confirm the success of SA17-streptavidin-FITC aptamer conjugation and be used as a visual control on SA17 binding to SA cells efficacy test.

The protocol followed to test SA17 was the same as in section 3.5 but by flowing the conjugated SA17-streptavidin-FITC instead of the SA61 aptamer solution. Figure 3.34 does not show any visible fluorescence as should be expected if SA17 was bound to *Staphylococcus cells* and analyzing figure 3.35 the same conclusion could be reached. The darker site from the experimental images showed cellular presence in the channel and time point signal 'after Hoechst 33342' supported this statement. As should be expected, there was an established difference between both measurement sites of the channel (region with higher cell agglomeration and lower). Summing all the above observations, was possible to conclude that SA17 was not in fact being bound to SA existent cells and thus, could not be used neither as a detection aptamer nor a capture one due to the lack of binding efficacy.

Throughout the entire set of assays performed since the beginning of the project, the approaches of attempting to development a chip to direct capture and detect *Staphylococcus aureus* bacterium cells were misfortunated by the failure in using the purchased aptamers. The aptamer-sandwich method initially conceived theory could not be set in practice, and so there was not a technique where the sensitivity could be tested. Nevertheless, due to the lack of alternatives to work with, regarding this matter, it was decided to assess the sensitivity of the beads physical capture approach. (Figure 3.36)

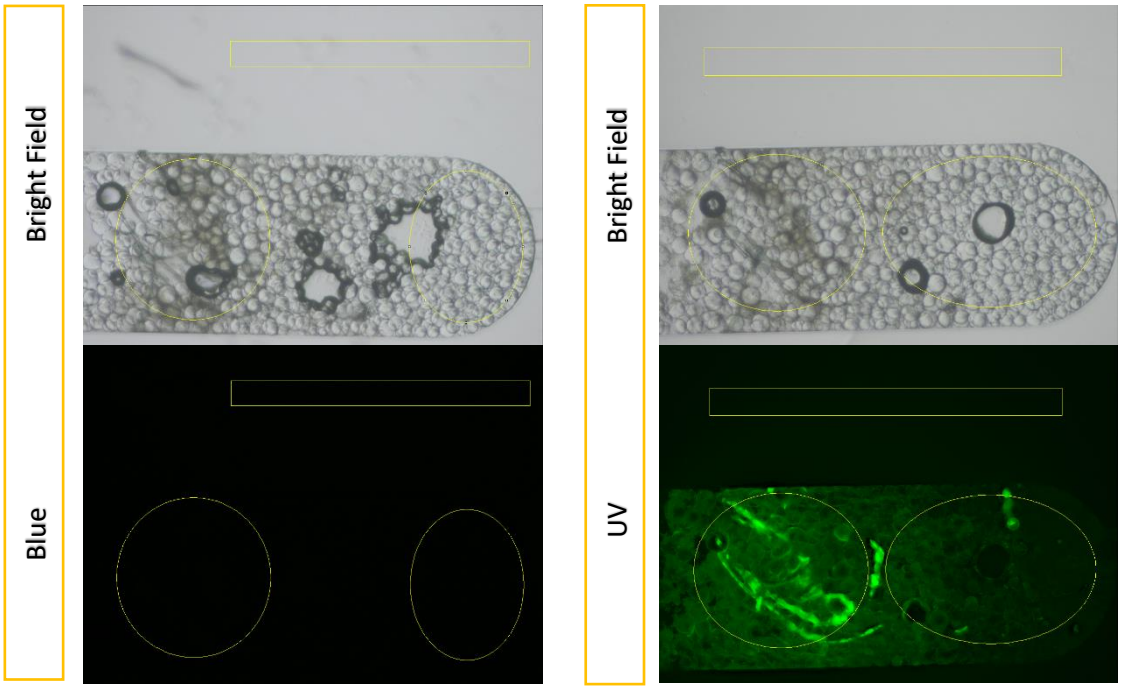

Figure 3.34 Experimental images from SA17 assay, after the washing step. Channels with Spherical silica® beads and a $4 * 10^8$ cells/mL *Staphylococcus aureus solution. Left: First time point – after a 2 µM SA17-streptavidin-FITC solution; Right: Second time point – after a 2.5 µg/mL Hoechst 33342 solution. All the experimental images were acquired in Olympus Microscope CHX41, exposure time: 50ms – for BrightField; 2s – for Fluorescence use, Filters: Blue and UV, gain: 0 dB, magnification:10x.*

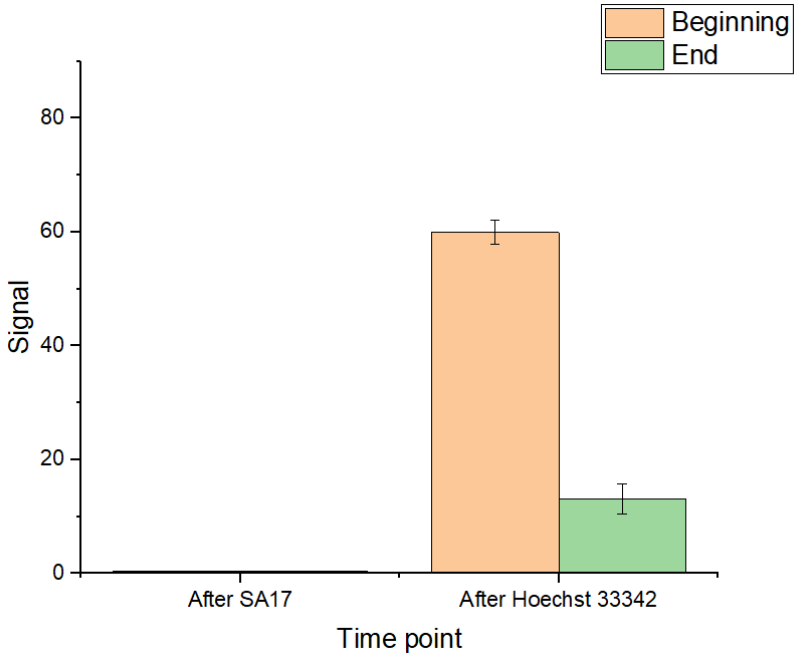

Figure 3.35 Mean fluorescence intensity signal measured on a section of the column after the washing step. Values from a $4 * 10^8$ cells/mL *SA solution on Spherical silica® beads; First time point – After SA17-streptavidin-FITC solution – related to the Blue filter acquisition and the secont time point – After Hoechst 33342 – related to the UV one. The Beginning and End labels are refereed to the different measured sites in the column. (Aquisition: Olympus Microscope CHX41, exposure time: 2s, gain: 0 dB, magnification:10x.)*

Guideline 6

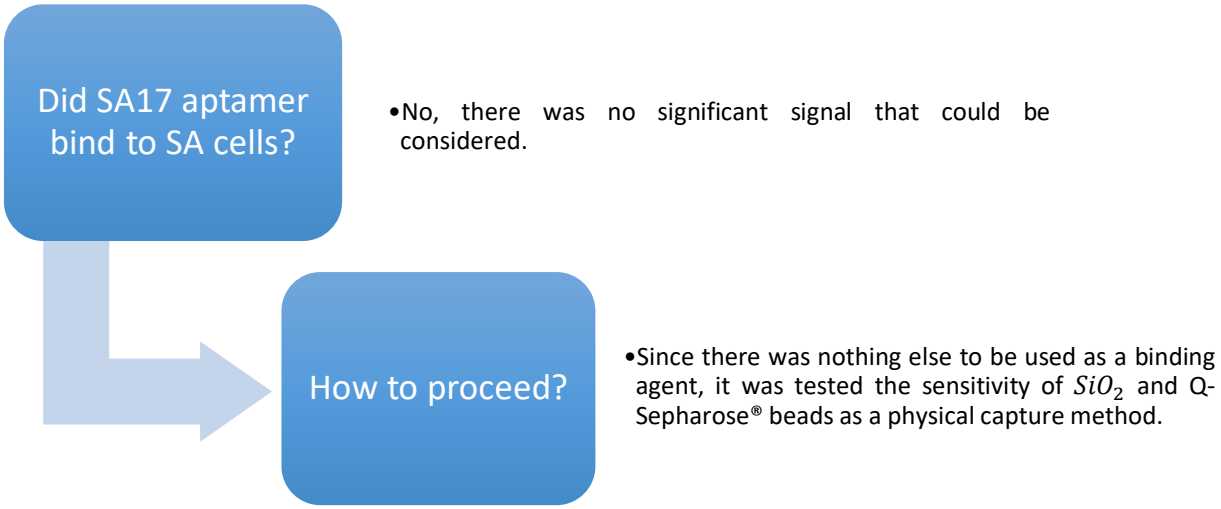

Figure 3.36 Schematic of the sixth guideline.

3.7 Beads capture method: Sensitivity

In spite of the binding assays failure, the truth is it was possible to observe some degree of cellular capture by bead action. Although happening only by physical interaction, the following approach was to test the sensitivity of the method. In one hand, SiO_2 beads are small, highly dense and were able to concentrate SA cells in the beginning of the column (inlet side), in the other hand, Q-Sepharose® beads are positively charged and could have some type of interaction on the bacterium cell surface, ending up attracting them.

To perform this sensitivity test, columns were packed, individually, with both bead types and a certain *Staphylococcus aureus* cell concentrated solution (Table 3.2) was flowed through the channel. Afterwards, Hoechst 33342 dye was also passed through to assess the cellular presence in the column, followed by a washing step. Regarding Hoechst's measurement signal, it was excited using UV filter from Olympus microscope and the analysis on ImageJ software resourced the blue channel splintered image. In this assay, it was selected the blue channel measurements instead of the green one, due to the single used dye, meaning this experiment was isolated from the previous ones and no green emission dyes were used.

Table 3.2 Tested SA solution concentrations in cells/mL.

cells/mL	~ $4*10^8$	~ $2*10^8$	~ $8*10^7$	~ $4*10^7$	~ $4*10^6$	~ $4*10^5$	~ $8*10^3$

3.7.1 Spherical silica® Beads

From the experimental images of figure 3.37 was clearly the decreasing in fluorescence across the lowering of the SA cells solution concentrations, having the results displayed on figure 3.38, supported this fact. From that analysis, was possible to ascertain that the physical capture by Spherical silica® beads had a registered sensibility that stopped around ~ $8*10^7$ cell/mL concentration. Lower concentrations had similar mean fluorescence intensities to those measured on a channel with a Hoechst 33342 solution without SA cells (Control), which marked the detection limit. From the experimental and analytical results, there was also a relevant difference in both measuring sites of the channel (beginning - Left side – and End – Right side), on the experiments where SA cells concentration fluorescence was above the detection limit. SiO_2 beads ability of physically capture SA cells was mostly related to their already mentioned properties in size that reduced considerably the channel's free space. Adding that, the distinct cells concentration led to SA agglomerates formation, ending up by creating a physical trapping mechanism.

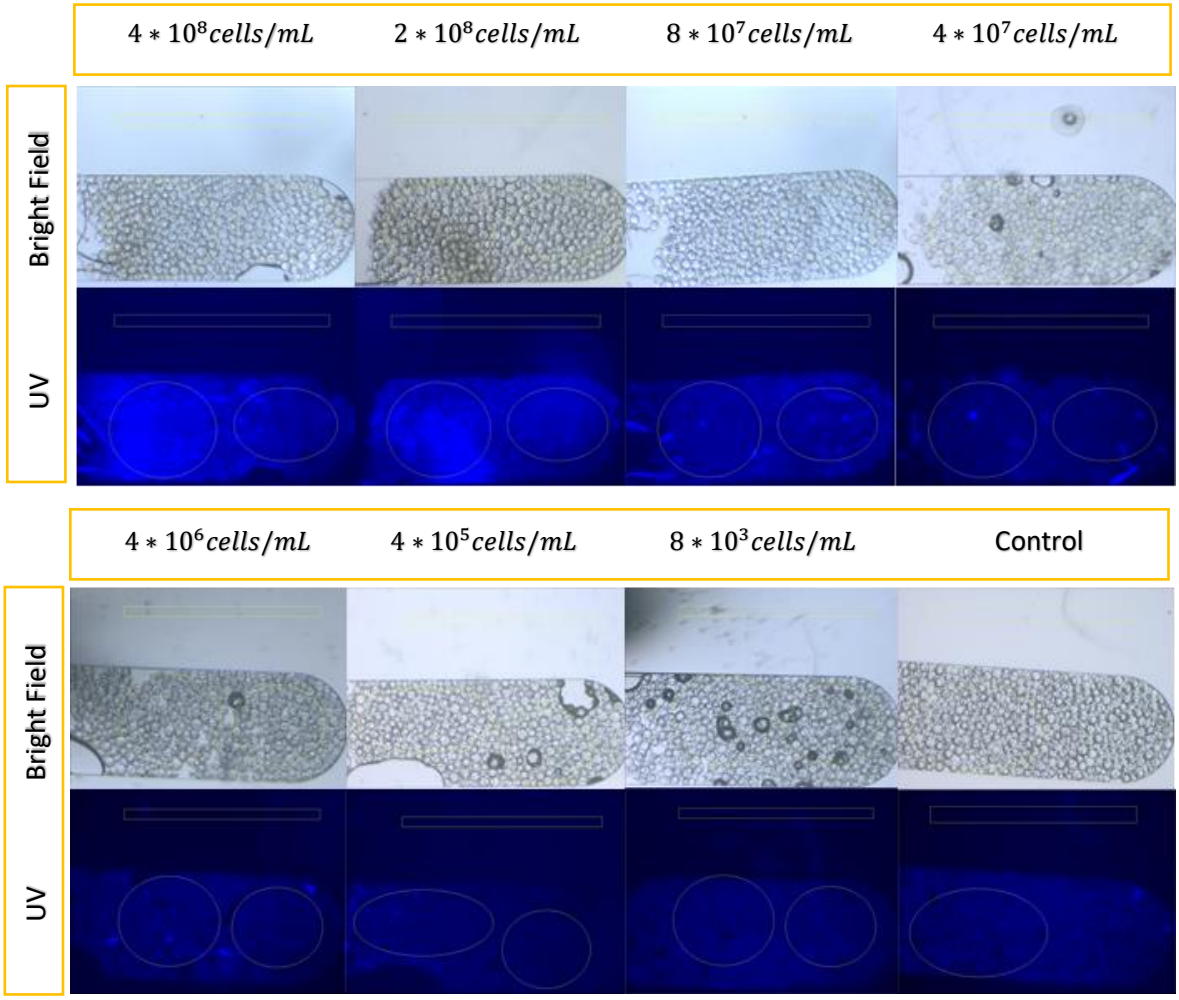

Figure 3.37 Experimental images from the sensibility assessment of SiO_2 beads physical capture method, after the washing step. Channels with Spherical silica® beads, different concentrations of SA cells solutions and a 2,5 µg/mL Hoechst 33342 solution. All the experimental images were acquired in Olympus Microscope CHX41, exposure time: 50ms – for BrightField; 2s – for Fluorescence use, Filters: UV, gain: 0 dB, magnification:10x.

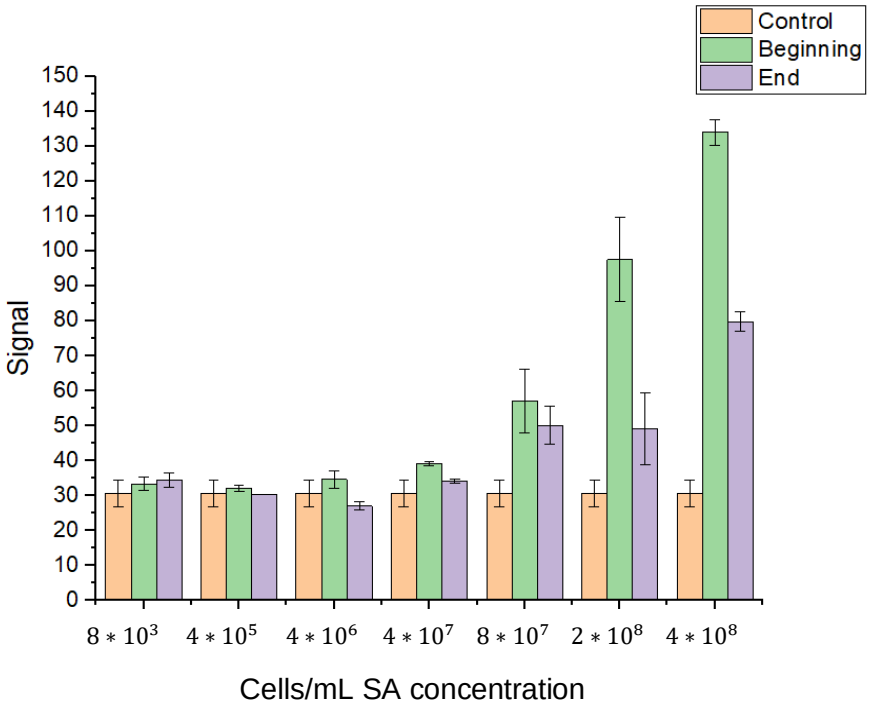

Figure 3.38 Mean fluorescence intensity signal measured on a section of the column after the washing step. Values of multiple concentrations of SA cells solutions on Spherical silica® beads, using Hoechst 33342 as a detection dye. The Beginning and End labels are refereed to the different measured sites in the column. (Aquisition: Olympus Microscope CHX41, exposure time: 2s, gain: 0 dB, magnification:10x.)

3.7.2 Q-Sepharose® Beads

From the experimental images and analytical results of figures 3.39 and 3.40 it was possible to conclude, that in comparison to the Spherical silica® beads, these had a higher sensibility regarding its physical capture of SA cells. The non-specific signal of Hoechst 33342 on Q-Sepharose® beads, used as control and defined as detection limit was higher, nevertheless a plausible detection could be performed by lowering SA concentration until $4 * 10^7 cells/mL$. Unlike SiO_2 beads, it was not registered a notorious difference on the fluorescence intensity signal measured across both the column sites. This could mean that the trapping effect between beads and SA cells was due to the positive charge characteristic of Q-Sepharose®, having an influence near SA cells surface and allowing a uniform detection across the channel. Even if, due to an higher free interspace, smaller cell agglomerates would have been formed and could get evenly distributed through the column and not congregate in the beginning, that does not justify the higher sensibility regarding Q-Sepharose® capture method. Also, a closer look to figure 3.40, allowed the detection of a possible irregularity. On the experiment with a $4 * 10^6 cells/mL$ SA solution, both replicas had the significant difference in the signal emission, which was supported by the chosen experimental image of figure 3.39, that appears brighter and does not go according the correspondent mean intensity displayed. The bar error elucidates that $4 * 10^6 cells/mL$ could either be considered above or bellow the detection limit. In this case, another replica should have been made to clarify this situation.

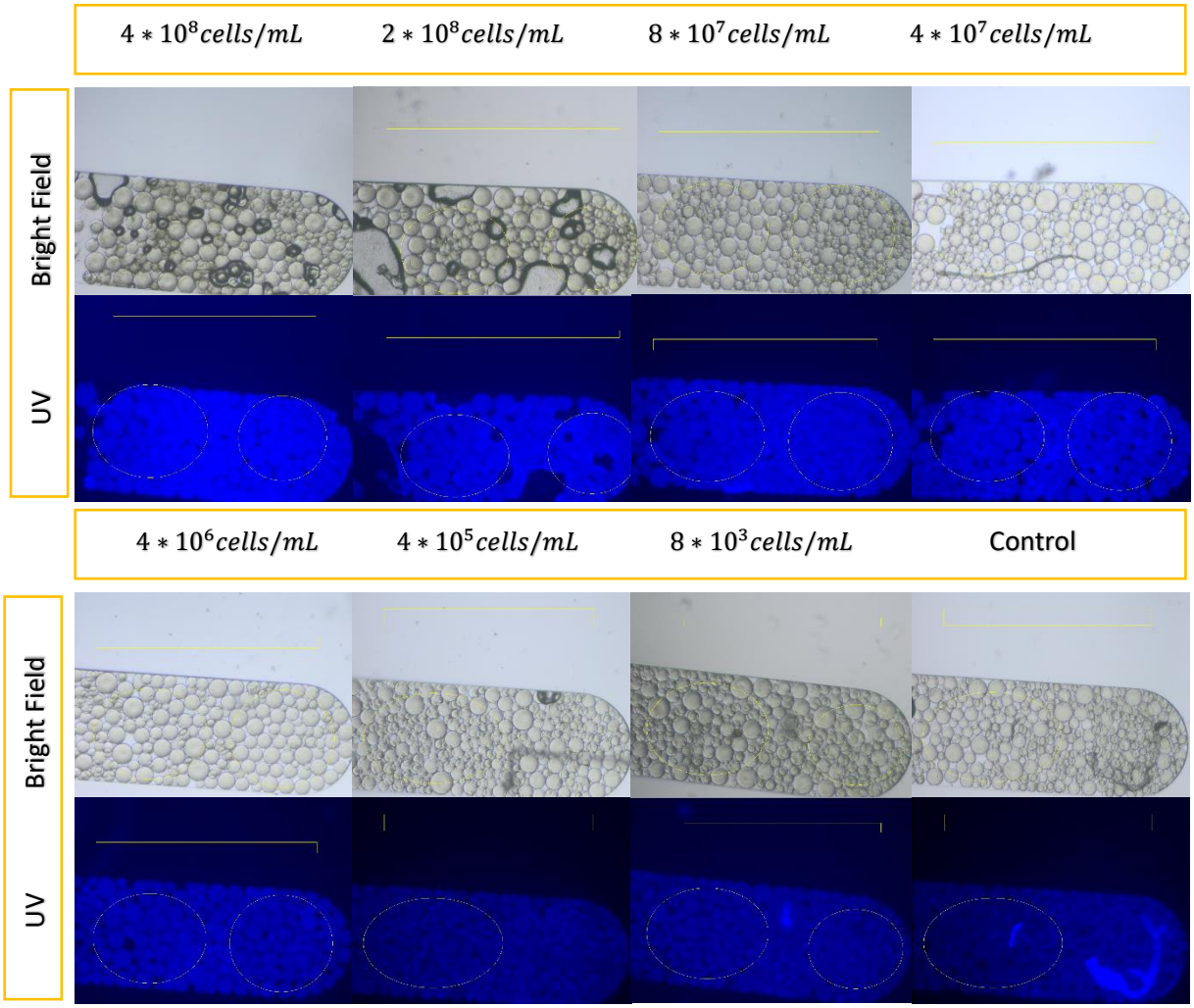

Figure 3.39 Experimental images from the sensibility assessment of Q-Sepharose® beads physical capture method, after the washing step. Channels with Q-Sepharose® beads, different concentrations of SA cells solutions and a 2,5 µg/mL Hoechst 33342 solution. All the experimental images were acquired in Olympus Microscope CHX41, exposure time: 50ms – for BrightField; 2s – for Fluorescence use, Filters: UV, gain: 0 dB, magnification:10x.

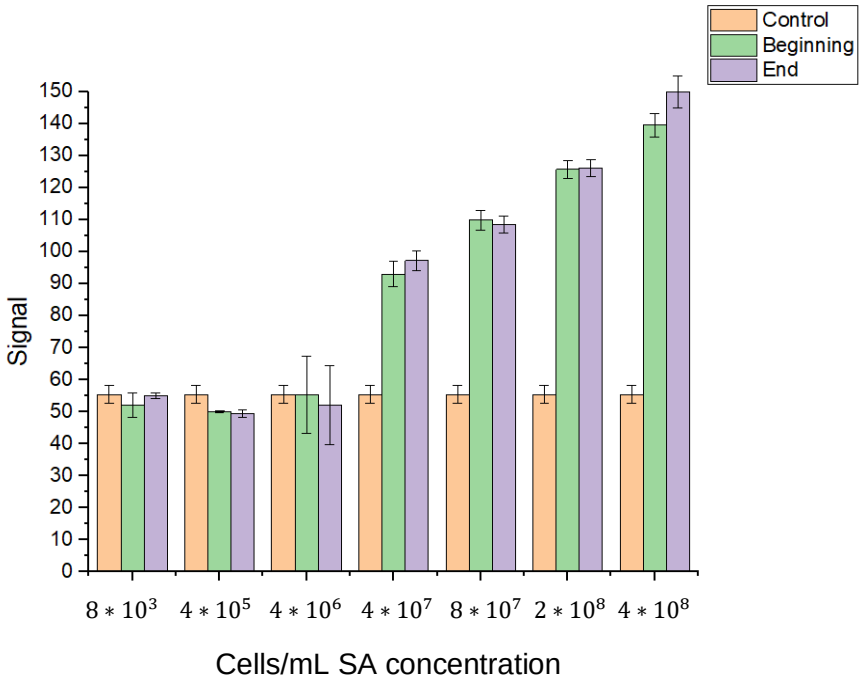

Figure 3.40 Mean fluorescence intensity signal measured on a section of the column after the washing step. Values of multiple concentrations of SA cells solutions on Q-Sepharose® beads, using Hoechst 33342 as a detection dye. The Beginning and End labels are refereed to the different measured sites in the column. (Aquisition: Olympus Microscope CHX41, exposure time: 2s, gain: 0 dB, magnification:10x.)

Chapter 4

Conclusion and Future Outlooks

Bacterial detection plays an important role in therapeutically approaches and pathology identification. The need to assess the main origin of certain clinical manifestations is the pillar to set the appropriated course of treatments. Although existing innumerous technics in the matter of bacterial detection, these are prone to a wide variety of drawbacks. Current practices are time and cost consuming and rely on methods that increase quantitatively the target of the sample in order to reach an appealing sensitivity. The use of microfluidic chips is considered to be an innovative tool in the means of screening, promising unique advantages that are keen to overcome the burden on current applications. Since, a microfluidic system is able to miniaturize a wide range of process, the need for reagents and other product waste is also reduced, achieving low rates of consumption among the used components. Besides being cost saving, as small volumes are being used to mimic an exponentially higher process, the time to perform the scaled down equated process is also reduced. Regarding bacteria detection, the microfluidic field as the possibility of assemble a technique to directly detect certain pathogens without the need of DNA acquisition and amplification.

On the course of the development of this project, a microfluidic chip was manufactured, aiming to direct capture and detect bacterial cells from the testing model of *Staphylococcus aureus* (SA). The chip basis was set to be composed of nano-porous beads, used as a capturing surface, allowing an enhancement of the capture area when compared to the micro-bare-channels. This capturing surface would act as an immobilization platform for a specific *S. aureus* targeting molecule, creating a selection-specific-approach that could be used among other desired targets. Upon capturing, other molecule target-specific, containing an identification marker, would set to be flowed through the beads to bind to the capture target, creating a molecule-target-molecule sandwich-type method. Regarding the success of an assembled, the capture-detection sensitivity of the method should also be assessed. To the present work, aptamers were chosen to act as molecule-targeting probes. Two aptamers were selected from the literature, where is stated their optimal binding efficiency to *S.aureus* cells [66] to attempt accomplishing the described approach. SA17 was purchased with a biotin molecule to allow the bead immobilization and SA16 with Atto 430LS molecule, a fluorophore to be able to be detected. Although the referred success on that literature binding assays, there was the need to assess the aptamers

binding efficacy. On that matter different beads were tested against a highly concentrated SA solution to evaluate the physical trapping ability of each. From the results analysis, Spherical silica beads® were selected, thus were prone to slow down the cells flow through the column, acting as a temporary capturing agent. The beads test results, showed that this trapping-effect was set time enough, that SA61 could be flowed and detected. On this assessment assay, the fluorescence measurements show no significant signal, although cellular content was clearly present in the channel. This gave rise to multiple questions. If the aptamers is specific to SA cells, why the bound was not occurring? Was the aptamer folding technique performed correctly or its tri-dimensional final structure was not achieved? And if so, why? Was the media folding used the ideal for this situation? Does the aptamer bind to the cells surface and so, there is the need to understand if the bacteria viability is being compromised across the assays protocol?

To continue the development of the project, one of those questions gained the need to be clarified and so, a viability assessment assay was performed resourcing two different dyes as probes. Hoechst 33342 and EvaGreen™, are able to stain every cell (alive or dead) and only compromised targets, respectively, creating an Alive/Dead cell evaluation test. From the results analysis, different conclusions could be obtained. The signal acquisition among distinct approaches of the dyes usage, led to the assumption of a binding competition between the dyes, where factors such as single or simultaneous flow of Hoechst 33342 and EvaGreen™ resulted in widely distinct measurements. Nevertheless, the initial question was able to be assessed and in fact, the high concentrations of *S. aureus* solutions and the need to perform centrifugation steps to achieved such concentration values, was indeed bursting the cells. This conclusion was even more clarified when the same assay was performed resourcing a much lower cellular concentration, which was traduced in a non-significant staining from EvaGreen™ dye action (marker for death cells).

After the reach of this solution, the natural path action was to re-try the binding efficacy tests on SA61 detection aptamer, using this new concentration, which showed to be enough to still slow down the SA cells flow through the microfluidic channel, using Hoechst's dye to confirm cellular presence upon the aptamers passage. Unfortunately, the binding was not yet successful and thus not related to viability issues. The following approach was to perform the same assessment for the capture aptamer type, SA17, modified to act as a detection molecule by the conjugation of a fluorescence fluorophore, aiming to avoid the negative results by using SA17 on both functions. Nevertheless, also this aptamer showed no binding efficacy against SA cells, which lead to the emergent questioning about the correct folding of both aptamers. Due to the project time boundaries, further evaluation was not able to be performed in trouble shooting the negative results of the binding assays, leaving this matter to further analysis. Nevertheless, there was still a visible capturing method that followed across the entire project's development: physical capture by the bead-packed columns. As a final approach, two different bead-types were assessed in their physical effects retaining bacterial cells in the column, using Hoechst 33342 to confirm cellular presence. Q-Sepharose® and Spherical silica® beads were packed prior to specific SA cells solutions concentrations to be flowed. Q-Sepharose® beads showed a higher sensitivity in comparison, where the lowest detection was set on ~ $4*10^7$ *cells/mL* solution. This number is extremely

far from being considered an ideal detection tool, as was already expected, nevertheless it was a mean of addressing the sensibility aspect of techniques.

Due to the faced issues during the course of the work hereby described, the need to continue addressing the intended goal is keen to be a path that follows what has been set so far. The attempt of clarifying the encountered binding issues and assess feasible features on why aptamers were not binding, is somehow appealing. Regardless, the negative results, the initial idea behind what was initially designed is an interesting approach, and so, besides the cellular viability already tested hypothesis on what was compromising the bound between aptamers and SA cells, other questions are keen to be answered. For instance, assessing the folding processes trying distinct protocols and buffers, upon literature study, that differ either in composition or physiological properties can be an approach to continue the binding trouble shooting. Since the reason behind the binding infectivity is yet unknown, this can be sorted as an aimed evaluation. The odd factor was both aptamers not being able to be bound-successful, since are reported for having a high efficiency within the presented target, which leads to the assumption based on the fact, that whatever interfered on this process, acted equally upon both aptamers.

Other approach seen as future work could be using the “sandwich” initial idea, changing the targeting molecules from aptamers to antibodies. Although aptamers assemble a wide range of stated advantages over antibodies, the truth is, these last are an extremely sensitive approach in the matter of targeting and bounding. Thus, antibodies can be specific selected and also be keen to perform an antibody-target-antibody interaction, since can also be used as immobilization and detection tools, resourcing feature addition (such as a fluorophore).

Chapter 5

References

[1] Sengupta S, Chattopadhyay MK, Grossart HP. The multifaceted roles of antibiotics and antibiotic resistance in nature. Front Microbiol. 2013; 4:47. doi: 10.3389/fmicb.2013.00047

[2] The antibiotic alarm. Nature. 2013; 495(7440):141.

[3] Michael CA, Dominey-Howes D, Labbate M. The antibiotic resistance crisis: causes, consequences, and management. Front Public Health. 2014; 2:145. doi: 10.3389/fpubh.2014.00145

[4] L. Zeng, L. Wang, J. Hu. Current and Emerging Technologies for Rapid Detection of Pathogens, Biosensing Technologies for the Detection of Pathogens - A Prospective Way for Rapid Analysis. IntechOpen. 2018 doi: 10.5772/intechopen.73178

[5] Harikrishnan J., Himanshu S., Bruce K G. Applications of Microfluidics for Molecular Diagnostics. Humana Press. 2013; 305:334 doi: 10.1007/978-1-62703-134-9_20

[6] 3.3 Unique Characteristics of Prokaryotic Cells - Biology LibreTexts. https://bio.libretexts.org/Bookshelves/Microbiology/Book%3A_Microbiology_(OpenStax)/03%3A_The_Cell/3.3%3A_Unique_Characteristics_of_Prokaryotic_Cells, September 2019.

[7] Dorothee M., Meghan B., and Arash K. Cell Biology of Prokaryotic Organelles. Cold Spring Harb Perspect Biol. 2010 Oct; 2(10): a000422. doi: 10.1101/cshperspect.a000422

[8] 20.1A: Phylogenetic Trees. https://bit.ly/2PccYVld, September 2019

[9] Koonin E. V.. Carl Woese's vision of cellular evolution and the domains of life. RNA biology. 2014;11(3), 197–204. doi:10.4161/rna.27673

[10] Hubert E. B., The human microbiome. Advances in Medical Sciences. 2017; 62(2) 414:420 doi: 10.1016/j.advms.2017.04.005.

[11] Steele-Mortimer O, Subtil A. Editorial overview: Host-microbe interactions: bacteria. War and peace: the fragile equilibrium between bacteria and host. Curr Opin Microbiol. 2014;17:v–vii. doi:10.1016/j.mib.2014.01.001

[12] Baron S, editor. Medical Microbiology. 4th edition. Galveston (TX): University of Texas Medical Branch at Galveston; 1996. https://www.ncbi.nlm.nih.gov/books/NBK7627/, October 2019

[13] Peterson JW. Bacterial Pathogenesis. Baron S, editor. Medical Microbiology. 4th edition. Galveston (TX): University of Texas Medical Branch at Galveston; 1996. Chapter 7. https://www.ncbi.nlm.nih.gov/books/NBK8526/, September 2019

[14] Singer M. Pathogen-pathogen interaction: a syndemic model of complex biosocial processes in disease. Virulence. 2010;1(1):10–18. doi:10.4161/viru.1.1.9933

[15] Mohseni M, Sung S, Takov V. Chlamydia. StatPearls. Treasure Island (FL): StatPearls https://www.ncbi.nlm.nih.gov/books/NBK537286/, September 2019

[16] Allocati N, Masulli M, Alexeyev MF, Di Ilio C. Escherichia coli in Europe: an overview. Int J Environ Res Public Health. 2013;10(12):6235–6254. 2013. doi:10.3390/ijerph10126235

[17] Whittaker R, Economopoulou A, Dias JG, et al. Epidemiology of Invasive Haemophilus influenzae Disease, Europe, 2007-2014. Emerg Infect Dis. 2017;23(3):396–404. doi:10.3201/eid2303.161552

[18] Iglewski BH. Pseudomonas. Baron S, editor. Medical Microbiology. 4th edition. Galveston (TX): University of Texas Medical Branch at Galveston; 1996. Chapter 27.: https://www.ncbi.nlm.nih.gov/books/NBK8326/, October 2019

[19] Ashurst JV, Truong J, Woodbury B. Salmonella Typhi. StatPearls [Internet]. Treasure Island (FL): StatPearls Publishing; https://www.ncbi.nlm.nih.gov/books/NBK519002/, October 2019

[20] Tong SY, Davis JS, Eichenberger E, Holland TL, Fowler VG Jr. Staphylococcus aureus infections: epidemiology, pathophysiology, clinical manifestations, and management. Clin Microbiol Rev. 2015;28(3):603–661. doi:10.1128/CMR.00134-14

[21] Patterson MJ. Streptococcus. IBaron S, editor. Medical Microbiology. 4th edition. Galveston (TX): University of Texas Medical Branch at Galveston; 1996. Chapter 13. https://www.ncbi.nlm.nih.gov/books/NBK7611/, October 2019

[22] Davies J, Davies D. Origins and evolution of antibiotic resistance. Microbiol Mol Biol Rev. 2010;74(3):417–433. doi:10.1128/MMBR.00016-10

[23] Aminov RI. A brief history of the antibiotic era: lessons learned and challenges for the future. Front Microbiol. 2010;1:134. 2010. doi:10.3389/fmicb.2010.00134

[24] Nelson, M. L., Dinardo, A. , Hochberg, J. and Armelagos, G. J. Brief communication: Mass spectroscopic characterization of tetracycline in the skeletal remains of an ancient population from Sudanese Nubia 350–550 CE. Am. J. Phys. Anthropol. 2010; 143: 151:154. doi:10.1002/ajpa.21340

[25] National Center for Biotechnology Information. PubChem Database. Tetracycline, CID=54675776, https://pubchem.ncbi.nlm.nih.gov/compound/Tetracycline, November 2019

[26] Bosch F, Rosich L. The contributions of Paul Ehrlich to pharmacology: a tribute on the occasion of the centenary of his Nobel Prize. Pharmacology. 2008;82(3):171–179. doi:10.1159/000149583

[27] Kong KF, Schneper L, Mathee K. Beta-lactam antibiotics: from antibiosis to resistance and bacteriology. APMIS. 2010;118(1):1–36. doi:10.1111/j.1600-0463.2009.02563.x

[28] Ventola CL. The antibiotic resistance crisis: part 1: causes and threats. P T. 2015;40(4):277–283.

[29] Munita JM, Arias CA. Mechanisms of Antibiotic Resistance. Microbiol Spectr. 2016;4(2):10.1128/microbiolspec.VMBF-0016-2015. doi:10.1128/microbiolspec.VMBF-0016-2015

[30] Fair RJ, Tor Y. Antibiotics and bacterial resistance in the 21st century. Perspect Medicin Chem. 2014;6:25–64. 2014; doi:10.4137/PMC.S14459

[31] Nepal G, Bhatta S. Self-medication with Antibiotics in WHO Southeast Asian Region: A Systematic Review. Cureus. 2018;10(4):e2428. 2018. doi:10.7759/cureus.2428

[32] Chokshi A, Sifri Z, Cennimo D, Horng H. Global Contributors to Antibiotic Resistance [published correction appears in J Glob Infect Dis. 2019 Jul-Sep;11(3):131]. J Glob Infect Dis. 2019;11(1):36–42. doi:10.4103/jgid.jgid_110_18

[33] Manyi-Loh C, Mamphweli S, Meyer E, Okoh A. Antibiotic Use in Agriculture and Its Consequential Resistance in Environmental Sources: Potential Public Health Implications. Molecules. 2018;23(4):795. Published 2018 Mar 30. doi:10.3390/molecules23040795

[34] Taylor TA, Unakal CG. Staphylococcus Aureus StatPearls [Internet]. Treasure Island (FL): StatPearls Publishing; 2019 https://www.ncbi.nlm.nih.gov/books/NBK441868/ , November 2019

[35] DeLeo FR, Diep BA, Otto M. Host defense and pathogenesis in Staphylococcus aureus infections. Infect Dis Clin North Am. 2009;23(1):17–34. doi:10.1016/j.idc.2008.10.003

[36] Myles IA, Datta SK. Staphylococcus aureus: an introduction. Semin Immunopathol. 2012;34(2):181–184. doi:10.1007/s00281-011-0301-9

[37] Stapleton PD, Taylor PW. Methicillin resistance in Staphylococcus aureus: mechanisms and modulation. Sci Prog. 2002;85(Pt 1):57–72. doi:10.3184/003685002783238870

[38] Harkins CP, Pichon B, Doumith M, et al. Methicillin-resistant Staphylococcus aureus emerged long before the introduction of methicillin into clinical practice. Genome Biol. 2017;18(1):130. Published 2017 Jul 20. doi:10.1186/s13059-017-1252-9

[39] Franco-Duarte R, Černáková L, Kadam S, et al. Advances in Chemical and Biological Methods to Identify Microorganisms-From Past to Present. Microorganisms. 2019;7(5):130. Published 2019 May 13. doi:10.3390/microorganisms7050130

[40] Linda V., Jia Li., David E. H., John D. P., Rosaleen J. A., Sylvain O., Paul W. G. Methods for the detection and identification of pathogenic bacteria: past, present, and future. Chemical Society Reviews. Issue 16, 2017 doi: 10.1039/c6cs00693k

[41] P. Rajapaksha, A. Elbourne, S. Gangadoo,R. Brown, D. Cozzolino, J. Chapman ORCID. A review of methods for the detection of pathogenic microorganisms. Analyst. Issue 2, 2019. doi: 10.1039/C8AN01488D

[42] Ashraf MW, Tayyaba S, Afzulpurkar N. Micro Electromechanical Systems (MEMS) Based Microfluidic Devices for Biomedical Applications. Int J Mol Sci. 2011;12(6):3648–3704. doi:10.3390/ijms12063648

[43] Emily M. C. Microfluidic Visualisation and Analysis of Multiphase Flow Phenomena at the Pore Scale. Imperial College London. 2014

[44] Tabeling, Patrick & Troian, Sandra. Introduction to Microfluidics. Physics Today. 2006; 59. 58-. 10.1063/1.2435685.

[45] Luka G, Ahmadi A, Najjaran H, et al. Microfluidics Integrated Biosensors: A Leading Technology towards Lab-on-a-Chip and Sensing Applications. Sensors (Basel). 2015;15(12):30011–30031. Published 2015 Dec 1. doi:10.3390/s151229783

[46] Iliescu C, Taylor H, Avram M, Miao J, Franssila S. A practical guide for the fabrication of microfluidic devices using glass and silicon. Biomicrofluidics. 2012;6(1):16505–1650516. doi:10.1063/1.3689939

[47] Gökaltun A, Kang YBA, Yarmush ML, Usta OB, Asatekin A. Simple Surface Modification of Poly(dimethylsiloxane) via Surface Segregating Smart Polymers for Biomicrofluidics. Sci Rep. 2019;9(1):7377. Published 2019 May 14. doi:10.1038/s41598-019-43625-5

[48] Gokaltun A, Yarmush ML, Asatekin A, Usta OB. Recent advances in nonbiofouling PDMS surface modification strategies applicable to microfluidic technology. Technology (Singap World Sci). 2017;5(1):1–12. doi:10.1142/S2339547817300013

[49] Velve-Casquillas G, Le Berre M, Piel M, Tran PT. Microfluidic tools for cell biological research. Nano Today. 2010;5(1):28–47. doi:10.1016/j.nantod.2009.12.001

[50] Mairhofer J, Roppert K, Ertl P. Microfluidic systems for pathogen sensing: a review. Sensors (Basel). 2009;9(6):4804–4823. doi:10.3390/s90604804

[51] Jayamohan, Harikrishnan & Sant, Himanshu & Gale, Bruce. (2013). Applications of Microfluidics for Molecular Diagnostics. 10.1007/978-1-62703-134-9_20.

[52] Grieshaber D, MacKenzie R, Vörös J, Reimhult E. Electrochemical Biosensors - Sensor Principles and Architectures. Sensors (Basel). 2008;8(3):1400–1458. Published 2008 Mar 7. doi:10.3390/s80314000

[53] Drake CR, Miller DC, Jones EF. Activatable Optical Probes for the Detection of Enzymes. Curr Org Synth. 2011;8(4):498–520. doi:10.2174/157017911796117232

[54] Jackson MP. Detection of Shiga toxin-producing Shigella dysenteriae type 1 and Escherichia coli by using polymerase chain reaction with incorporation of digoxigenin-11-dUTP. J Clin Microbiol. 1991;29(9):1910–1914.

[55] Terekhov SS, Smirnov IV, Stepanova AV, et al. Microfluidic droplet platform for ultrahigh-throughput single-cell screening of biodiversity. Proc Natl Acad Sci U S A. 2017;114(10):2550–2555. doi:10.1073/pnas.1621226114

[56] Okumus B, Baker CJ, Arias-Castro JC, et al. Single-cell microscopy of suspension cultures using a microfluidics-assisted cell screening platform. Nat Protoc. 2018;13(1):170–194. doi:10.1038/nprot.2017.127

[57] Janeway CA Jr, Travers P, Walport M, et al. Immunobiology: The Immune System in Health and Disease. 5th edition. New York: Garland Science; 2001. The structure of a typical antibody molecule. https://www.ncbi.nlm.nih.gov/books/NBK27144/, November 2019

[58] Jan H. A therapeutic battle: Antibodies vs. Aptamers.Research paper. Nanoscience master program. NS109.

[59] Forthal DN. Functions of Antibodies. Microbiol Spectr. 2014;2(4):1–17.

[60] Schroeder HW Jr, Cavacini L. Structure and function of immunoglobulins. J Allergy Clin Immunol. 2010;125(2 Suppl 2):S41–S52. doi:10.1016/j.jaci.2009.09.046

[61] Parashar A. Aptamers in Therapeutics. J Clin Diagn Res. 2016;10(6):BE01–BE6. doi:10.7860/JCDR/2016/18712.7922

[62] Kaur H, Bruno JG, Kumar A, Sharma TK. Aptamers in the Therapeutics and Diagnostics Pipelines. Theranostics. 2018;8(15):4016–4032. Published 2018 Jul 1. doi:10.7150/thno.25958

[63] Chames P, Van Regenmortel M, Weiss E, Baty D. Therapeutic antibodies: successes, limitations and hopes for the future. Br J Pharmacol. 2009;157(2):220–233. doi:10.1111/j.1476-5381.2009.00190.x

[64] Olympus. CKX41 Inverted Microscope. https://www.olympus-lifescience.com/pt/microscopes/inverted/ckx41/, September 2019

[65] Amine-Reactive Crosslinker Chemistry. ThermoFisher. https://www.thermofisher.com/pt/en/home/life-science/protein-biology/protein-biology-learning-center/protein-biology-resource-library/pierce-protein-methods/amine-reactive-crosslinker-chemistry.html , September 2019

[66] Chang YC, Yang CY, Sun RL, Cheng YF, Kao WC, Yang PC. Rapid single cell detection of Staphylococcus aureus by aptamer-conjugated gold nanoparticles. *Sci Rep*. 2013;3:1863. doi:10.1038/srep01863